Univerzita Karlova

1. lékařská fakulta

Studijní obor: Biochemie a patobiochemie

UNIVERZITA KARLOVA
1. lékařská fakulta

Fyziologický ústav AV ČR, v. v. i.

Oddělení bioenergetiky

Mgr. Jana Kovalčíková

Funkční charakterizace nových komponent savčího mitochondriálního proteomu

Functional characterisation of new components of mitochondrial proteome

Disertační práce

Školitel: RNDr. Marek Vrbacký, Ph.D.

Praha, 2018

Prohlášení:

Prohlašuji, že jsem závěrečnou práci zpracovala samostatně a že jsem řádně uvedla a citovala všechny použité prameny a literaturu. Současně prohlašuji, že práce nebyla využita k získání jiného nebo stejného titulu.

Souhlasím s trvalým uložením elektronické verze mé práce v databázi systému meziuniverzitního projektu Theses.cz za účelem soustavné kontroly podobnosti kvalifikačních prací.

V Praze, 5.4.2018

Jana Kovalčíková

Identifikační záznam:

KOVALČÍKOVÁ, Jana. *Funkční charakterizace nových komponent savčího mitochondriálního proteomu [Functional characterisation of new components of mitochondrial proteome]*. Praha, 2018. 104 s., 6 příl. Dizertační práce (Ph.D.). Univerzita Karlova v Praze, 1. lékařská fakulta. Vedoucí práce Vrbacký, Marek.

Acknowledgements

I thank, first of all, my supervisor RNDr. Marek Vrbacký, Ph.D. for his valuable guidance, broad knowledge going hand in hand with constructive criticism. I highly appreciate RNDr. Tomáš Mráček, Ph.D. and MUDr. Josef Houštěk, DrSc., who were not only great mentors but also eminent specialists in the mitochondrial field and far beyond. I would like to express my gratitude to all members of the Department of Bioenergetics, Institute of Physiology, CAS, for help, mental support and friendly atmosphere during the entire PhD studies and research. I would like to also thank to all collaborative departments for their valuable contributions. This thesis would not have been carried out without the support of the grant projects from Charles University Grant Agency (726214), Grant Agency of the Czech Republic (P303/11/0970, 14-36804G), Ministry of Education, Youth and Sports of the Czech Republic (LL1204) and Czech Health Research Council (16-33018A).

Finally, I express my sincere gratitude to my family and Mgr. Miroslav Mikeš for their support and endless trust in me.

Abstrakt

Mitochondriální proteom savců je tvořen ~1500 různými proteiny, z nichž není stále přibližně jedna čtvrtina plně charakterizována.

Jedním z těchto proteinů je TMEM70 podílející se na biogenezi eukaryotické F_1F_o-ATP syntázy. Mutace v *TMEM70* způsobují izolovaný nedostatek ATP syntázy, což často vede u pacientů k letálním neonatálním mitochondriálním encefalokardiomyopatiím. Abychom porozuměli molekulárnímu mechanismu působení TMEM70, vytvořili jsme konstitutivní *Tmem70* knockout myší model, který byl embryonálně letální s narušenou biogenesí ATP syntázy. Následně vytvořený myší indukovatelný *Tmem70* knockout model byl letální v 8. týdnu po indukci. Především vykazoval funkční poruchu jater, což je v kontrastu k převážně kardiologickému fenotypu u lidí v počátku onemocnění. Analýza jaterních mitochondrií odhalila tvorbu labilních subkomplexů ATP syntázy postrádajících podjednotku c. V případě deficitu TMEM70 tedy nebyl inkorporován c-oligomer do ATP syntázy, což vedlo ke kritickému poškození produkce energie mitochondriemi, analogickému k dysfunkci TMEM70 u lidí. V modelech s deficitem TMEM70 dosáhl nedostatek ATP syntázy limitu pro jeho patologický projev, který jsme stanovili na 30 %. Pozorovali jsme také kompenzační zvýšení obsahu většiny komplexů OXPHOS, ale neočekávaně také ANT a PiC, komponent ATP syntasomu, které by měly být asociovány s ATP syntázou.

Studovali jsme také podjednotku ATP syntázy DAPIT (kódovanou *Usmg5* genem). Vytvořili jsme potkany s deficiencí DAPIT, kteří byli plně životaschopní, ale měli nižší tělesnou hmotnost, výrazně snížené množství tukové tkáně a hypertrofii pravé komory srdeční. Pozorovali jsme normální množství ATP syntázy, nicméně byla přítomna převážně v monomerní formě, což ukazuje na úlohu DAPIT při tvorbě dimerů ATP syntázy. Funkce ATP syntázy byla snížena o ~10 % v játrech i v srdci. Její vyšší citlivost k inhibitoru oligomycinu než k aurovertinu naznačuje, že DAPIT blokuje vazebné místo oligomycinu na F_o části.

Závěrem můžeme shrnout, že jsme vytvořili unikátní modely deficitu mitochondriálních proteinů a charakterizovali funkci proteinů TMEM70 a DAPIT.

Klíčová slova: mitochondriální proteom, mitochondriální patologie, F_1F_o-ATP syntáza, TMEM70, DAPIT, *Usmg5*, knockout modely

Abstract

It has been estimated that the mammalian mitochondrial proteome consists of ~1500 distinct proteins and approximately one quarter of them is still not fully characterized.

One of these proteins is TMEM70, protein involved in the biogenesis of the eukaryotic F_1F_o-ATP synthase. *TMEM70* mutations cause isolated deficiency of ATP synthase often resulting in a fatal neonatal mitochondrial encephalocardiomyopathies in patients. To understand the molecular mechanism of TMEM70 action, we generated constitutive *Tmem70* knockout mice, which led to embryonic lethal phenotype with disturbed ATP synthase biogenesis. Subsequently generated inducible *Tmem70* mouse knockout was lethal by the week 8 post induction. It exhibited primarily impaired liver function, which contrasts with the predominantly cardiologic phenotype at disease onset in humans. Liver mitochondria revealed formation of labile ATP synthase subcomplexes lacking subunit c. Thus, in case of TMEM70 deficiency c-oligomer was not incorporated into ATP synthase, which led to critical impairment of mitochondrial energy provision, analogous to TMEM70 dysfunction in humans. In TMEM70 deficient models, the ATP synthase deficiency reached the 'threshold' for its pathologic presentation, which we quantified at 30 %. We observed compensatory increases in the content of most OXPHOS complexes but unexpectedly also of ANT and PiC, components of ATP synthasome, which should associate with ATP synthase.

We also studied ATP synthase subunit DAPIT (coded by *Usmg5* gene). We generated DAPIT deficient rats, which were fully viable but had lower body weight, pronounced decrease of fat tissue and right ventricular hypertrophy. We observed normal levels of assembled ATP synthase, however, it was predominantly present in the monomeric form, pointing at the role of DAPIT in formation of ATP synthase dimers. ATP synthase function was reduced by ~10 % in both liver and heart. Its higher sensitivity to inhibitor oligomycin than to aurovertin indicated that DAPIT shields oligomycin binding site at F_o moiety.

In conclusion, we generated unique models of mitochondrial proteins deficiency and characterised TMEM70 and DAPIT function.

Key words: mitochondrial proteome, mitochondrial pathology, F_1F_o-ATP synthase, TMEM70, DAPIT, *Usmg5*, knockout models.

Contents

List of abbreviations 10
1 INTRODUCTION 12
1.1 Mitochondria 12
1.2 The mammalian mitochondrial genome and proteome 14
1.2.1 Mitochondrial genome and its expression 14
1.2.2 Mitochondrial protein databases 17
1.3 Oxidative phosphorylation system 19
1.3.1 Respiratory chain 19
1.3.2 ATP synthase 21
1.3.2.1 Structure of ATP synthase 21
1.3.2.2 Assembly of ATP synthase 23
1.3.2.3 Function of ATP synthase 25
1.3.3 Mitochondrial diseases and therapy 26
1.3.3.1 ATP synthase defects of mtDNA origin 27
1.3.3.2 ATP synthase defects of nDNA origin 28
1.3.3.2.1 Nuclear genes mutations causing ATP synthase deficiency 28
1.3.3.3 Link between genotype and phenotype in ATP synthase disorders 29
1.3.4 New proteins involved in biogenesis and structure of ATP synthase 30
1.3.4.1 TMEM70 protein 30
1.3.4.2 DAPIT protein 34
2 AIMS OF THE STUDY 36
3 MATERIALS AND METHODS 37
3.1. Animal and cell models 37
3.1.1 Ethics Statement 37
3.1.2 Generation of Tmem70-deficient mice 37
3.1.3 Generation of DAPIT-deficient rats 38
3.1.4 Cell culture and generation of knockdown clones 38
3.1.5 Collection of mouse embryos 39
3.2 Molecular methods 39
3.2.1 Genotyping 39
3.2.2 RT-PCR 40
3.3 Biochemical methods 40
3.3.1 Electrophoresis and Western blot analysis 40
3.3.2 ATPase in-gel activity assay 43

3.3.3 Respiratory measurements 44
3.3.4 ROS production 45
3.3.5 Enzyme activity measurement 45
3.3.6 Adenine nucleotide analysis 46
3.3.7 Blood analysis 46
3.3.8 Determination of caspase activities 46
3.3.9 Determination of glutathione level 47
3.3.10 Triglycerides level determination 47
3.4 Microscopic methods 47
3.4.1 Whole mount confocal microscopy 47
3.4.2 Transmission Electron Microscopy 48
3.5 Physiological methods 49
3.5.1 Body weight and food intake monitoring 49
3.5.2 Echocardiography 49
3.6. Statistics 49
4 RESULTS 50
4.1 Effect of *Tmem70* knockout in mice (aim 1) 50
4.1.1 Whole body *Tmem70* mouse knockout (publication A) 50
4.1.1.1 Embryonic lethality 50
4.1.1.2 Developmental retardation of c*Tmem70*$^{-/-}$ embryos 51
4.1.1.3 Disrupted mitochondrial ultrastructure in c*Tmem70*$^{-/-}$ embryos 53
4.1.1.4 ATP synthase deficiency in c*Tmem70*$^{-/-}$ embryos 54
4.1.1.5 Altered mitochondrial energetic function in c*Tmem70*$^{-/-}$ embryos 55
4.1.1.6 Affected postnatal heart phenotype of *Tmem70* heterozygous mice 56
4.1.2 Inducible *Tmem70* knockout mouse (unpublished data) 58
4.1.2.1 Viability of i*Tmem70*$^{-/-}$ mice 58
4.1.2.2 Effectivity of *Tmem70* excision 59
4.1.2.3 ATP synthase isolated deficiency i*Tmem70*$^{-/-}$ mice 60
4.1.2.4 Altered mitochondrial energetic function in i*Tmem70*$^{-/-}$ mice 63
4.1.2.4 Oxidative stress in i*Tmem70*$^{-/-}$ mice 64
4.1.2.5 Physiological parameters in liver of i*Tmem70*$^{-/-}$ mice 65
4.2 Effect of DAPIT deficiency in rats (aim 2, unpublished data) 67
4.2.1 Lower body weight and heart hypertrophy of DAPIT deficient rats 67
4.2.2 Affected heart function in DAPIT deficient rats 68
4.2.3 ATP synthase defect in DAPIT deficient rats 69

4.3 Components of mitochondrial ATP synthasome in fibroblasts of patients with ATP synthase deficiency (aim 3, publication B) 72
4.4 ATP synthase 'threshold' in ATP synthase deficiencies (aim 4, manuscript prepared for submission) 74
4.4.1 Knockdown of ATP synthase central stalk subunits - clone characterisation 74
4.4.2 Cellular energetics and ROS production in relation to residual ATP synthase activity 75
5 DISCUSSION 77
6 CONCLUSIONS 86
7 SUMMARY 87
8 REFERENCES 88
9 APPENDIX 104

List of abbreviations

ADP	- adenosine diphosphate
ALT	- alanine aminotransferase
ANT	- ADP/ATP translocase
AST	- aspartate aminotransferase
ATP	- adenosine triphosphate
AWTd	- diastolic anterior wall thickness
AWTs	- systolic anterior wall thickness
BAT	- brown adipose tissue
BN-PAGE	- blue native polyacrylamide gel electrophoresis
BW	- body weight
hrCN-PAGE	- high resolution clear native polyacrylamide gel electrophoresis
CoQ	- coenzyme Q
DAPIT	- diabetes-associated protein in insulin-sensitive tissues
EOH	- early-onset hypotonia
FADH	- flavin adenine dinucleotide
FCCP	- carbonyl cyanide-p-trifluoromethoxyphenylhydrazone
FD	- facial dysmorphism
FS	- fractional shortening
FTT	- failure to thrive
HA	- hyperammonemia
HCMP	- hypertrophic cardiomyopathy
HPLC	- high-performance liquid chromatography
HR	- heart rate
HW	- heart weight
IUGR	- intrauterine growth retardation
IMM	- inner mitochondrial membrane
IMS	- intermembrane space
IMPI	- integrated mitochondrial protein index
LA	- lactic acidosis
LRPPRC	- leucine-rich PPR-motif containing protein
LV	- left ventricle
LVDd	- left ventricle diastolic dimension
LVDs	- left ventricle systolic dimension
LW	- liver weight
3-MGA	- 3-methylglutaconic aciduria
MILS	- maternally inherited Leight syndrome
mtDNA	- mitochondrial deoxynucleic acid
MTERF4	- mitochondrial transcription terminator factor 4
NA	- neuroporus anterior
NADH	- nicotinamide adenine dinucleotide
NARP	- neuropathy, ataxia and retinis pigmentosa

nDNA	- nuclear deoxynucleic acid
OCR	- oxygen consumption rate
OMM	- outer mitochondrial membrane
OT	- outer tract
PAH	- pulmonary arterial hypertension
PiC	- inorganic phosphate carrier
PIC	- protease inhibitor cocktail
POLRMT	- MtDNA RNA polymerase
OXPHOS	- oxidative phosphorylation
pmf, Δp	- proton motive force
PMR	- psychomotor retardation
PWTd	- diastolic posterior wall thickness
PWTs	- systolic posterior wall thickness
RC	- respiratory chain
RCR	- respiratory control ratio
ROS	- reactive oxygen species
rRNA	- ribosomal ribonucleic acid
RV	- right heart ventricle
SB	- Sorensen's phosphate buffer
SDHA	- succinate dehydrogenase A
SOD	- superoxide dismutase
STZ	- streptozotocine
TAM	- tamoxifen
TCA	- tricarboxylic acid
TFAM	- transcription factor A
TIM	- translocases of inner membrane
TMEM70	- transmembrane protein 70
TOM	- translocase of outer membrane
tRNA	- transfer ribonucleic acid
UCP	- uncoupling protein
Usmg5	- Up-regulated during skeletal muscle growth 5
VDAC	- voltage-dependent anion channels
WPW	- Wolf-Parkinson-White pre-excitation syndrome
$\Delta\Psi_m$	- mitochondrial membrane potential

1 INTRODUCTION

Incomplete knowledge of biochemical processes in mitochondria forms a barrier between the mitochondrial disease and its possible treatment. Recently, a lot of effort has focused on the mitochondrial research to shed more light on the mitochondrial function. Many mitochondrial proteins have unknown function and generating animal knockout models is a proven way to clarify it. I have set out to contribute to the research of mitochondrial proteins by analysing rodent models of deficiency of TMEM70 and DAPIT - new proteins related to ATP synthase. In addition, I focussed on more general prerequisites for the pathological presentation of ATP synthase deficiencies. Here I summarise the overview of literature relevant for this research.

1.1 Mitochondria

Mitochondria are eukaryotic organelles playing critical role in cellular energy metabolism, small molecule metabolism, ion homeostasis, immune signalling and cell death. According to the current hypothesis, mitochondria originated from once free-living cells (Sagan, 1967). As the cell with the most related genome was identified α-proteobacterium *Rickettsia prowazekii*, which likely entered host cell via symbiosis during eukaryotic evolution ~1.5-2 billion years ago (Andersson et al., 1998). Pioneering electron microscopy studies in the 1950's revealed that mitochondria are composed by two membranes (Palade, 1953) - outer and inner mitochondrial membrane (OMM, IMM) separated by intermembrane space (IMS). IMM surrounds intramitochondrial space termed matrix (Figure 1). Although mitochondria are often depicted as singular oval-shaped structures, they usually undergo fusion and fission processes that give rise to the very dynamic mitochondrial reticulum (Bereiter-Hahn, 1990).

The OMM is partially permeable to ions and metabolites and contains three isoforms of protein pores termed porins also known as the voltage-dependent anion channels (VDAC) (Szabo and Zoratti, 2014).

The IMM surface is enlarged by invaginations called cristae and together with matrix is the main place of metabolic processes in mitochondria. The membrane composition differs from that of OMM. IMM is enriched with phospholipid cardiolipin and contains almost no sterols (Horvath and Daum, 2013). Roughly 80 % of membrane is composed of proteins (Guidotti, 1972). Many of these proteins are involved in transport of metabolites and ions between cytosol and matrix (Szabo and Zoratti, 2014) and in the process of oxidative

phosphorylation (OXPHOS) (Nicholls and Ferguson, 2013). OXPHOS system itself is essential in cellular energy provision as it produces ~90 % of cellular adenosine triphosphate (ATP).

The matrix is a compartment where tricarboxylic acid (TCA) cycle, β oxidation of free fatty acids and pathways of amino acid oxidation take place (Nelson and Cox, 2017) and it also hosts pathways of haem metabolism (Barupala et al., 2016).

The IMS coordinates processes between matrix and cell cytoplasm. It includes signalling pathways, exchange of proteins, lipids, or metal ions. Important protein of IMS is cytochrome c, which is mobile component of OXPHOS and mediator of apoptosis (Herrmann and Riemer, 2010).

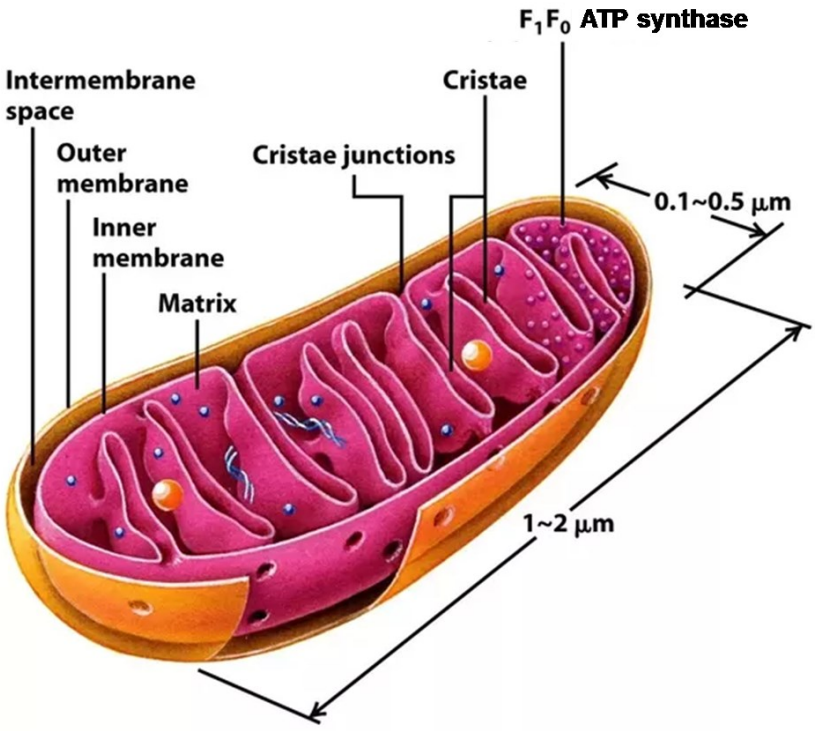

Figure 1. Structure of mitochondria. *Mitochondria are composed of the outer and inner membranes, which are separated by the intermembrane space. The inner mitochondrial membrane surface is enlarged by cristae connected with intermembrane space by cristae junctions. Inside of mitochondria is a space termed 'matrix'. Adopted and modified from (Lodish et al., 2007).*

Mitochondria have their own genome (mtDNA) that encodes transfer RNAs (tRNAs), ribosomal RNAs (rRNAs) and (in case of mammals) only 13 mitochondrial proteins. The most of the α-proteobacterium genome was transferred to the cell nucleus during evolution. The one of the possible explanations, why mitochondria retained the genome for a few proteins, is their hydrophobicity that might embarrass their import across mitochondrial membranes (Falkenberg

et al., 2007). Most of the mitochondrial proteins are encoded by nuclear genome (nDNA), synthesised in cytosol and transported into the mitochondria by protein translocase systems, which are primarily translocase of OMM – TOM complex and translocases of inner membrane – TIM complexes (Wasilewski et al., 2017).

1.2 The mammalian mitochondrial genome and proteome

1.2.1 Mitochondrial genome and its expression

In vast majority of species, mtDNA is maternally inherited. Mammalian mtDNA is double stranded, circular and in humans it consists of 16569 bp. In mammals it encodes 13 proteins involved in OXPHOS. It encodes also 2 rRNAs and 22 tRNAs that play roles in intra-mitochondrial proteosynthesis (Anderson et al., 1981, Andrews et al., 1999).

Human somatic cell contains 1000-5000 copies of mtDNA associated with many proteins forming particles termed 'nucleoids'. The main protein packaging mtDNA into nucleoids is transcription factor A (TFAM) protein (Kukat and Larsson, 2013, Kukat et al., 2015). In addition, Twinkle helicase involved in replication (Spelbrink et al., 2001) and many other proteins associate with nucleoids (Hensen et al., 2014). Moreover, NDUFS6, C7ORF55, and FASTKD1 were validated as novel mitochondrial nucleoid proteins using peroxidase-catalysed proximity biotinylation, APEX (Han et al., 2017). Nucleoids are thus places of initial processing of mtRNA and ribosome assembly (Bogenhagen et al., 2014). Other particles containing RNAs and RNA-binding proteins are RNA granules in close proximity to mitochondrial nucleoids. These are centres for posttranscriptional RNA processing and ribosome biogenesis (Antonicka and Shoubridge, 2015).

Each molecule of mtDNA is composed of heavy (H) and light (L) strand. Most of genes are encoded on the H-strand of mtDNA, eight tRNAs and one polypeptide are encoded by the L-strand. Mitochondrial genome is highly compact and lacks introns. The mtDNA molecules have a small non-coding region controlling mtDNA expression that contains the origin of leading H-strand replication and main promoters for transcription. It forms a triplex structure known as a displacement loop (D-loop). L-strand also contains a single promoter region for transcriptional initiation (Falkenberg et al., 2007) (Figure 2).

The human mtDNA is replicated by DNA polymerase γ (POLG) with help of additional components of mtDNA replication machinery, which are topoisomerase, Twinkle mtDNA helicase, mitochondrial RNA polymerase, RNaseH1, mitochondrial single-stranded DNA-binding protein and mitochondrial DNA ligase III. The replication mechanism of mtDNA

is still not fully understood. mtDNA is replicated most likely according to the strand-displacement model (Young and Copeland, 2016).

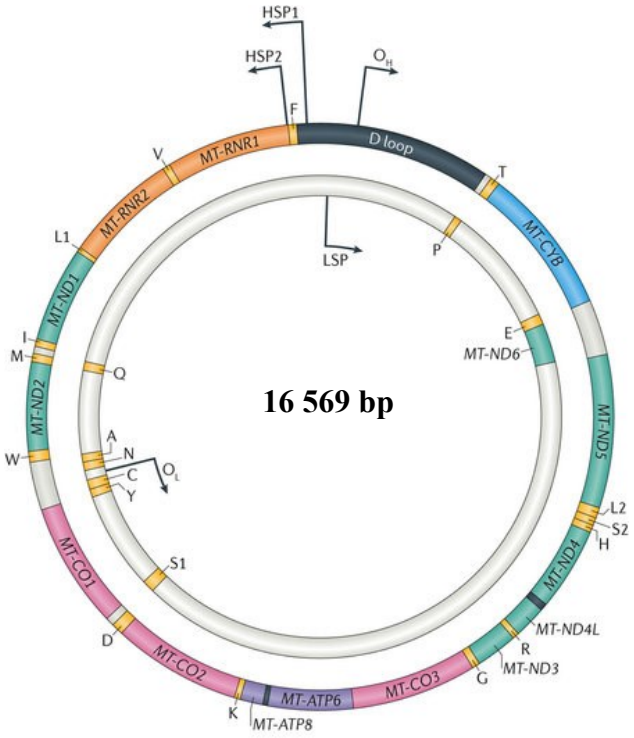

Figure 2. Structure of the human mitochondrial genome. *Human molecular genome is circular, double stranded DNA molecule. It is composed of heavy (H) and light (L) strand. H-strand includes a 1.1-kb non-coding region called displacement loop (D-loop) on heavy strand containing origin for transcription (O_H) and replication (HSP) of mtDNA. The L-strand also contains origin for its replication (O_L) and transcription (LSP). mtDNA encodes 2 rRNA, 22 tRNAs, and 11 mRNAs for 13 proteins of respiratory complexes. Single letters (Q, L) indicate tRNA gene. Adopted and modified from (Gorman et al., 2016).*

Moreover, mtDNA RNA polymerase (POLRMT), which has promoter binding specificity and catalytic polymerase activity, is responsible for mtDNA transcription (Gaspari et al., 2004). TFAM (Shi et al., 2012), mitochondrial transcription factors B1 and B2 (Falkenberg et al., 2002) and mitochondrial transcription elongation factor (TEFM) (Minczuk et al., 2011) are also required for efficient transcription. Transcription produces polycistronic precursor RNAs, which are processed to individual mRNAs, rRNAs and tRNAs by a protein-only RNase P complex (Holzmann et al., 2008) and ELAC2 (Brzezniak et al., 2011) associated with nucleoids (Bogenhagen et al., 2014). Produced RNAs (except ND6 mt-mRNA) undergo post-transcriptional modifications. The only known modification

of mt-mRNAs is the addition of a poly(A) tail catalysed by mitochondrial poly(A) polymerase (mtPAP) (Tomecki et al., 2004).

The 13 mitochondrial genes encode seven complex I subunits (ND1-ND6, ND4L), cytochrome b, three complex IV subunits (COXI-III) and two subunits of the F_o part of ATP synthase (ATP a and A6L) (Falkenberg et al., 2007). They are translated on mitochondrial ribosomes (mitoribosomes) composed of a 39S large (mt-LSU) and 28S small (mt-SSU) subunits, which are complexes of mitoribosomal proteins (MRPs) encoded in nucleus and a catalytic 12S mt-rRNA and 16S mt-rRNA. The initiating codons recognised by the mitoribosome are AUG, AUA and AUU, to which f-Met-tRNAMet is recruited. Termination codons are UAA and UAG (Mai et al., 2017).

The remaining respiratory chain subunits and all other proteins required in mitochondria (for example proteins of Krebs cycle, protein import, fatty and amino acid oxidation, apoptosis, biosynthesis of ketone bodies, pyrimidines, haem and urea) are encoded in a cell nucleus and translated in cytoplasm. Transcription of respiratory genes is regulated by nuclear regulatory factors NRF-1, NRF-2 and ERRα and their co-activators PGC-1a, PGC-1b, and PRC (Scarpulla, 2006). Synthesised protein precursors are imported into mitochondria by specialised transporters that recognize signal of mitochondrial targeting sequence, which specifies distribution of protein precursors to OMM, IMM, IMS or matrix. Major protein import pathways to mitochondria are through the channel of TOM protein complex and through TIM23 to matrix or TIM22 translocase to IMM (Wasilewski et al., 2017). To avoid accumulation of unfolded proteins in mitochondria, the crosstalk between mitochondria and nucleus is important. It is triggered by the mitochondrial unfolded protein response (UPRmt), which regulates transcription of mitochondrial proteins but its signalling mechanism in mammals remains still unclear (Wasilewski et al., 2017).

Expression of mitochondrial proteins is regulated in dependency on tissue energy demands. It is controlled not only by previously mentioned factors but also by mtDNA copy number, which is supposedly controlled by nuclear encoded Twinkle helicase (Tyynismaa et al., 2004, Milenkovic et al., 2013).

1.2.2 Mitochondrial protein databases

Knowledge of the mitochondrial proteome is essential for studying mitochondrial functions and diseases. It has been estimated that the mammalian mitochondrial proteome consists of ~1500 distinct proteins (Calvo and Mootha, 2010). There have been several efforts to establish such an inventory as a universal tool for mitochondrial biology researchers. However, not a single method can identify all mitochondrial proteins, therefore solid inventories depend on integrative approaches. The most common strategies are searching for mitochondrial targeting sequences, mass spectrometry (MS)-based proteomics, microscopy, and analysis of sequence homology. One of the prominent inventories MitoCarta database was compiled in 2008. It includes 1013 human genes and 1098 mouse genes and was assembled as inventory using multiple experimental and computational approaches (Pagliarini et al., 2008). Mitochondria were isolated and purified from 14 mouse tissues to identify enriched mitochondrial proteins by in-depth mass spectrometry. In addition to the MS, GFP epitope tagging followed by microscopy, literature curation and several *in silico* sequence analyses were integrated using Bayesian algorithms. In 2015, MitoCarta inventory was updated to MitoCarta 2.0 containing 1158 human genes and 1158 mouse genes encoding for mitochondrial proteins (Calvo et al., 2016) and then updated yet again to MitoCarta+ (1166 human mitochondrial proteins) (Floyd et al., 2016).

Similar database to MitoCarta is Integrated Mitochondrial Protein Index (IMPI) developed using machine learning to predict mitochondrial protein localisation in human, mouse, rat and cow. IMPI version Q3 2017 contains 1550 human genes encoding proteins localised in mitochondria - 1130 known to be mitochondrial and 420 predicted to be mitochondrial using the evidence in MitoMiner (Smith and Robinson, 2016). MitoMiner (http://mitominer.mrc-mbu.cam.ac.uk) is an integrated web resource of mitochondrial localisation evidence and phenotype data for mammals, zebrafish and yeasts. It comprises number of sources including both MitoCarta and IMPI reference sets, the Human Protein Atlas (Uhlen et al., 2015), mitochondrial targeting sequence prediction tools (iPSORT, MitoProt, TargetP, MitoFates) and many others.

The Gene Ontology (GO) database is a relational database comprised of the Gene Ontology ontologies (Cellular Component, Biological Process, Molecular Function) as well as the annotations of genes and gene products to terms in those ontologies. Major model organism databases and other bioinformatics resource centres contribute to the project that is maintained and annotated by the Gene Ontology Consortium and is available at geneontology.org (Gene

Ontology, 2008). Gene Ontology term Mitochondrion (Cellular Component, GO:0005739) 1647 human mitochondrial genes are found in this database.

The overlap of mitochondrial entries in IMPI, MitoCarta2.0 and Gene Ontology Database is shown in Figure 3.

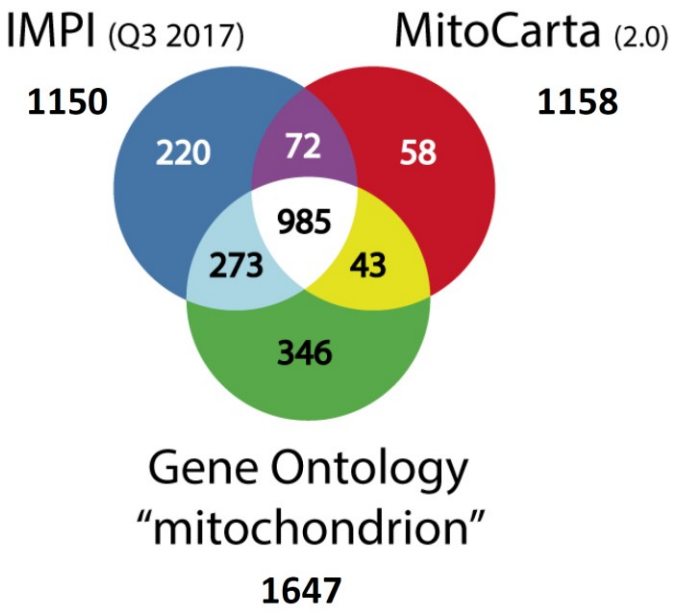

Figure 3. Overlap of mitochondrial protein databases. *Integrated Mitochondrial Protein Index (IMPI) is collection of 1550 genes encoding proteins with strong evidence for cellular localisation within the mammalian mitochondrion (human, mouse, rat and cow). MitoCarta2.0 is an inventory of 1158 human and mouse genes encoding proteins with strong support of mitochondrial localisation. 1647 human mitochondrial genes were found in Gene Ontology (GO) database. Adopted and modified from www.mrc-mbu.cam.ac.uk/impi (THE MITOCHONDRIAL PROTEOME (IMPI).*

1.3 Oxidative phosphorylation system

OXPHOS and TCA cycle are key metabolic pathways in mitochondria. OXPHOS is composed of five protein complexes I-V designated as CI, CII, CIII, CIV, CV (ATP synthase), then two mobile electron carriers [(coenzyme *Q* (Co*Q*) and cytochrome c]. OXPHOS complexes are localised in the IMM and formed by proteins coded by 13 mitochondrial genes and at least 77 nuclear genes (Calvo and Mootha, 2010).

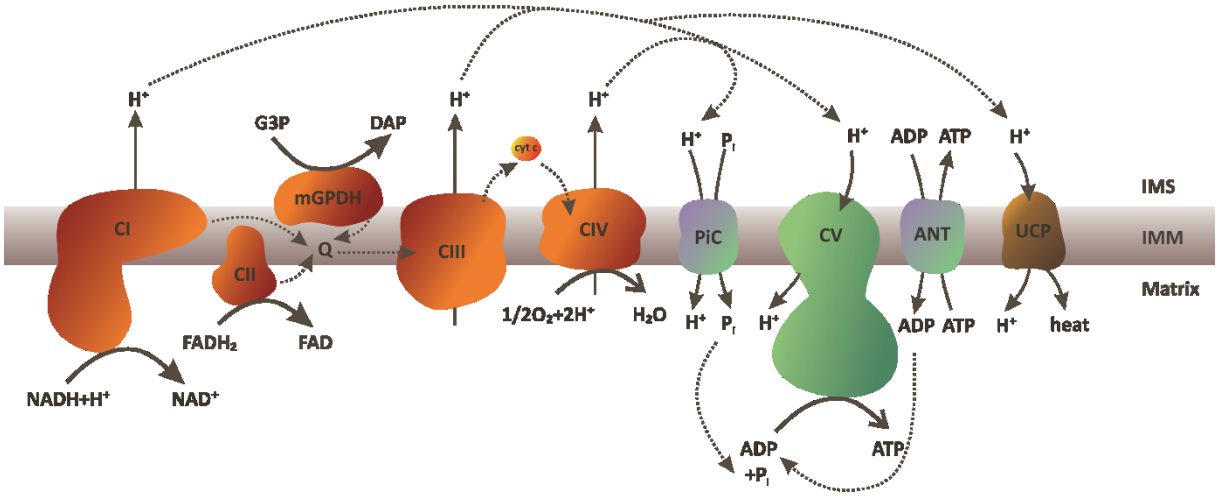

Figure 4. Oxidative phosphorylation system (OXPHOS). *The key components of the OXPHOS are four complexes of respiratory chain (CI–CV) and ATP synthase (CV). Other source of electrons is mitochondrial glycerol-3 phosphate dehydrogenase (mGPDH) that oxidizes glycerol-3-phosphate (G3P) to dihydroxyacetone phosphate (DAP). Essential for ATP production by ATP synthase are also ADP/ATP translocase (ANT) and inorganic phosphate carrier (PiC). Proton gradient is also used by uncoupling proteins (UCP), e.g. UCP1 present in mitochondria of brown adipose tissue. IMS – intermembrane space, IMM – inner mitochondrial membrane.*

1.3.1 Respiratory chain

Mitochondrial respiratory chain (RC) is composed of complexes CI-CIV (Table 1) which transport electrons from reduced coenzymes NADH and $FADH_2$ to molecular oxygen reducing it to H_2O. RC has also other sources of electrons such as glycerol-3 phosphate dehydrogenase, especially in brown adipose tissue, electron-transferring flavoprotein dehydrogenase (ETF:Q) and dihydroorotate dehydrogenase (Nicholls and Ferguson, 2013). Electrons entering OXPHOS originate from metabolised sugars and lipids through a series of reactions such as glycolysis, β-oxidation and TCA cycle.

Table 1. *Mammalian complexes I-IV of respiratory chain and their properties including catalytic function, total number of subunits, subunits encoded by mtDNA, molecular weight of whole complex, prosthetic groups and number of known factors necessary for complex assembly.*

	CI	CII	CIII	CIV
	NADH dehydrogenase	Succinate dehydrogenase	Cytochrome bc_1 complex	Cytochrome *c* oxidase
Catalytic function	NADH:ubiquinone oxidoreductase EC 1.6.5.3	succinate:ubiquinone oxidoreductase EC 1.3.5.1	ubiquinol: ferricytochrome *c* oxidoreductase EC 1.10.2.2	ferrocytochrome *c*: oxygen oxidoreductase EC 1.9.3.1
Number of subunits (mtDNA encoded)	45 (7)	4 (0)	11 (1)	13 (3)
Molecular weight (kDa)	~1000	~130	~240	~20
Prosthetic groups	FMN, 8 [Fe-S] clusters	FAD, 3 [Fe–S] clusters, haem *b*	haem *b* and c_1, 2 [Fe–S]	Haem *a* and a_3, Cu_A, Cu_B
Assembly factors	13	4	6	>20
References	(Sanchez-Caballero et al., 2016, Wirth et al., 2016)	(Bezawork-Geleta et al., 2017)	(Schagger et al., 1986, Iwata et al., 1998, Fernandez-Vizarra and Zeviani, 2015)	(Tsukihara et al., 1996, Kadenbach and Huttemann, 2015)

These electrons are transported through complexes of RC containing prosthetic groups serving as electron carriers (Figure 4). According to chemiosmotic theory, transport of electrons through CI, CIII, and CIV is coupled with transmembrane proton pumping from matrix across IMM into IMS contributing to proton gradient (ΔpH) required for ATP generation by F_1F_o-ATP synthase (also complex V, CV) (Mitchell, 1961). Proton gradient as well as other concentration gradients across IMM are utilised by many membrane transporters. They transport ions, metabolites and other molecules across the IMM. For example, ADP/ATP translocase (ANT) and inorganic phosphate carrier (PiC) transport substrates for ATP synthesis into mitochondrial

matrix. Some transporters can be specialised as for example, uncoupling proteins (UCP – Figure 4) (Nelson and Cox, 2017).

Complexes of RC require ancillary factors, which have a function in assembly, stabilisation of subunits or complex intermediates, insertion of prosthetic groups, or other, yet unidentified, functions. Mutations in these factors may cause severe diseases (Fernandez-Vizarra and Zeviani, 2015, Kadenbach and Huttemann, 2015, Sanchez-Caballero et al., 2016, Bezawork-Geleta et al., 2017).

Furthermore, respiratory complexes form higher structures termed 'supercomplexes'. In mammalian mitochondria, supercomplexes were observed in stoichiometry of $CI/CIII_2/CIV_{1-4}$, $CI/CIII_2$, and $CIII_2/CIV_{1-2}$. Their function remains unclear but it is generally assumed that they facilitate substrate channelling (Milenkovic et al., 2017).

1.3.2 ATP synthase

Mitochondrial ATP synthase (F_1Fo-ATP synthase Complex V, CV, EC 3.6.3.14) is IMM multiprotein complex of the molecular weight of ~650 kDa. It is the main producer of ATP in cells in the process of oxidative phosphorylation.

1.3.2.1 Structure of ATP synthase

Mammalian ATP synthase is composed of 18 different subunits (α_3, β_3, γ, δ, ε, a, b, c_8, d, e, f, g, F_6, A6L, OSCP, IF1, MLQ a DAPIT), some of them present in multiple copies per holoenzyme. Enzymatic complex can be subdivided into several functional domains: globular catalytic F_1 part, proton translocating membrane F_o part of ATP synthase (named according to sensitivity to oligomycin) and two connecting central and peripheral stalks (Figure 5) (Ackerman and Tzagoloff, 2005, Wittig and Schagger, 2008, Walker, 2013). Crystal structure of bovine mitochondrial F_1-ATPase was firstly determined at 2.8 Å resolution in 1994 (Abrahams et al., 1994). F_1 part is oriented to the matrix and is composed of $\alpha_3\beta_3$ hexamer and central stalk subunits γ, δ and ε. Central stalk is connected to the membrane F_o part formed by c-subunit oligomer (c-ring) and a, e, f, g, A6L and b. Subunit b together with subunit d, F_6 and OSCP forms peripheral stalk. Two of the F_o subunits, a and A6L are encoded by mtDNA (Anderson et al., 1981, Fearnley and Walker, 1986), while the other subunits are encoded by nDNA. IF1 subunit is a small regulatory subunit connected with F_1 part at low pH and prevents switching the ATP synthase to its hydrolytic mode. Interestingly, its premature form binds only to monomeric ATP synthase while mature IF1 only to dimeric or multimeric ATP synthase (Wittig et al., 2010). Finally, new accessory subunits of ATP synthase identified

in the membrane-embedded F_o domain are DAPIT and MLQ (6.8 kDa proteolipid) but their exact placement and function in the complex are not yet known (Chen et al., 2007, Meyer et al., 2007).

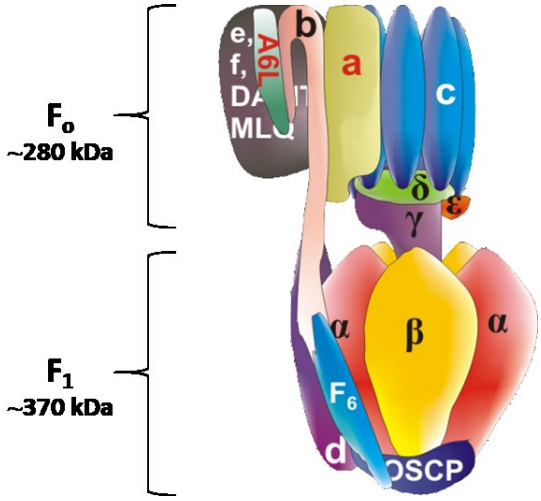

Figure 5. Structure of ATP synthase. *Mammalian ATP synthase is divided into catalytic F_1 and membrane F_o and two stalks together composed by 18 different subunits. F_1 moiety is composed of $\alpha_3\beta_3$ hexamer, central stalk of γ, δ and ε subunits, F_o part contains a, e, f, g, A6L and b, which is shared with peripheral stalk. Peripheral stalk includes also d, F_6 and OSCP. Moreover, DAPIT and MLQ are associated with ATP synthase (Hejzlarova et al., 2014).*

ATP synthase can also form higher structure entities, namely dimers, oligomers and specific interactions with other proteins (Seelert and Dencher, 2011). Subunits DAPIT and MLQ, probably play a role in ATP synthase dimerization (Wittig and Schagger, 2008). These two subunits are extra in mammals (Chen et al., 2007). On the other hand, mammals lack subunits i/j, k, l, which are present in ATP synthase of *Saccharomyces cerevisiae* and i/j, k, e together with subunit a form the dimerization surface in yeast (Guo et al., 2017). Dimerization in mammals can be also regulated by coupling factor B (Belogrudov, 2002, 2010). It was also shown in yeasts (Davies et al., 2012, Hahn et al., 2016) and mammals (Strauss et al., 2008) that ATP synthase dimer formation is essential for mitochondrial cristae modulation. Moreover, dimerization can also optimise ATP synthase performance (Strauss et al., 2008). Two monomers interact via F_o part of ATP synthase involving subunits a, e, g, b and A6L (Wittig and Schagger, 2008, Wittig et al., 2010). One of the higher structures, in which is ATP synthase involved, is ATP synthasome. It is proposed that this supramolecular structure is composed of ATP synthase, ADP/ATP translocase (ANT) and inorganic phosphate carrier (PiC). As ATP synthase needs adenosine diphosphate (ADP) and inorganic phosphate for ATP production,

it may function as catalytic unit. It was originally reported in rat liver (Ko et al., 2003, Chen et al., 2004) but also later in bovine heart (Murray et al., 2004, Wittig and Schagger, 2008, Seelert and Dencher, 2011). Still, a little is known about its relative abundance in comparison with free forms of its components, its stoichiometry or regulation of ATP synthasome biogenesis.

Both ANT and PiC do have several tissue specific isoforms. PiC has two isoforms: PiC-A isoform (a heart-type isoform) is highly abundant in heart and skeletal muscle whilst PiC-B isoform (a liver-type isoform) is expressed ubiquitously (Fiermonte et al., 1998). Human isoforms are encoded by just one gene (SLC25A3) and generated by alternative splicing of exon IIIA or exon IIIB which differs in 13 amino acids (Dolce et al., 1994).

Four isoforms of ANT have been identified in human genome (Dahout-Gonzalez et al., 2006). ANT1 (*SLC25A4*, heart-type isoform) is specific to heart and skeletal muscle, ANT2 (*SLC25A5*, liver-type isoform) is expressed ubiquitously and ANT3 (*SLC25A6*) is expressed in highly proliferative cells and tissues (Stepien et al., 1992). The fourth isoform, ANT4 (*SLC25A31*, testes-specific isoform), is predominantly detected in human liver, testis and brain (Dolce et al., 2005). Only three isoforms encoding ADP/ATP carriers have been identified in rodents (ANT1, ANT2, ANT4), the fourth isoform ANT3 is present only as pseudogene (Dahout-Gonzalez et al., 2006).

It has also been reported in rat liver that ATP synthasome is a part of the larger complex, which also includes succinate dehydrogenase and mitochondrial ATP-binding cassette protein 1. (Ardehali et al., 2004). Moreover, it was proposed that ATP synthasome, mitochondrial creatine kinase, VDAC and tubulin form mitochondrial interactosome (Timohhina et al., 2009).

1.3.2.2 Assembly of ATP synthase

Biogenesis of ATP synthase is a complex process not fully understood so far (Figure 6). Current knowledge of ATP synthase assembly is mainly based on the yeast model of *Saccharomyces cerevisiae* (Ackerman and Tzagoloff, 2005, Rak et al., 2009, Rak et al., 2011, Ruhle and Leister, 2015). Biogenesis proceeds via several modules. It starts with the independently assembled soluble F_1 module (α_3, β_3, γ, δ and ε). The second assembly module is the c-ring representing the first intermediate in F_o assembly. Assembled F_1 module binds via the stalk subunits to the c-oligomer, independently of other F_o subunits, to form a larger ATP synthase intermediate. Then subunits of peripheral stalk (b, d, F6 and OSCP) and other membrane subunits of F_o (e, f, g, DAPIT, MLQ) are added (Hejzlarova et al., 2014).

Using mtDNA depleted mammalian cell, it was shown that the two last added subunits are a and A6L (Wittig et al., 2010).

ATP synthase biogenesis is assisted by numerous auxiliary factors. Most of them are yeast specific (Ackerman and Tzagoloff, 2005, Hejzlarova et al., 2014, Ruhle and Leister, 2015) and have several different functions. In F_o biogenesis, Aep1p, Aep2p and Atp25p are needed for efficient expression of subunit c, which is in yeasts encoded by mtDNA, and c-ring formation. Additionally, Atp22p promotes synthesis of subunit a and Oxa1p stabilises subunit a association with c-ring. Other factors playing role in F_o assembly are Atp23p, Mia40 and ATP10p. F_1 biogenesis requires Atp11p, Atp12p, Fmc1p and Hsp90 chaperones. Finally, central stalk biogenesis and F_1F_o assembly are assisted by Ina17 and Ina22 factors (Ruhle and Leister, 2015). Most of these factors are not present in mammalian cells, because their functions are not needed. Thus, only three factors are conserved between yeast and humans - ATPAF1 (Atp11p), ATPAF2 (Atp12p) important in the $\alpha_3\beta_3$ hexamer formation of F_1 part of ATP synthase (Wang et al., 2001) and partial homolog of Atp23p (Osman et al., 2007, Zeng et al., 2007). Moreover, new assembly factor TMEM70 specific for mammals has been described in humans (Cizkova et al., 2008).

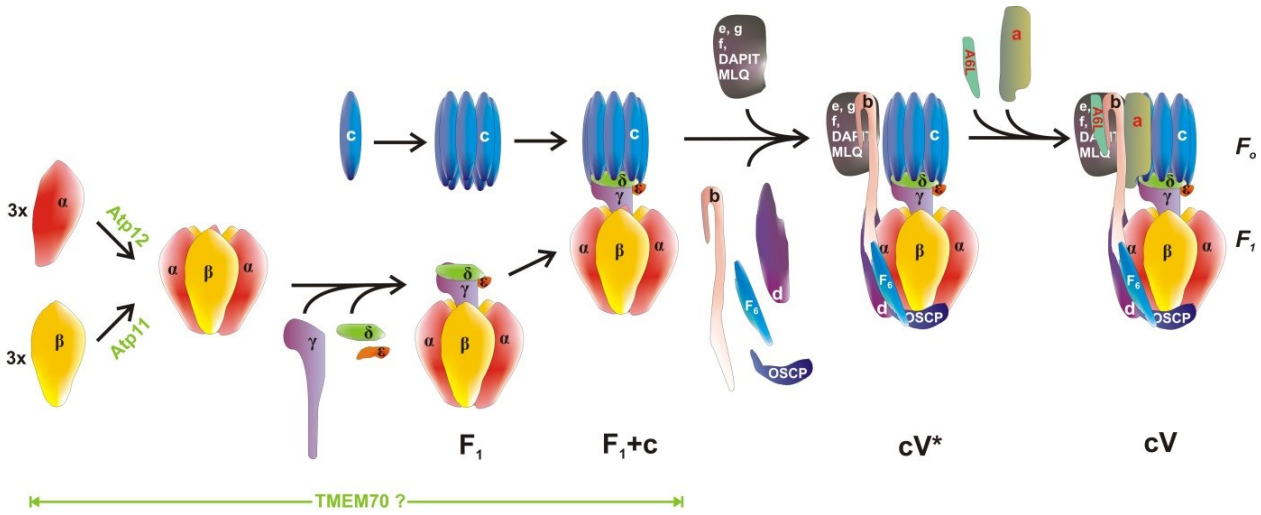

Figure 6. Scheme of ATP synthase assembly. *Mitochondrial ATP synthase assembly starts with the formation of $\alpha_3\beta_3$ hexamer to which subunits γ, δ and ε of the central stalk are added. Assembled F_1 module binds via the stalk subunits to the c-oligomer and it is followed by addition of other F_o subunits (e, f, g, DAPIT, MLQ) and peripheral stalk (b, d, F6 and OSCP) forming cV*. Two last added subunits forming complete cV are a and A6L which are encoded by mtDNA. Assembly factors Atp11 and Atp12 are involved in $\alpha_3\beta_3$ hexamer formation. The role of TMEM70 assembly factor is proposed in early steps of ATP synthase biogenesis. Adopted from (Hejzlarova et al., 2014).*

1.3.2.3 Function of ATP synthase

ATP synthase operates as a molecular motor which utilises proton gradient across the inner mitochondrial membrane. The term proton motive force (pmf, Δp) was first used by Peter Mitchel who proposed that Δp drives the ATP synthase to produce ATP from ADP and Pi (Mitchell, 1961). The protons pass IMM and drive c-oligomer rotation which is transmitted by the central stalk to the catalytic F_1 part which changes conformation of $\alpha_3\beta_3$ hexamer in cycles (Walker, 2013). Subsequently the ADP, Pi and ATP binding-change mechanism on ATP synthase results in ATP production (Boyer, 1975). During one c-oligomer rotation, γ subunit turns 360° taking each β subunit through three states (β_{TP}, β_{DP} and β_E). These three states have different affinity for nucleotides. β_E-site is closed (empty) when binding ADP and phosphate, ATP is formed at β_{DP}-site and is released from β_{TP}-site as it opens and converts back to β_E-site (Abrahams et al., 1994). In the end of one cycle three molecules of ATP are produced per three β subunits. Effectivity of the enzyme is dictated by the number of protons, translocated from IMS to matrix, required for a full rotation of γ subunit. This is in turn defined by a number of c subunits forming the ring in any respective species. Most effective in this regard is the mammalian enzyme, in which c-oligomer is composed of 8 c subunits (Walker, 2013). For uncovering the mechanisms behind the synthesis of ATP, Paul D. Boyer and John E. Walker were awarded the Nobel prize in chemistry.

The detailed mechanism, how protons pass through the IMM, has been extensively studied. It has been proposed that protons from intermembrane space pass across membrane between subunits a and c (Walker, 2013). It was predicted that it occurs through two half channels, one opened into IMS and the second into matrix (Vik and Antonio, 1994, Junge et al., 1997), which were recently observed by cryo-electron microscopy on yeast (Guo et al., 2017), bovine (Zhou et al., 2015) and alga *Polytomella* (Allegretti et al., 2015, Klusch et al., 2017) F-ATP synthase. The yeast and bovine a subunit consists of five transmembrane α helixes and one amphipathic α helix along the plane of membrane surface. Two of α helixes are tilted and tightly in contact with the c-ring (Zhou et al., 2015, Guo et al., 2017) (Figure 7). This model is similar to that in alga *Polytomella* (Allegretti et al., 2015, Klusch et al., 2017). Also, subunit b seems to form the IMS half channel together with subunit a. According all these observations, the model of proton translocation was proposed (Figure 7). The proton entering half-channel from IMS neutralizes glutamate residue of the c subunit, which can enter hydrophobic environment of the membrane and c-ring rotate because of Brownian motion (Vik and Antonio, 1994, Junge et al., 1997). In the matrix half-channel, the proton is bound by conserved arginine of subunit a and then is lost into the matrix. It was also suggested that protonated glutamate

enters hydrophobic environment of lipid bilayer in locked conformation that is changed into open conformation in hydrophilic environment (Pogoryelov et al., 2010).

In anoxic conditions, ATP synthase can reverse its function and hydrolyse ATP. Produced energy drives c-ring in counter clockwise direction and pumps protons to the outward site of IMM leading to formation of $\Delta\Psi_m$ (Walker, 2013).

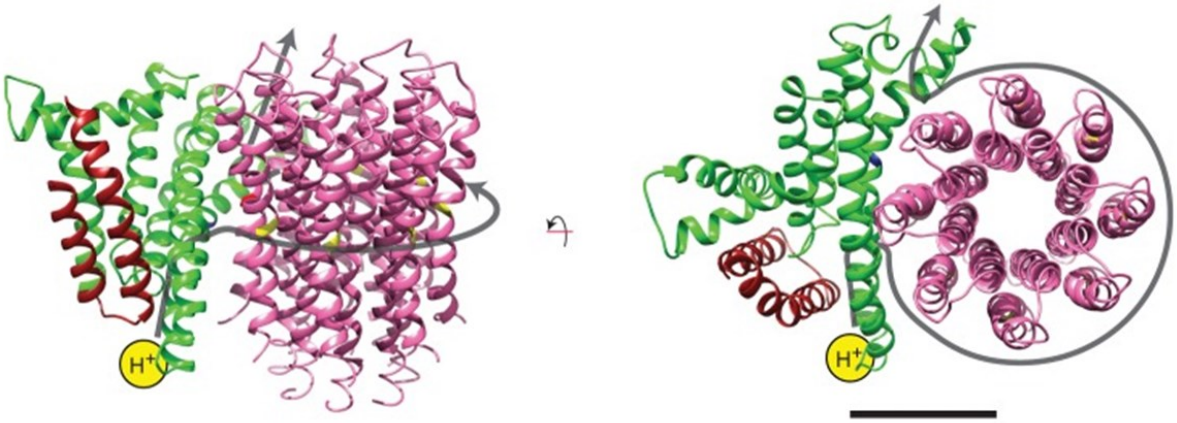

Figure 7. Model of proton translocation through mammalian F-type ATP synthase. *Membrane intrinsic helix hairpins of subunit a (green), subunit b (red) and c8-oligomer (pink) in bovine F_1F_o ATP synthase. Protons (yellow) reach the aqueous half-channel in intermembrane space of mitochondria formed by subunits a and b. When the c-subunit with proton approaches the hydrophilic half-channel on the matrix side, the proton can escape into the matrix. Scale bar, 25 Å. Adopted from (Zhou et al., 2015).*

1.3.3 Mitochondrial diseases and therapy

Mitochondrial diseases are biochemically characterised by the defect of oxidative phosphorylation. It can lead to the serious dysfunctions of tissues with high energy demands such as heart, muscle and brain. In addition, liver, pancreas, kidney and bone marrow can be affected as well. Mutations causing diseases of mitochondrial respiratory chain have been described in number of structural genes including all mtDNA genes (Dimauro and Davidzon, 2005, Calvo and Mootha, 2010, Gorman et al., 2016, Frazier et al., 2017). When OXPHOS is defective, mitochondrial energy provision is insufficient. The estimated prevalence of mitochondrial diseases varies between countries and studies but recent estimate based on large cohort gives it as approximately 20 cases per 100000 individuals (Gorman et al., 2015, Gorman et al., 2016). Mitochondrial diseases have usually very severe impact. At present, however, patients depend only on symptomatic treatments to alleviate complications. The development of new targeted therapies is still in the beginning. Nevertheless, a few

promising approaches already exist, for example gene therapy in LHONs, heteroplasmy shifting or liver transplants (Gorman et al., 2016, Viscomi, 2016). In the case of mtDNA encoded diseases, novel reproductive technologies called mitochondrial replacement therapy may represent effective treatments. Here, during in vitro fertilisation enucleated egg with mitochondria is donated to a women who has a high risk of mutated heteroplasmic mtDNA transmission to a child (Craven et al., 2017).

First mutations in mtDNA that cause maternally inherited diseases were reported in 1988 (Holt et al. 1988). Hundreds of mtDNA mutations are listed in MITOMAP inventory, (Ruiz-Pesini et al., 2007)]. The majority of mtDNA mutations are heteroplasmic which means a mixture of wildtype and mutated mtDNA inside of the cell. Typically, >50 % of mutated mtDNA are required to result in cellular defect (Gorman et al., 2016).

The first identified mutation in nDNA gene causing defect in OXPHOS was in *SDHA* encoding CII subunit (Bourgeron et al., 1995). The number of mutations in nuclear genes causing mitochondrial diseases is still increasing. Affected genes are not only these coding proteins of OXPHOS but can also be proteins with other functions, e.g. in mtDNA maintenance and expression, transport of molecules across membranes, metabolic pathways, mitochondrial fusion and fission, membrane dynamics or function as structural proteins (Vafai and Mootha, 2012, Gorman et al., 2016, Frazier et al., 2017).

As of November 23 2017, 289 mitochondrial disease genes have been identified (35 mtDNA encoded genes and 254 nuclear encoded disease genes), which account only for ~60 % of patients with suspected mitochondrial diseases (Frazier et al., 2017).

To the group of most severe metabolic disorders belong inborn defects of ATP synthase. They are manifested by encephalocardiomyopathies and predominantly affect the paediatric population (Houstek et al., 2006). Isolated ATP synthase defects can be caused by mutations in mtDNA (Holt et al., 1990) or nDNA (Houstek et al., 1999).

1.3.3.1 ATP synthase defects of mtDNA origin

Two subunits of ATP synthase are encoded by mtDNA. Mutations in mtDNA gene *MT-ATP6* for subunit a manifest mainly as NARP syndrome (neuropathy, ataxia and retinis pigmentosa) or maternally inherited Leigh syndrome (MILS) (Baracca et al., 2007). On the other hand, less common mutations in the gene *MT-ATP8* for A6L subunit manifested with hypertrophic cardiomyopathy (Jonckheere et al., 2008). In these cases, the function of F_o proton

channel, ATP synthase stability or protein-protein interactions can be affected. Nowadays, mtDNA mutations are routinely scanned and diagnosed.

1.3.3.2 ATP synthase defects of nDNA origin

The first case of ATPase deficiency with no mutation in mtDNA genes and possible nuclear origin was found in 1992. The child suffered with persistent 3-methylglutaconic aciduria (3-MGA), severe neonatal lactic acidosis (LA) and hypertrophic cardiomyopathy. The ATPase activity was very low and respiratory rate was low and tightly coupled in muscle mitochondria. Also mitochondria with ultrastructural abnormalities were observed (Holme et al., 1992).

Later in 1999, mitochondrial disorder of nuclear origin (OMIM 604273) caused by isolated ATP synthase deficiency was described in a patient with the fatal neonatal cardiomyopathy (Houstek et al., 1999). This child suffered with severe LA, cardiomegaly, and hepatomegaly and died 2 days after birth. The ATP synthase amount decreased to the 30 % of enzyme content in controls. The similar type of defect was found in other patients (Mayr et al., 2004, Sperl et al., 2006, Hejzlarova et al., 2014, Magner et al., 2015). Isolated deficiency of ATP synthase is autosomal hereditary mitochondrial disease which affects children and has fatal consequences (Houstek et al., 2006). Lower amount of ATP synthase causes insufficient ATP production and increased production of reactive oxygen species (ROS). It leads to damage of tissues with high energy demands such as heart, skeletal muscle and brain (Houstek et al., 2004, Mracek et al., 2006). Most of patients suffer from neonatal lactate acidosis, 3-methyl glutaconic aciduria, hypertrophic cardiomyopathy and central nervous system disorder (Sperl et al., 2006, Magner et al., 2015). Although each symptom is treated by supportive treatment, there is a need of causal therapy approach, which is still not available.

1.3.3.2.1 Nuclear genes mutations causing ATP synthase deficiency

Mutations in *ATP5A1* (Jonckheere et al., 2013) and *ATP5E* (Mayr et al., 2010) coding, respectively, subunits α and ε of F_1 moiety of ATP synthase were identified in patients with isolated ATP synthase deficiency. As was previously shown in ε subunit knockdown in HEK293 cells, mitochondrial content of assembled ATP synthase is decreased and this leads to the accumulation of c subunit (Havlickova et al., 2010). In addition, mutations of genes linked to ATP synthase biogenesis - *ATP12* (De Meirleir et al., 2004) and *TMEM70* (Cizkova et al., 2008) were also identified. Mutations in *TMEM70* are more common in comparison with

rare in *ATP5A1*, *ATP5E* or *ATP12* (see Table 2). All these mutations share a similar biochemical phenotype with distinct decrease of fully assembled and functional ATP synthase, yet differ in molecular mechanism, incidence and pathogenic effect on patients.

All these mutations commonly cause the inability of ATP synthase to utilise membrane potential ($\Delta\Psi_m$) for ATP production. Subsequently it leads to stimulation of mitochondrial ROS production (Baracca et al., 2007, Cizkova et al., 2008). Therefore, energy deprivation together with oxidative stress represents key factors in the pathogenesis of isolated defects of ATP synthase (Mracek et al., 2006).

1.3.3.3 Link between genotype and phenotype in ATP synthase disorders

The phenotypic presentation of mitochondrial diseases is highly variable in mitochondrial genetic defects and pathology can manifest only when a threshold level is exceeded. Rossignol et al. demonstrated that ATP synthase can be inhibited by oligomycin up to critical value without affecting the rate of mitochondrial respiration or ATP synthesis until threshold level is exceeded as shown in rats (Rossignol et al., 2000, Rossignol et al., 2003). In this regard, it is interesting that in patients with pathological manifestation, levels of ATP synthase ranging between 30 and 10 % of controls can be observed (Houstek et al., 2006). This suggests existence of spare capacity for ATP synthase. In control cells/tissues, it remains unclear, where lies the true threshold of ATP synthase defects required to trigger pathology.

1.3.4 New proteins involved in biogenesis and structure of ATP synthase

1.3.4.1 TMEM70 protein

In 2006, TMEM70 was identified by integrative genomics as a potential gene coding for mitochondrial protein of unknown function and its GFP tagged form was localised in mitochondria (Calvo et al., 2006). *TMEM70* gene is located on chromosome 8 and encodes 260 amino acids precursor, which has together with mitochondrial N-terminal importing sequence molecular weight of 29 kDa. Processed TMEM70 is transmembrane protein of inner mitochondrial membrane, which has 179 amino acids and molecular weight of 21 kDa (Hejzlarova et al., 2011). It contains conserved DUF1301 domain and two potentially transmembrane regions (Hejzlarova et al., 2011). Both 21 amino acid long N-terminal and 98 amino acid long C-terminal sequences are exposed into mitochondrial matrix (Jonckheere et al., 2011, Kratochvilova et al., 2014) (Figure 8). TMEM70 is present in considerably lower quantities than structural subunits, similarly to other ancillary factors (Hejzlarova et al., 2011). Its homologs were found in eukaryotes but not in yeasts and fungi (Cizkova et al., 2008, Houstek et al., 2009).

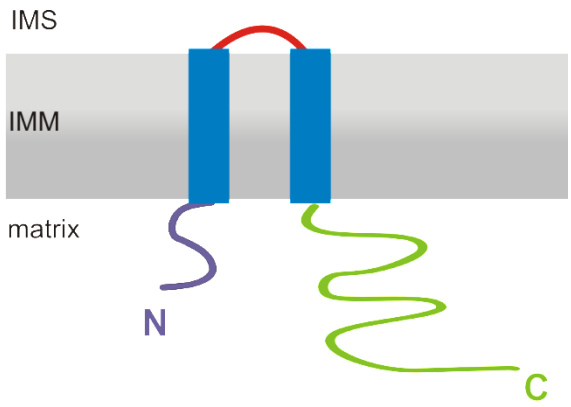

Figure 8. Structure and orientation of TMEM70 protein. *TMEM70 protein is localised in the inner mitochondrial membrane (IMM). C and N-terminal sequences are both oriented into the matrix. IMS - intermembrane space.*

Several dozens of cases with TMEM70 mutation were identified (Hejzlarova et al., 2014). These patients have isolated ATP synthase deficiency and are homozygous or compound heterozygotes (different mutations at each allele) of particular mutation.

The most common *TMEM70* mutation in patients is c317-2A>G in the second intron removing splicing side prior to the third exon. Very labile transcript is produced from this

mutant allele. ATP synthase from these patients is not fully assembled and F_1 subcomplex is accumulated but still the small amount of assembled and functional ATP synthase is present. Complementation of patient fibroblast cell lines restored biogenesis and function o ATP synthase (Cizkova et al., 2008). Up to now about 50 patients with this mutation were found (see Table 2). Patients often die during first few years and most often in the first months of life but 10-year survival rate is still 63 % (Magner et al., 2015). Critical for the patients is survival of the postnatal period, and many of the metabolic defects and cardiac disorder can improve thereafter (Honzik et al., 2010).

While the c317-2A>G mutation is relatively often associated with the Roma population (Wortmann et al., 2009, Honzik et al., 2010, Torraco et al., 2012, Stojanovic and Doronjski, 2013, Braczynski et al., 2015, Magner et al., 2015, Sarajlija et al., 2017), less common pathogenic mutations of this gene were found in other ethnical groups. For example, in Arab Muslims and Turkish families (see Table 2).

Recently new *TMEM70* mutation c.440T>C (p.I147T) has been identified in Asian population. Patient caring single mutant allele of this gene was without pathological effects. Other family members carrying this mutation in combination with mutations in other genes exhibited defective heart function. On the other hand, c.440T>C mutation did not have higher effect in cases of multiple mutations (Wang et al., 2016).

Table 2: ***Nuclear DNA mutations associated with isolated deficiency of ATP synthase.*** *Adapted and updated from (Hejzlarova et al., 2014).*

Gene	Mutation	Clinical phenotype	References
ATP5A1	c.985C>T missense (p.R329C) (c.–49+418C>T substitution)	Severe neonatal encephalopathy	(Jonckheere et al., 2013)
ATP5E	c.35A>G missense (p.Y12C)	Neonatal respiratory distress, LA, 3-MGA, severe peripheral neuropathy, exercise intolerance	(Mayr et al., 2010)
ATPAF2	c.280T>A missense (p.W94R)	3-MGA, LA, neonatal encephalopathy, dysmorphism	(De Meirleir et al., 2004)
TMEM70	c.317–2A>G splicing	IUGR, LA, HA, EOH, FD, HCMP, 3-MGA, cataract, encephalopathy, FTT, PMR, PAH	(Cizkova et al., 2008, Wortmann et al., 2009, Honzik et al., 2010, Tort et al., 2011, Torraco et al., 2012, Stojanovic and Doronjski, 2013, Catteruccia et al., 2014, Braczynski et al., 2015, Diodato et al., 2015, Magner et al., 2015, Sarajlija et al., 2017)
	c.317–2A>G/c.118_119insGT frameshift (p.S40CfsX11)	LA, 3-MGA, HA, HCMP, FD, PMR,	(Cizkova et al., 2008, Honzik et al., 2010, Cameron et al., 2011, Magner et al., 2015)
	c.317–2A>G/c.494G>A missense (p.G165D)	LA, 3-MGA, HA, HCMP, Reye-like syndrome, exercise intolerance	(Scaglia et al., 2002, Shchelochkov et al., 2010)
	c.336T>A nonsense (p.Y112X)	IUGR, LA, HA, HCMP, FD, PMR	(Spiegel et al., 2011, Magner et al., 2015)
	c.316+1G>T splicing	IUGR, Encephalopathy, HCMP, EOH, LA, FD	(Spiegel et al., 2011, Magner et al., 2015)
	c.238C>T nonsense (p.R80X)	IUGR, EOH, LA, 3-MGA, HA, HCMP, multiorgan failure, dysmorphism,	(Spiegel et al., 2011, Diodato et al., 2015, Magner et al., 2015)

	c.578_579delCA frameshift (p.N198X)	IUGR, EOH, LA, 3-MGA, FD, cataract, Encephalopathy, HCMP, PMR	(Spiegel et al., 2011, Magner et al., 2015)
	c.211–450_317–568del (2290bp deletion) frameshift	IUGR, HCMP, LA, 3-MGA, PMR	(Tort et al., 2011)
	g.2436–3789 in-frame deletion (1353bp)	IUGR, LA, HA, HCMP, PMR, ptosis	(Jonckheere et al., 2011)
	c.317–2A>G/c.628A>C missense (p.T210P)	HCMP, LA, 3-MGA, HA, PAH, WPW	(Torraco et al., 2012, Catteruccia et al., 2014, Magner et al., 2015)
	c.535C>T missense (p.Y179H)	IUGR, LA, EOH, FD, HCMP, bilateral cataract, PMR, HA	(Atay et al., 2013, Magner et al., 2015)
	c.317–2A>G/c.349_352del frameshift (p.I117A, p.224X?)	IUGR, LA, PMR, HCMP, EOH, dysmorphism, HA	(Diodato et al., 2015)
	c.317–2A>G/c.783A>G frameshift (p.X261Wext17)	IUGR, LA, PMR, HCMP, dysmorphism	(Diodato et al., 2015)
	c.701A>C missense (p.H234P)	IUGR, LA, 3-MGA, PMR, HCMP, HA, EOH, dysmorphism, leukoencephalopathy, PAH	(Catteruccia et al., 2014, Diodato et al., 2015)
	c.317–2A>G/c.251delC	Hypoglycemic seizures, epilepsy	(Magner et al., 2015)
	c.317–2A>G/c.470T>A	n.a.	(Magner et al., 2015)
	c.359delC	n.a.	(Magner et al., 2015)
	c.440T>C (p.I147T)	no pathological effects	(Wang et al., 2016)

n.a., not available; 3-MGA, 3-methylglutaconic aciduria; EOH, Early-Onset Hypotonia; FD, facial dysmorphism; FTT, Failure To Thrive; HA, hyperammonemia; HCMP, Hypertrophic Cardiomyopathy; IUGR, Intrauterine growth retardation; LA, Lactic Acidosis; PAH, pulmonary arterial hypertension; PMR, Psychomotor Retardation; WPW, Wolf-Parkinson-White pre-excitation syndrome.

Interestingly, ATP synthase deficiency caused by *TMEM70* mutation is associated with higher levels of complexes III and IV of respiratory chain, which seems to be compensatory response by the cell (Havlickova Karbanova et al., 2012).

As was already mentioned, ATP synthase is important in the formation of mitochondrial cristae. It was also published that mitochondria with mutation in *TMEM70* are swollen and irregularly shaped with loss or aggregated cristae and fragmented mitochondrial network (Jonckheere et al., 2011, Braczynski et al., 2015, Diodato et al., 2015, Sladkova et al., 2015). The morphology of these mitochondria is restored by complementation of the *TMEM70* defect in fibroblasts (Jonckheere et al., 2011).

It was recently shown, that *Tmem70* gene is hypermethylated and its mRNA downregulated in the liver of rats treated with hepatocarcinogen thiocetamid for 28 days. It indicates that aberrant epigenetic regulation of this gene leads to the shift of metabolism from oxidative phosphorylation to glycolysis. It may mean that TMEM70 is involved in tumour development (Mizukami, Watanabe, et al., 2017, Mizukami, Yafune, et al., 2017). It is in agreement with already reported ATP synthase downregulation in many types of carcinomas (Isidoro et al., 2004).

Despite the fact that TMEM70 protein is essential for ATP synthase biogenesis, its detailed molecular function remains to be determined. It was indicated that TMEM70 is involved in early stages of ATP synthase assembly (Houstek et al., 1999) and takes part in F_1 stabilisation and assistance in further steps of assembly (Torraco et al., 2012).

1.3.4.2 DAPIT protein

Protein DAPIT (diabetes-associated protein in insulin-sensitive tissues) is 58 amino acids long with one putative transmembrane helix (Paivarinne and Kainulainen, 2001) and calculated molecular mass of 6.4 kDa (Carroll et al., 2006). DAPIT is highly conserved in vertebrates and insects. The chromosomal location of its gene *Usmg5* (Up-regulated during skeletal muscle growth 5) is 1q54 in rat, 19D1 in mouse and 10q24 in human (Kontro et al., 2015).

DAPIT was shown to be associated with the mammalian mitochondrial ATP synthase (Chen et al., 2007, Meyer et al., 2007, Lee et al., 2015) and it was also suggested that DAPIT might be associated with lysosomal V-ATPase (Kontro et al., 2012). Moreover, it was observed in the DAPIT knock-down HeLa cells that DAPIT regulates ATP synthase population in mitochondria. Although ATP synthase activity was smaller, levels of α and β subunit mRNAs were not changed due to suppressed DAPIT protein expression in HeLa cells (Ohsakaya et al., 2011).

Interestingly, DAPIT was also shown to play an important role in the cell metabolism. Its transcript (mRNA) was firstly identified in a rat type 1 diabetes model induced by streptozotocin (STZ), in which DAPIT level is downregulated in insulin-sensitive skeletal and heart muscle (Paivarinne and Kainulainen, 2001). In contrary, it has also been published that STZ induction of diabetes up-regulates DAPIT protein levels in rat heart muscle, skeletal muscles and epidydimal adipose tissue and strikingly down-regulates in liver and *musculus plantaris*. However, levels were not changed in STZ induced diabetic mouse calf skeletal muscle complex (Kontro et al., 2012). It has also been found that its over-expression in HEK293T cells modulates glucose metabolism through higher glucose utilisation leading to increased lactate production (Kontro et al., 2015). Furthermore, hyperglycaemia up-regulated the DAPIT protein in the Schwann cells of neonatal rats (Zhang et al., 2010). Hence, DAPIT may be a novel glucose sensitive protein that affects mitochondrial function in diabetic tissues.

Moreover, over-expressed DAPIT in HEK293T cells was also found to be associated with an epithelial to mesenchymal (EMT)-like transition by changing E-cadherin to N-cadherin and upregulating a few key junction/adhesion proteins. Cell migration was slowed down and cell growth by G1 arrest, cell detachment was enhanced. In addition, mitochondrial $\Delta\Psi_m$ and superoxide levels were increased. It also led to the translocation of hypoxia inducible factor 1α (HIF1α) and β-catenin transcription factors to nucleus (Kontro et al., 2015).

Furthermore, DAPIT was also increased in the brain synaptosomes of a mouse model of Parkinson's disease (McFarland et al., 2008), and results of Gene Expression Omnibus (GEO) screening suggested up-regulation of *USMG5* in various cancers, in high weight gainers adipose tissue and in cardiac deficiencies (Barrett et al., 2013, Kontro et al., 2015).

Based on histologic analyses, DAPIT of human/rat origin is highly expressed in tissues with high energetic demands (heart, skeletal muscle, brain) and epithelial cells that actively transport nutrients and ions (Kontro et al., 2012).

2 AIMS OF THE STUDY

The aim of this study was to characterise the function of new components of mammalian mitochondrial proteome. Specifically, I focused on two proteins related to ATP synthase – TMEM70 and DAPIT. TMEM70 is necessary for ATP synthase assembly, and its deficiency causes severe diseases but its detailed function remains unclear. The second protein I focused on, DAPIT, is known to associate with ATP synthase but its role in the protein complex is not yet clear. It has been suggested that DAPIT might play a role in ATP synthase dimer formation. I also followed other higher order structures formed by ATP synthase and namely I studied ATP synthasome formation in physiological and pathological models of ATP synthase content variation. Finally, I was interested in the limiting content of ATP synthase to be present in cells to avoid pathological presentation and tried to determine the threshold for its content.

The specific aims of the thesis were:

1) To characterise the function of TMEM70, the new assembly factor of the mitochondrial ATP synthase, using animal knockout model:
   a) Generate and characterise the constitutive *Tmem70* knockout mouse model.
   b) Prepare inducible *Tmem70* knockout mouse model to characterise consequences of TMEM70 absence in adult animals.

2) To characterise the function of DAPIT in ATP synthase complex using rat knockout model.

3) To examine the effect of ATP synthase defects (including TMEM70 deficiency) on ATP synthasome components in patient cells and in mice.

4) To examine the threshold limit of ATP synthase defects in human cell lines.

3 MATERIALS AND METHODS

3.1. Animal and cell models

3.1.1 Ethics Statement

Animal care and experiments were approved by the Animal Care Committees of the Institute of Physiology and Institute of Molecular Genetics of the Czech Academy of Sciences (study ID#174/2010) in compliance with national and institutional guidelines (ID#12135/2010-17210). All human samples were obtained on the basis of written informed consent and handled in accordance with the Code of Ethics of the World Medical Association.

3.1.2 Generation of Tmem70-deficient mice

A few different types of *Tmem70* knockout were generated and analysed within this dissertation thesis (Figure 9). All TMEM70 deficient mice were prepared in collaboration with the Transgenic Unit of the Institute of Molecular Genetics, CAS.

TMEM70 deficient constitutive mice were generated using JM8.A4 embryonic stem (ES) cells harbouring knockout first allele (Tmem70$^{tm1a(KOMP)Wtsi}$) obtained from the KOMP repository (trans-NIH Knock-Out Mouse Project, ID: CSD29597, www.komp.org (The Knockout Mouse Project). Using laser-assisted technique ES cells were injected into 8-cell stage embryos of strain C57BL/6J-*Tyr*$^{c-2J}$ to generate chimeric mice. Tmem70tm1a$^{+/-}$ mice were crossed with Cre recombinase expressing strain Gt(ROSA)26Sor$^{tm1(ACTB-cre,-EGFP)Ics/Ics}$ (Birling et al., 2012) to convert tm1a allele into tm1b allele (Figure 9). Both tm1a and tm1b mice exhibited identical phenotype - lethality at 9.5 *days post coitum* (E9.5) and thus Tmem70tm1a (further denoted as **c*Tmem70*$^{-/-}$) mice were used to analyse the lethal impact of *Tmem70* deletion and the ATP synthase biogenesis.

To obtain viable adult *Tmem70*$^{-/-}$ mice, the tamoxifen (TAM) inducible conditional knockout was generated - B6.Tmem70$^{tm1d(KOMP)Wtsi}$ (further denoted as **i*Tmem70*$^{-/-}$). This strain was produced by crossing of Tmem70$^{tm1c(KOMP)Wtsi}$ (produced by crossing of Tmem70$^{tm1a(KOMP)Wtsi}$ with Gt(Rosa)26Sor(CAG-Flpo,-EYFP) with mice harbouring inducible whole-body Cre recombinase. Then, *Tmem70* gene was cut out by Cre recombinase, which is activated by gavage administered TAM (Sigma T5648; 5 consecutive days, 5 mg/day/mouse - dissolved in EtOH and mixed 1:1 with sunflower oil). Control mice were administered EtOH mixed 1:1 with sunflower oil only. Mice were provided food and water *ad libitum* and housed under 12 h light–dark cycles.

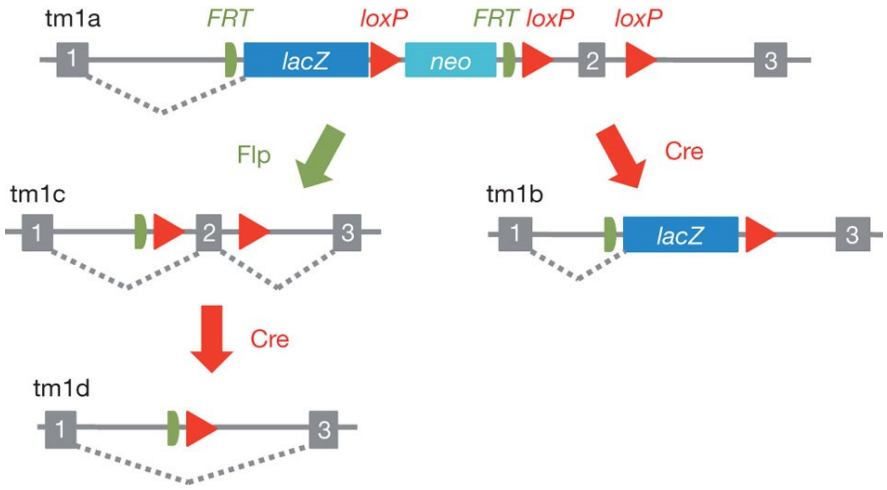

Figure 9. Schematic of the 'knockout-first' conditional allele. *The 'knockout-first' allele (tm1a) contains an IRES:lacZ trapping cassette and a floxed promoter-driven neo cassette inserted into the intron of a gene, disrupting gene function. Flp (flippase) converts the 'knockout-first' allele to a conditional allele (tm1c), restoring gene activity. Cre deletes the promoter-driven selection cassette and floxed exon of the tm1a allele to generate a lacZ-tagged allele (tm1b) or deletes the floxed exon of the tm1c allele to generate a frameshift mutation (tm1d), triggering nonsense mediated decay of the deleted transcript (Skarnes et al., 2011).*

3.1.3 Generation of DAPIT-deficient rats

The DAPIT deficient rats were prepared at the Department of Genetics of Model Diseases of the Institute of Physiology, CAS.

The *Usmg5* knockout rats (DAPIT deficient) were prepared by microinjections of fertilised ova from SHR/Ola by ZFN mRNA (Sigma) at concentration 5 ng/microliter.

Rats were provided food and water *ad libitum* and housed under 12 h light–dark cycles.

3.1.4 Cell culture and generation of knockdown clones

Cells were cultivated under standard conditions (37 °C, 5 % CO_2 atmosphere) in the high-glucose DMEM medium (Life Technologies, 31966-021) supplemented with 10 % foetal bovine serum (Life Technologies, 10270-106), 2 mM HEPES, and antibiotics (100 U/mL penicillin, 100 µg/mL streptomycin, Life Technologies, 15140-122).

To produce knockdown clones, HEK293 cells were transfected with plasmids carrying pre-designed shRNAs (MISSION shRNA Plasmid DNA, Sigma-Aldrich) complementary with transcripts *ATP5C1*, *ATP5D* and *ATP5E* coding for the ATP synthase subunits γ, δ and ε, respectively. As a transfection reagent, Metafectene Pro (Biontex) was used according

to the manufacturer's instructions in the ratio 2:1 to µg of plasmid DNA. Individual clones were isolated and kept under antibiotic selection (puromycin 1 µg/mL).

Primary fibroblast cultures derived from skin biopsies of 3 healthy individuals, 7 patients with an isolated ATP synthase defect due to the homozygous nucleotide substitution 317-2A>G in the gene *TMEM70* (Cizkova et al., 2008), a patient with c.35A>G missense mutation in the gene *ATP5E* coding for the subunit F_1-ε (Mayr et al., 2010), and a patient harbouring m.9205delTA frameshift mutation in the mitochondrial gene *MT-ATP6* coding for the subunit F_o-a (Jesina et al., 2004, Hejzlarova et al., 2015) were cultivated under standard conditions (Mayr et al., 2010).

3.1.5 Collection of mouse embryos

Mouse embryos were harvested at stage 9.5 dpc from timed pregnant females. The morning of the vaginal plug was considered as embryonic day 0.5 (E0.5). Embryos were dissected out of the membranes under a dissection microscope and further processed as outlined below.

3.2 Molecular methods

3.2.1 Genotyping

Genotyping was performed on DNA from yolk sac, mouse tail lysates and tissues. Yolk sacs and mouse tails were incubated overnight at 56 °C in 30 µL (yolk sac) or 400 µL (tail) PCR buffer with non-ionic detergents (10 mM Tris-HCl, 50 mM KCl, 2.5 mM $MgCl_2$, 0.1 mg/ml Gelatin, 0.45 % (v/v) IGEPAL CA-630 (Sigma, I7771), and 0.45 % (v/v) Tween 20) containing Proteinase K (100 µg/ml). DNA from tissues was isolated using Invisorb Spin Tissue Mini Kit (Stratec).

Lysates and isolated DNA were diluted to 10 ng of DNA/µL of PCR grade water. PCR was run with DreamTaq polymerase (0.6 U) and buffer (Thermo Scientific), 1.5 mM dNTPs (Sigma) and following primer (Generi Biotech) combinations:

	forward (5'→3')	reverse (5'→3')	wildtype forward (5'→3')
tm1a	TATATCCCCTCCCCCGTTAG	CACTGCAACTCGGCCTTTA	
tm1b	ACGGTTTCCATATGGGGATT	CACTGCAACTCGGCCTTTA	GCATGCACCACCACTGTGTAG
tm1d	GGAGGTCATCATTGACTGTCTTC	CACTGCAACTCGGCCTTTA	

Moreover, tm1a PCR products were cleaved by *Sac1* (BioLabs) restriction enzyme for 3 h at 37 °C. Tm1a, tm1b and tm1d PCR products were resolved by 1 % agarose gel electrophoresis.

3.2.2 RT-PCR

To perform quantitative RT-PCR, whole embryo RNA was isolated using RNase mini-kit (Qiagen) and the total RNA from tissues was isolated by the Trizol reagent (Life Technologies). cDNA was synthesised from 40-100 ng of RNA by reverse transcription (SCRIPT cDNA Synthesis Kit, Jena Biosciences). The following predesigned primer/probe sets (TaqMan Gene Expression Assays, Life Technologies) were used: *Tmem70* (Mm00466179_m1), *Atp5a1* (Mm00431960_m1), and *B2m* (Mm00437762_m1). qPCR amplifications were carried out on ViiA 7 instrument (Life Technologies) with the following cycling protocol: 95 °C for 15 min, and 40 cycles at 95 °C 20 s and 60 °C for 1 min. All reactions were done in duplicate and 1 µL of diluted (1:1) cDNA was used in each 10 µL reaction using HOT FIREPol probe qPCR Mix (Solis Biodyne). ΔCt was calculated for all genes. Standard curves for all genes were created by serially diluting wildtype embryo cDNA. The Ct of all genes was related to Ct of housekeeper reference *B2m*.

3.3 Biochemical methods

3.3.1 Electrophoresis and Western blot analysis

Frozen embryos stored at -86 °C were pulverised in liquid nitrogen and homogenised with PBS with protease inhibitor cocktail (PIC, 1:500, Sigma P8340) in a glass-glass micro-homogeniser (1 ml, Fisher Scientific, FB56673).

Tmem70$^{+/+}$ and *Tmem70*$^{+/-}$ mice (5 weeks and 14 weeks old mice males) and i*Tmem70*$^{-/-}$ mice males were anesthetised by CO_2 and sacrificed by cervical dislocation. Heart homogenates (5 %, w/v) or liver homogenates (10 %, w/v) were prepared at 4 °C in STE medium [0.25 M (heart) or 0.32 M (liver) sucrose, 10 mM Tris-HCl, 2 mM EDTA, pH 7.4] with protease inhibitor cocktail (PIC 1:500, Sigma P8340) using glass-teflon homogeniser (4 strokes at 650 rpm) and filtered through coarse nylon screen (100 µm mesh). Protein concentration was determined by Bicinchoninic Acid Kit for Protein Determination (Sigma), and homogenates were stored at -80 °C.

DAPIT rats (6-month-old rats) were killed in CO_2 narcosis. Tissue homogenates were prepared and mitochondria from tissues (heart, liver,) were isolated by differential centrifugation as before (Mracek et al., 2009, Pecinova et al., 2011).

Fibroblast mitochondria were isolated by hypotonic shock cell disruption (Mayr et al., 2010).

The protein concentration was estimated by Bradford's method (Bradford, 1976) (Bio-Rad) or by Bicinchoninic Acid Kit for Protein Determination (Sigma).

Prepared samples were separated under denatured or native conditions by electrophoreses. Individual electrophoretic buffers are summarised in Table 3.

For SDS-PAGE embryos, tissue homogenates, mitochondria and HEK cells were denatured for 15 min at 56 °C in a sample lysis buffer containing 50 mM Tris-HCl pH 7.0, 4 % (w/v) SDS, 10 % (v/v) glycerol and 0.1 M DTT (1,4-Dithiothreitol). Mitochondria and fibroblast samples were also denatured for 15 min at 65 °C in a sample lysis buffer containing 50 mM Tris-HCl pH 7.0, 4 % (w/v) SDS, 10 % (v/v) glycerol, and 2 % (v/v) 2-mercaptoethanol. Afterwards, proteins were separated on 10 % (homogenates, mitochondria) or 12 % (cells) polyacrylamide minigels (Bio-Rad MiniProtean III) using the Tricine buffer system (Schägger 2006).

Under native conditions tissue homogenates and cells were centrifuged 10 min at 20000 *g*. Pellets were diluted in solubilisation buffer A containing 50 mM NaCl, 2 mM 6-aminohexanoic acid, 50 mM imidazole, 1 mM EDTA, pH 7, and solubilised for 20 min at 0 °C using detergent (2 g n-dodecyl-β-D-maltoside/g protein or 2 g digitonin/g protein) and centrifuged for 20 min at 30000 *g* to remove cell debris. The supernatants were mixed with glycerol (5–10 %) and Coomassie Brilliant Blue G-250 dissolved in 5 mM 6-aminohexanoic acid so that the final ratio of this dye and detergent in the sample was 1:8. BN-PAGE was run on 4-13 % (animal samples) or 4-8 % (cell samples) gradient mini gels using the imidazole buffer system (Wittig et al., 2006, Pecinova et al., 2011).

In case of high resolution clear native PAGE (hrCN-PAGE) supernatants were mixed with glycerol (5–10 %) and 1 µl of 0.1 % Ponceau S/50 % glycerol for each approximately 50 µl of sample. Detergents were also added into cathode buffer (see Table 3) (Wittig and Schagger, 2009).

Table 3. Buffers for SDS-PAGE, BN-PAGE, hrCN-PAGE (final concentrations)

Cathode buffers	**SDS**	**BN**	**hrCN**
Tris (mM)	100	-	-
Tricine (mM)	100	50	50
SDS (%)	0.1	-	-
Imidazole (mM)	-	7.5	7.5
n-dodecyl-β-D-maltoside (%)	-	-	0.02
Sodium deoxycholate (%)	-	-	0.05
Coomassie dye (%)	-	0.02 and 0.002	-
pH*	~8.25	~7.0	~7.0

Cathode buffer for hrCN should be prepared immediately before electrophoresis.
*Adjust pH by Tricine or imidazole if difference is higher than 1 pH unit (at 25 °C).
Mix for several hours.

Anode buffers	**SDS**	**BN**	**hrCN**
Tris (mM)	100	-	-
Imidazole (mM)	-	25	5
pH	~8.9	~7.0	~7.0

pH is adjusted before the addition of SDS.

Gel buffers (3x GB)	**SDS**	**BN**	**hrCN**
Tris (M)	3	-	-
SDS (%)	0.3	-	-
Imidazole (mM)	-	75	75
6-aminocapronic acid (M)	-	1.5	1.5
pH	~8.45	~7.0	~7.0

AB - Acrylamide/bisacrylamide mix (48 % acrylamide, 1.5 % bisacrylamide)

Electrophoreses were followed by Western blot as described previously (Hejzlarova et al., 2011, Kratochvilova et al., 2014). Gels were blotted onto PVDF membrane (Immobilon-FL, Merck Millipore) by semi-dry electrotransfer (1 h at 0.8 mA/cm^2). Immediately after blotting, blue native blots were destained with methanol to decrease background fluorescence. All Western blots were blocked in 5 % non-fat milk dissolved in TBS (Tris-buffered saline containing 150 mM NaCl, 10 mM Tris-HCl, pH 7.5) for 1 h prior to incubations with primary (2 h at room temperature/overnight at 4 °C) (see Table 4) and infrared fluorescent secondary antibodies (45–60 min at room temperature Alexa Fluor 680, Life Technologies; IRDye 800, Rockland Immunochemicals, Li-Cor).

Table 4. List of used primary antibodies.

Target	MW (kDa)	Host/clonality	Antibody source/catalog no.
F_1-α	55	mo/P	Clone 20D6 - Godinot (Jesina et al., 2004)
F_1-β	24	mo/M	Abcam ab117991
F_1-γ	33	rb/P	GeneTex GTX114275
F_1-δ	10	rb/P	GeneTex GTX101503
F_o-a	25	rb/P	Godinot (Dubot et al., 2004)
F_o-b	24	mo/M	Abcam ab117991
F_o-c	9	rb/P	(Jesina et al., 2004)
F_o-g	11	rb/P	GeneTex GTX111014
IF1	12/15	mo/M	Abcam ab110279
SDHA	70	mo/M	Abcam ab14715
Core 1	49	mo/M	Abcam ab 110252
Cox4	18	mo/M	Abcam ab14744
ANT	30	rb/P	(Kolarov et al., 1978)
PiC	35	mo/P	Sigma-Aldrich SAB1400208
MS603	-	mo/M	Abcam ab110412
DAPIT	10	rb/P	Proteintech Group 17716-1-AP
CPO-1 actin	44	mo/M	Calbiochem
SOD1	16	rb/P	Ab-Frontier LF-PA0013
SOD2	22	mo/M	Ab-Frontier LF-MA0030

mo/P - mouse polyclonal; rb/P - rabbit polyclonal; mo/M - mouse monoclonal

For membrane washing between individual incubations with antibodies, TBS supplemented with 0.1 % Tween-20 was used. Fluorescence was detected using Odyssey infrared imaging system (LI-COR Biosciences) and the signal was quantified using Aida 3.21 Image Analyzer software (Raytest).

3.3.2 ATPase in-gel activity assay

Enzyme in-gel activity staining was performed after separation of the respiratory complexes using BN-PAGE or hrCN-PAGE. The in-gel activity assay of the ATPase hydrolytic activity was performed as described (Wittig et al., 2007). Gels were pre-incubated in Tris/Glycine buffer containing 35 mM Tris, 270 mM glycine, pH 8.3 – 8.4. Than gels were

incubated in the assay mixture containing 14 mM $MgSO_4$, 0.2 % $Pb(NO_3)_2$ and 8 mM ATP in Tris/Glycine buffer until white precipitate was observed.

3.3.3 Respiratory measurements

The Seahorse XF°24 Analyzer (Seahorse Bioscience) was used to measure oxygen consumption and extracellular acidification in embryo homogenates and intact cells.

Fresh mouse embryos were homogenised in Assay medium (70 mM sucrose, 220 mM mannitol, 10 mM KH_2PO_4, 5 mM $MgCl_2$, 2 mM HEPES, 1 mM EGTA, 0.2 % BSA; pH 7.2) containing substrates for Complex I (10 mM pyruvate, 2 mM malate, 10 mM glutamate), 5 µM cytochrome *c*, 2 mM ADP, and PIC (1:500, Sigma). Hand homogenisation was performed in a glass-glass micro-homogeniser (13 complete strokes, 1 ml, Fisher Scientific, FB56673). Homogenates were transferred to XF-V7 24-well plates (Seahorse Bioscience) and spun down for 20 minutes at 2000 *g*, 4 °C to attach the homogenate to the plastic surface. Before measurement, the total volume in each well was adjusted to 500 µL with Assay medium plus substrates (same as for homogenisation). The oxygen consumption rate (OCR) was determined at 37 °C with Complex I substrates + ADP and then after subsequent additions of 10 mM succinate, 2 µM oligomycin, 4 µM FCCP, and 0.4 µM antimycin A. The data are presented as the OCR in picomoles O_2 per minute. The respiratory control ratio (RCR) was calculated from the respiration values after adding succinate (State 3) and oligomycin (State 4) – State3/State4.

The intact cells were seeded on poly-L-lysine (Sigma, P8920) coated plates on a day before the measurement (30000–40000 cells per well). The measurements were carried out in the XF base medium supplemented with 10 mM glucose, 1 mM pyruvate, 2 mM L-glutamine, and 0.2 % bovine serum albumin. Final concentrations of inhibitors were as follows: 1 µM oligomycin, 2 µM FCCP, 1 µM rotenone, 0.5 µM antimycine A, and 100 mM 2-deoxyglucose. Both oxygen consumption and extracellular acidification were normalised to the total DNA content that was estimated by the Quant-iT PicoGreen assay according to the manufacturer's instructions (ThermoFischer) after cells had been treated with a lysis buffer (20 mM Tris-HCl, 10 mM EDTA pH 7.4, 1 % (w/v) SDS, 50 µg/ml proteinase K) at 37 °C for 1 h.

The OROBOROS Oxygraph-2k (Oroboros Instruments) was used to determine oxygen consumption of freshly prepared tissue homogenates in an assay medium containing 80 mM KCl, 3 mM $MgCl_2$, 5 mM KH_2PO_4, 1 mM EDTA, 10 mM Tris-HCl (pH 7.3) at 37 °C (mice) or 30 °C (rats).

Final concentrations of substrates and inhibitors were as follows: 10 mM glutamate, 10 mM pyruvate 2.5 mM malate, 10 mM succinate, 1.5 mM ADP, 0.2 µM oligomycin (titrated), 1.5 µM FCCP.

The oxygen consumption was expressed in pmol oxygen/s/mg protein.

3.3.4 ROS production

ROS production was estimated as CM-H_2DCFDA (chloromethyl derivative of 2',7'-dichlorodihydrofluorescein diacetate, Life Technologies) fluorescence in a saline buffer (135 mM NaCl, 5 mM KCl, 0.4 mM KH_2PO_4, 1 mM $MgSO_4$, 1 mM $CaCl_2$, 20 mM HEPES, pH 7.4) supplemented with 10 mM glucose and 1 µM CM-H_2DCFDA and with or without inhibitors (1 µM oligomycin, 1 µM FCCP). Cells were seeded in poly-L-lysine coated 24-well plates a day prior to the measurement. Immediately after the cultivation medium was exchanged for the assay medium, the background fluorescence was recorded using a plate reader (Infinite M200, Tecan) with excitation set to 495 nm and emission 525 nm. After incubation at 37 °C for 2 h, an increase in the fluorescence was recorded with the same instrumental gain.

3.3.5 Enzyme activity measurement

Enzyme activities were determined spectrophotometrically at 37 °C in tissue homogenates.

Oligomycin-sensitive ATP synthase hydrolytic activity was measured in ATP-regenerating system according to Baracca et al. (Baracca et al., 1989). 10 µl of sample was mixed in cuvette with 490 µl of 5 mM Tris-HCl and sonicated (10 s at 20 % amplitude sonication). 500 µl of 2x concentrated measuring mixture [75 mM Tris-HCl, 10 mM $MgCl_2$, 20 mM KCl, 0.2 mM NADH, 0.4 mM 2-phosphoenolpyruvate, 0.5 mM ATP, 0.2 % BSA, 1 mM FCCP, 2 µM antimycin A, 1 µM rotenone, 8 U/ml lactate dehydrogenase + 8 U/ml pyruvate kinase (Sigma P0294)] was added. 1.5 min after starting the measurement 3 µM oligomycin was added. Oligomycin sensitive enzyme activity was calculated as difference of -/+ oligomycin and expressed as nmol/min/mg protein using molar absorption coefficient $\varepsilon_{340} = 6.22\ mM^{-1}.cm^{-1}$ (NADH).

Citrate synthase was measured as described in (Srere P. A. 1969). 10 µl of sample was mixed in cuvette with detergent (3 µg n-dodecyl-β-D-maltoside/1 µg of protein) for 1 min. Than H_2O, 0.1 mM DTNB and 0.1 mM acetyl-CoA were added. After 30 s of reaction, 0.5 mM oxaloacetate was added to reach final volume 1 ml. Enzyme activity was calculated

as difference of -/+ acetyl-CoA and was expressed as nmol/min/mg protein using molar absorption coefficient $\varepsilon_{412} = 13.6\ mM^{-1}.cm^{-1}$ (DTNB).

3.3.6 Adenine nucleotide analysis

To determine the level of adenine nucleotides, flash-frozen embryos stored in liquid nitrogen were homogenised and deproteinated by 6 % (v/v) perchloric acid in a glass-glass micro-homogeniser. Cells were snap frozen with liquid nitrogen in cultivation plates quickly after medium removal and harvested on ice into 6 % (v/v) perchloric acid. After centrifugation at 10000 *g* for 10 min (4 °C) collected supernatant was neutralised to pH 7 by 0.4 M triethanolamine + 1.8 M KOH. Neutralised samples were centrifuged at 10000 *g* for 2 min (4 °C) to remove precipitated salts. The content of ATP and ADP was determined by HPLC (high-performance liquid chromatography) as described in (Flachs et al., 2002).

3.3.7 Blood analysis

Blood was collected under isoflurane (2 %) anaesthesia from vena cava inferior. Complete blood count was analysed by automatic haematological analyser XN-1000 (Sysmex). Blood was also centrifuged for 5 min at 3000 *g*, 4 °C. Obtained plasma was analysed by biochemistry analyser Architect ci16200 (Abbott Diagnostics). Plasma enzymes AST and ALT contents were measured using Activated AST Reagent Kit (8L91, Abbott Diagnostics) and Activated ALT Reagent Kit (8L92, Abbott Diagnostics). Ammonia content was measured by MULTIGENT Ammonia Ultra Kit (6K89-30, Abbott Diagnostics). Analyses were performed at the Laboratory Methods Division, Institute of Experimental Medicine (IKEM), Prague.

3.3.8 Determination of caspase activities

The activities of caspases 3, 8 and 9 were assessed in tissue homogenate after addition of specific substrates Ac-DEVD-AMC, Ac-LETD-AFC and Ac-LEHD-AMC, respectively (Enzo Life Sciences, NY, USA). The activities were measured in a fluorescent mode using a TECAN Infinite M200 spectrofluorometer (Tecan Group AG, Switzerland). The excitation and emission wavelengths were 350 and 460 nm for caspase 3 and caspase 9, and 400 and 505 nm for caspase 8. Results were normalised to protein concentration (BCA) and expressed as percent of control (100 %). Measurement was performed at the Department of Physiology, Faculty of Medicine, Charles University, Hradec Králové.

3.3.9 Determination of glutathione level

Level of GSH was measured according to a slightly modified method of Rousar et al. (Rousar et al. 2012). Liver homogenates were added to ice-cold metaphosphoric acid (5 %, w/v) in the ratio of volumes 1:2, were shaken, and after incubation (10 min) were centrifuged 20000 *g* for 10 min (4 °C). The supernatant was stored at -80 °C until analysis. The GSH standards (0-1000 µM) were diluted in metaphosphoric acid (5 %, w/v) according to the procedure for sample preparation. The sample/standard (50 µl) was added to 1000 µl of 100 mM sodium phosphate buffer with 4 mM EDTA (pH 8). Next, 60 µl of the mixture was added to 900 µl of sodium phosphate buffer, and then 60 µl of 0.1 % o-Phthalaldehyde (w/v) in methanol was added. After 15 min sample incubation at room temperature in darkness, 75 µl of 1 M HCl was added and the fluorescence was detected (λ_{ex} = 340 nm; λ_{em} = 420 nm). Measurement was performed on an Aminco Bowman AB2 luminescence spectrofluorometer (Thermo, USA). Measurement was performed at the Department of Physiology, Faculty of Medicine, Charles University, Hradec Králové.

3.3.10 Triglycerides level determination

Triglycerides level was determined in liver tissue. 50 mg of liver tissue was incubated for 2 hours with 150 µl of 3M KOH in 65 % ethanol at 70 °C. Mixture was centrifuged 600 *g*/5 min and obtained supernatant was diluted 10 times by distilled water.

Level of triglycerides was determined by Triglycerides kit (Erba Lachema, BLT00059). Sample absorbance was measured spectrophotometrically at 500 nm.

3.4 Microscopic methods

3.4.1 Whole mount confocal microscopy

The embryos were isolated in ice-cold PBS, fixed overnight in 4 % paraformaldehyde at 4 °C, then rinsed and stored in PBS at 4 °C. Prior to further processing, photographs of the embryos were taken on an Olympus SZX dissecting microscope. For whole mount immunohistochemistry (Miller C. E. et al. 2005) the embryos were permeabilised and blocked in normal goat serum with 0.1 % Triton-X100 in TBS for 2 h, followed by 24 h incubation with the primary antibodies (alpha smooth muscle actin, clone 1A4, Sigma, 1:1000, and the rat anti-mouse CD31 clone MEC13.3 from BD Pharmingen, 1:500). After 3x2 h rinsing with PBS, the samples were incubated for 24 h with the appropriate goat secondary antibodies (Jackson Immuno) coupled with Alexa488 (anti-rat) and rhodamine red (anti-mouse). Hoechst 33342

nuclear stain was added to the secondary antibody solution. After thorough rinsing, the embryos were rapidly dehydrated in ethanol, cleared in xylene, and mounted into cavity slides (Fisher Scientific) in DEPEX permanent mounting media (Electron Microscopy Sciences) and coverslipped. After drying, the slides were examined on an upright Olympus FluoView confocal microscope using 4x-20x objective lenses. The images were assembled into plates and labeled using Adobe Photoshop. Digital image processing included background subtraction, level adjustment for each channel, and Unsharp Mask filtering. Measurement was performed at the Department of Cardiovascular Morphogenesis, Instituteof Physiology, CAS.

3.4.2 Transmission Electron Microscopy

Mouse embryos (E8.5, E9.5) were removed from mice, washed immediately in Sorensen's phosphate buffer (SB; 0.1 M phosphate, pH 7.2-7.4) at 37 °C and fixed with 2.5 % glutaraldehyde in SB during 1-2 h at 4 °C (Soplop N. H. et al. 2009). Then, fixed embryos were embedded into melted agarose at 37 °C, and agarose was allowed to harden on ice. Agarose-embedded embryos were post-fixed with 1 % OsO_4 in SB, dehydrated in ethanol series, and embedded in Epon-Durkupan. Ultrathin sections (70-90 nm) were cut with Ultramicrotome Leica EM UC6, mounted on copper grids, contrasted with a saturated aqueous solution of uranyl acetate, and examined in FEI Morgagni 268 transmission electron microscope operated at 80 kV and in FEI TECNAI G2 20 LaB6 electron microscope operated at 200 kV (Tan A. S. et al. 2015). The images were captured using Mega View III CCD camera (Olympus Soft Imaging Solutions). Quantitative data are presented as mean ± standard deviation. Analysis was performed at the Department of the Cell Nucleus, Institute of Molecular genetics CAS.

3.5 Physiological methods

3.5.1 Body weight and food intake monitoring

Body weight and food intake of i*Tmem70*$^{-/-}$ and i*Tmem70*$^{+/+}$ mice were monitored once a day at the same time for eight weeks post knockout induction.

3.5.2 Echocardiography

Transthoracic echocardiographic measurement of geometrical and functional parameters of the left heart ventricle (LV) was done using GE Vivid 7 Dimension (GE Vingmed Ultrasound, Horten, Norway) with 12 MHz high resolution matrix probe M12-L. Animals were anesthetised by inhalation of 2% isoflurane (Forane, Abbott), placed on a heated table and their temperature (rectal thermometer RET-4, Physitemp Instruments) was maintained within 36.5 and 37.5 °C. For echocardiographic evaluation, the following diastolic and systolic dimensions were measured: cavity diameter (LVDd, LVDs), anterior wall thickness (AWTd, AWTs), posterior wall thickness (PWTd, PWTs) and heart rate (HR). The main functional parameter, fractional shortening (FS%) was derived from these dimensions by the following formula: FS% = 100 × (LVDd – LVDs) / LVDd. All dimensions were measured in parasternal long and short axes view using two-dimensional and M-mode images. Repeated measurements in every view and mode were then averaged. Echocardiography was measured at the Department of Experimental Cardiology, Institute of physiology, CAS.

3.6. Statistics

Statistical analysis was performed by Student's t-Test (Excel function TTEST, two tailed distributions, two sample equal variance). Quantitative data are presented as mean ± standard deviation (SD), alternatively standard error of the mean (SEM). All results are the average of multiple samples (n).

4 RESULTS

Structure of the results section follows the formulated aims. The first chapter deals with the deleterious effect of constitutive and conditional *Tmem70* mouse knockouts. It summarises published results on constitutive knockout and continues with unpublished data on the inducible one. The second chapter discussing a rat model of DAPIT protein deficiency is solely based on unpublished data. The third chapter shows how ATP synthase defects influence components of its supramolecular structure ATP synthasome in patient's fibroblasts and mice. It describes results on a published paper and extends them with results on *Tmem70* mouse knockout model. Finally, the last chapter explores the threshold content of ATP synthase required for pathological presentation in mitochondrial function and oxidative stress. This chapter is based on manuscript prepared for submission.

4.1 Effect of *Tmem70* knockout in mice (aim 1)

4.1.1 Whole body *Tmem70* mouse knockout (publication A)

4.1.1.1 Embryonic lethality

Generation of constitutive *Tmem70* deficient mice ($Tmem70^{tm1a(KOMP)Wtsi}$ and $Tmem70^{tm1b(KOMP)Wtsi}$) led to viable heterozygous $Tmem70^{+/flox}$ mice (further denoted as **c*Tmem70*$^{+/-}$**) and embryonic lethal $Tmem70^{flox/flox}$ embryos (further denoted as **c*Tmem70*$^{-/-}$**) about 9.5 days *post coitum* (E9.5). The expression of *Tmem70* at the RNA level was ~60 % in c$Tmem70^{+/-}$ of that in $Tmem70^{+/+}$, while *Tmem70* mRNA was undetectable in c$Tmem70^{-/-}$ embryos (Figure 10 A). To study the lethality *in utero* the embryos from $Tmem70^{+/flox}$ inter-crosses were dissected at E8.9-E9.5 and genotyped (Figure 10 B). Total 481 embryos were analysed - c$Tmem70^{-/-}$ n=100, c$Tmem70^{+/-}$ n=260, $Tmem70^{+/+}$ n=121 (ratio: 0.8:2:0.9). All c$Tmem70^{-/-}$ embryos exhibited severe growth retardation phenotype (Figure 10 C). The genotyping of born animals (n = 212) followed the expected Mendelian ratio - $Tmem70^{+/+}$ n=71, c$Tmem70^{+/-}$ n=141.

4.1.1.2 Developmental retardation of c*Tmem70*$^{-/-}$ embryos

Due to the resorption of *cTmem70*$^{-/-}$ embryos past the day E9.5, we analysed embryo's morphology at this day and compared *cTmem70*$^{-/-}$ embryos to their littermates. c*Tmem70*$^{+/-}$ embryos were unaffected (Figure 10 C). The average size of the c*Tmem70*$^{-/-}$ was less than half of the controls, their body curvature was often still in a lordotic-like curvature, they had an open anterior neuropore (Figure 10 C, inset) and their somite number was <15 compared with the 25-somite stage of their littermates, all consistent with a 1-day developmental delay (i.e. E8.5). Also heart was retarded but without any other morphological discrepancies (Figure 11 A). Whole mount staining showed that the colonisation of cardiac cushions by mesenchymal cells was also reduced, similarly to the situation in E8.5 with only a few cells entering the cardiac jelly. Intravascular presence of erythrocytes indicated that functional circulation was already established. The heart was contracting at the time of isolation, and extent intensity of smooth muscle α-actin staining (marker of early myocardium) was normal (Figure 11 A).

To see if there is increase of apoptosis in *cTmem70*$^{-/-}$ and *cTmem70*$^{+/-}$, we carried out the whole mount staining for the active form of caspase 3. It showed only a few scattered cells in all genotypes, which indicated that widespread apoptosis is not a part of the mutant phenotype (not shown). Semithin sections (in addition to serial confocal sections) clearly demonstrated that the myocardium was on average composed from two cell layers (range 1-3). The connections between the cells appeared normal.

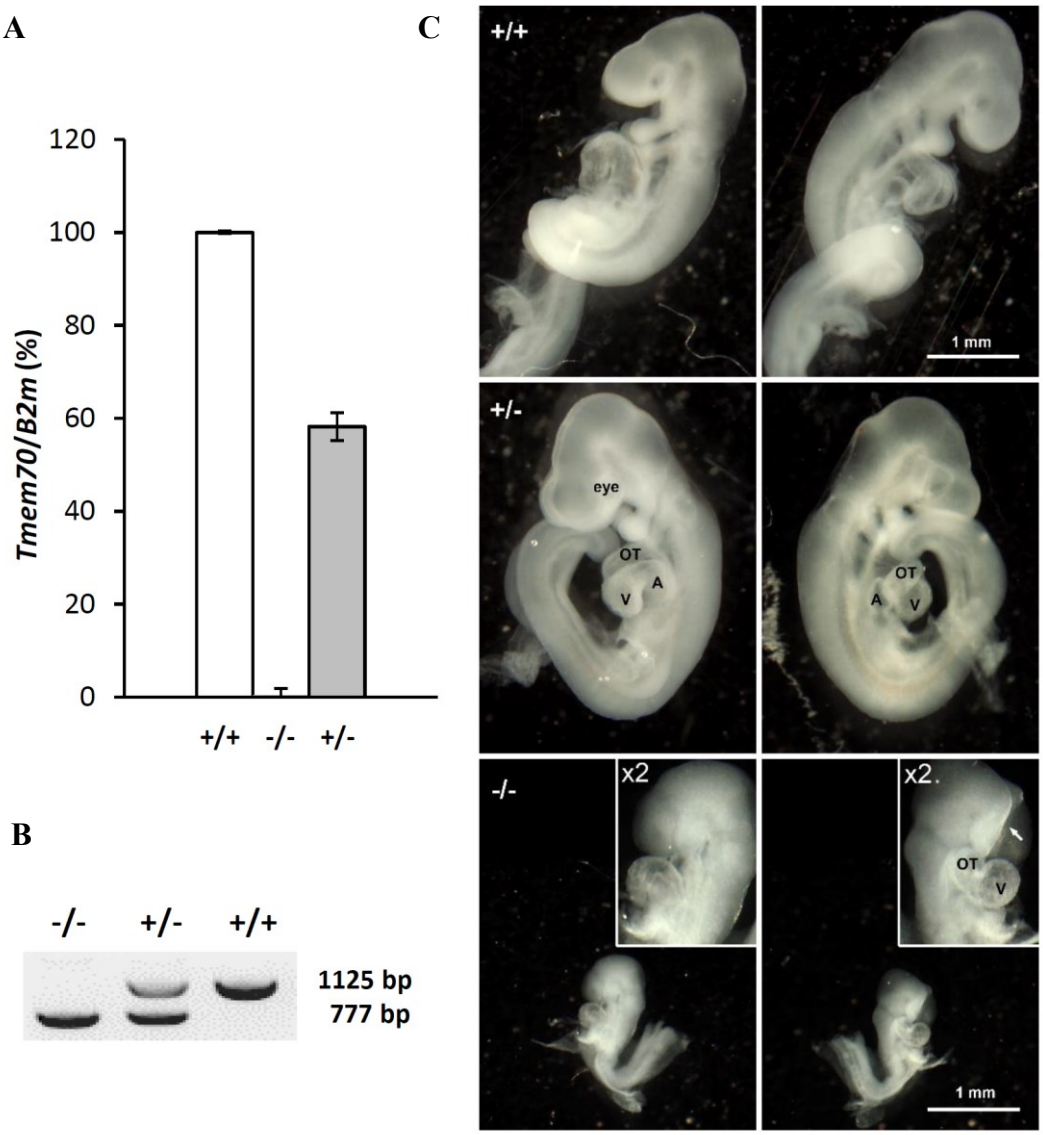

Figure 10. Tmem70 knockout mouse. ***(A)*** *RT-PCR quantification of Tmem70 mRNA (related to β2 microglobulin - B2m mRNA), n=2.* ***(B)*** *Genotyping of E9.5 embryos: +/+ allele is 1125 bp and -/- allele is 777 bp.* ***(C)*** *Optical microscopy of Tmem70$^{+/+}$ (+/+),* c*Tmem70$^{+/-}$ (+/-), and retarded* c*Tmem70$^{-/-}$ (-/-) E9.5 embryos. OT – heart outer tract, V – ventricle, A – atrium, arrow points to open neuroporus anterior, scale bar 1 mm.*

4.1.1.3 Disrupted mitochondrial ultrastructure in c*Tmem70*$^{-/-}$ embryos

It has been published that patients with *Tmem70* deficiency have disrupted mitochondrial cristae (Jonckheere et al., 2011, Braczynski et al., 2015, Diodato et al., 2015, Sladkova et al., 2015). To observe mitochondrial cristae morphology in E9.5 embryos we used transmission electron microscopy. We detected pronounced changes in mitochondrial morphology in the heart as a result of c*Tmem70*$^{-/-}$ knockout (Figure 11 B). Wildtype embryos contained 1.3 ± 0.1 mitochondria per µm^2 (n = 45 cells), with 83.4±3.4 % of mitochondria exhibiting normal ultrastructure. On the contrary, in c*Tmem70*$^{-/-}$ mouse embryos the average density of mitochondria did not differ from controls (1.4 ± 0.3 mitochondria per µm^2) but 80.5±1.3 % of mitochondria displayed atypical shapes and fewer cristae with altered morphology (n = 45 cells). In particular, the classical arrangement of trabecular cristae was often replaced by concentric or irregular cristae structures.

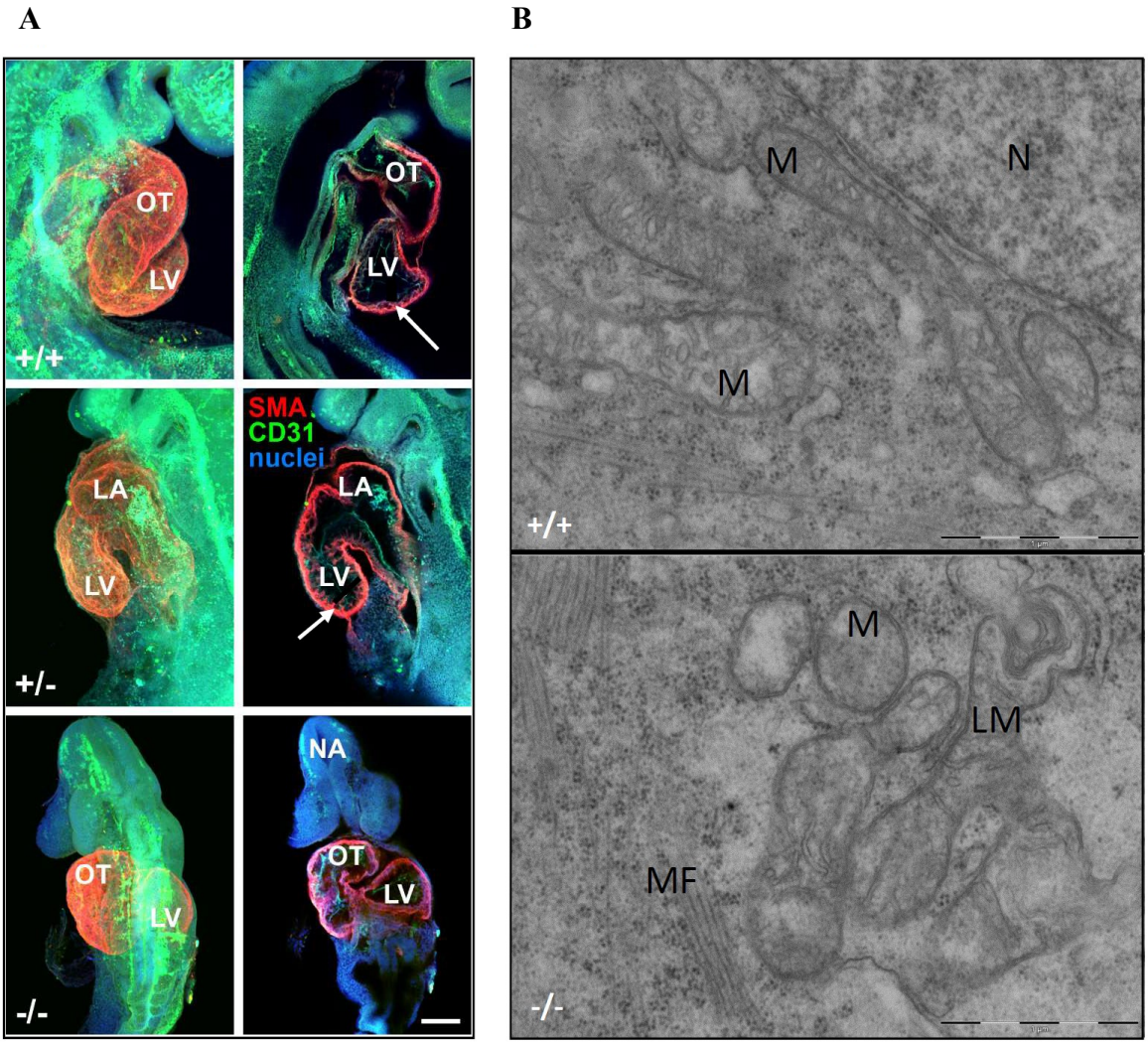

Figure 11. Impaired morphology of cTmem70$^{-/-}$ embryos. *(continues at the next page)*

Continues from the previous page. ***(A)*** *Whole mount immunohistochemistry; confocal microscopy of retarded heart of c*Tmem70$^{-/-}$ *(-/-) embryo in comparison with Tmem70$^{+/+}$ (+/+) and cTmem70$^{+/-}$ (+/-) E9.5 embryos: OT – outer tract, LV – left ventricle, LA – left atrium, NA – neuroporus anterior; SMA (alpha smooth muscle actin), red – myocardium; CD31, green – endocardium; Hoechst 33342, blue – nuclei; arrows point to emerging ventricular trabeculation, scale bar 100 µm.* ***(B)*** *Electron microscopy of disturbed cristae morphology of cTmem70$^{-/-}$ (-/-) compared to Tmem70$^{+/+}$ (+/+) heart mitochondria of E9.5 embryos. M – mitochondria, MF – myofibrils, LM – lysed mitochondria, N – nucleus, scale bar 1 µm.*

4.1.1.4 ATP synthase deficiency in c*Tmem70*$^{-/-}$ embryos

Patients with *Tmem70* deficiency exhibit a pronounced decrease of assembled ATP synthase (Cizkova et al., 2008). To confirm this defect in our model we analysed ATP synthase assembly and other OXPHOS complexes by native electrophoresis. Although the expression of subunit F_1-α (*Atp5A1*) in embryos did not differ between genotypes (data not shown), BN-PAGE followed by Western blot immunodetection (antibody against F_1-α subunit) showed that ATP synthase is strongly affected in c*Tmem70*$^{-/-}$ embryos. Fully assembled ATP synthase (F_oF_1) was decreased to 20 % and F_1 subcomplex was 3.5-4-fold accumulated (Figure 12 A, B). c*Tmem70*$^{+/-}$ embryos did not differ from *Tmem70*$^{+/+}$ embryos containing normal amounts of ATP synthase and low amount of F_1 subcomplex, related to CII (Figure 12 B). This resulted in 20-fold increase in F_1/F_oF_1 ratio in c*Tmem70*$^{-/-}$ embryos (Figure 12 C). A comparable decrease was observed with antibodies against F_o-a and F_o-c subunits, which were not present in the F_1 subcomplex. Any intermediates or F_o subunits containing aggregates were not present (Figure 12 A). In-gel ATPase hydrolytic activity confirmed impaired ATP synthase assembly and showed retained ATPase hydrolysing activity of F_1 subcomplex (Figure 12 A).

Following probing with antibodies against representative subunits of RC - succinate dehydrogenase A subunit (SDHA - CII), Core1 subunit (CIII), Cox4 subunit (CIV) showed nearly normal content of RC complexes in c*Tmem70*$^{-/-}$ in comparison to c*Tmem70*$^{+/-}$ or *Tmem70*$^{+/+}$ embryos (Figure 12 A).

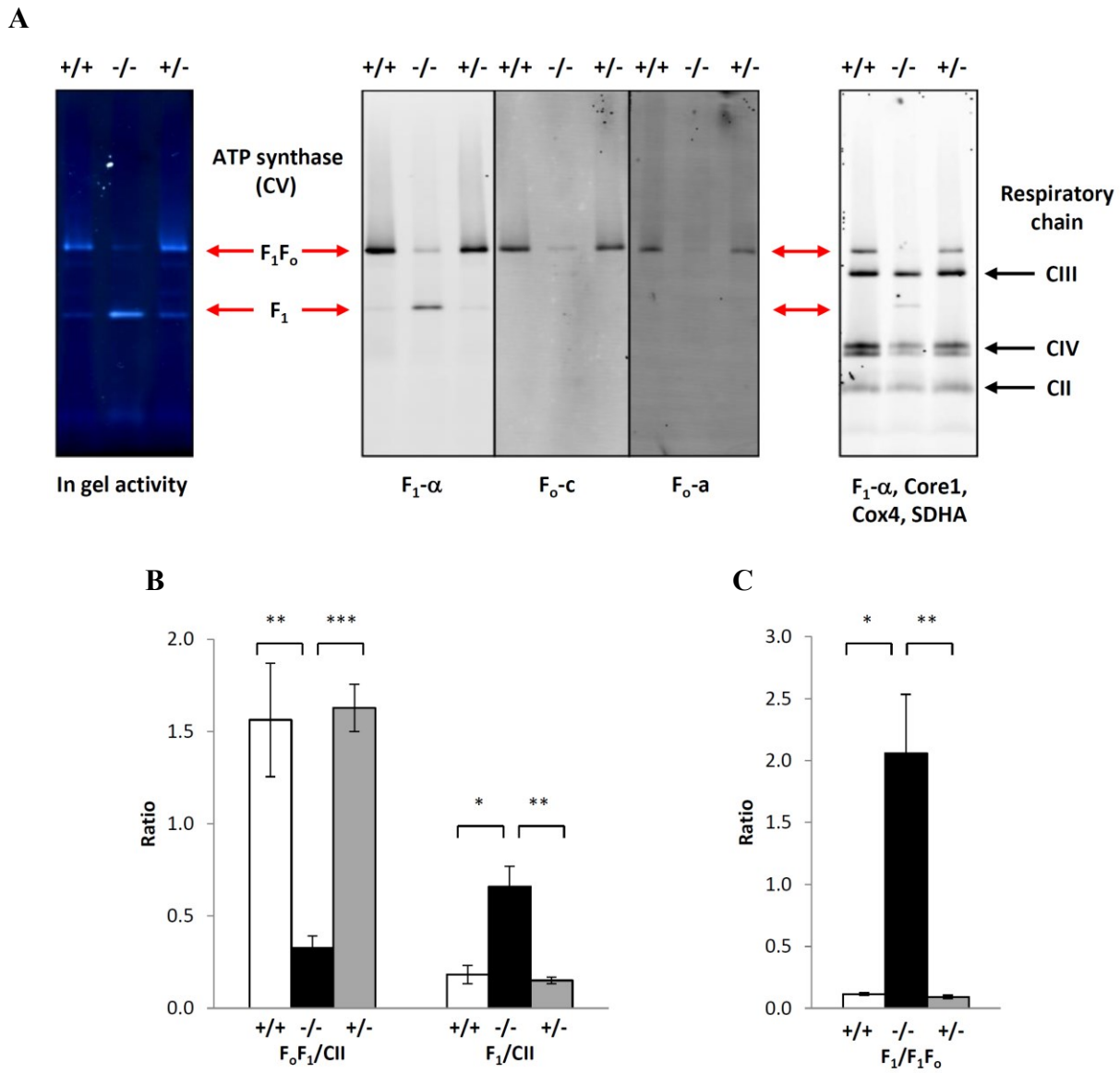

Figure 12. ATP synthase deficiency in cTmem70$^{-/-}$ embryos. (A) *BN-PAGE separation of ATP synthase and respiratory chain complexes using n-dodecyl-β-D-maltoside -solubilised proteins (2 g/g protein) of Tmem70$^{+/+}$ (+/+), cTmem70$^{-/-}$ (-/-) and cTmem70$^{+/-}$ (+/-) Tmem70 knockout E9.5 embryos, Western blot detection with antibodies to ATP synthase (subunits F_1-α, F_o-c, F_o-a), Complex II (CII, SDHA subunit), Complex III (CIII, Core 1 subunit), Complex IV (CIV, Cox4 subunit).* ***(B)*** *Quantification of ATP synthase content with respect to CII (F_1F_o – complex of ~ 6- kDa, F_1 – subassembly of ATP synthase catalytic part of ~ 370 kDa).* ***(C)*** *Relative content of F_1 and F_oF_1, n = 2–3. Data are mean±SD, * p≤0.05, ** p≤0.01, *** p≤0.001.*

4.1.1.5 Altered mitochondrial energetic function in c*Tmem70*$^{-/-}$ embryos

As the ATP synthase was affected, we tested overall OXPHOS function. The analysis of mitochondrial OXPHOS function on fresh embryo homogenates was measured on Seahorse XF^e analyzer by subsequent addition of different substrates. c*Tmem70*$^{-/-}$ embryos displayed much lower rates of ADP-stimulated (State 3) oxidation of RC substrates (pyruvate, glutamate,

malate, and succinate) normalised to SDHA content. Oligomycin sensitive oxidation of these substrates (State3-State4) was decreased by 68-71% in *Tmem70*$^{-/-}$ embryos in comparison to c*Tmem70*$^{+/-}$ and *Tmem70*$^{+/+}$ embryos. This leads to the 2-fold decrease of respiratory control ratio (RCR) (State 3/State 4) in c*Tmem70*$^{-/-}$ embryos (Figure 13 A). HPLC analysis of adenine nucleotides showed in *Tmem70*$^{-/-}$ embryos 2-fold decrease of ATP/ADP ratio (Figure 13 B). Immunodetection of antioxidants superoxide dismutases (SODs) revealed upregulation in the content of mitochondrial Mn-dependent SOD2 and in *Tmem70*$^{-/-}$ embryos. The same tendency was observed for Cu/Zn-dependent SOD1.

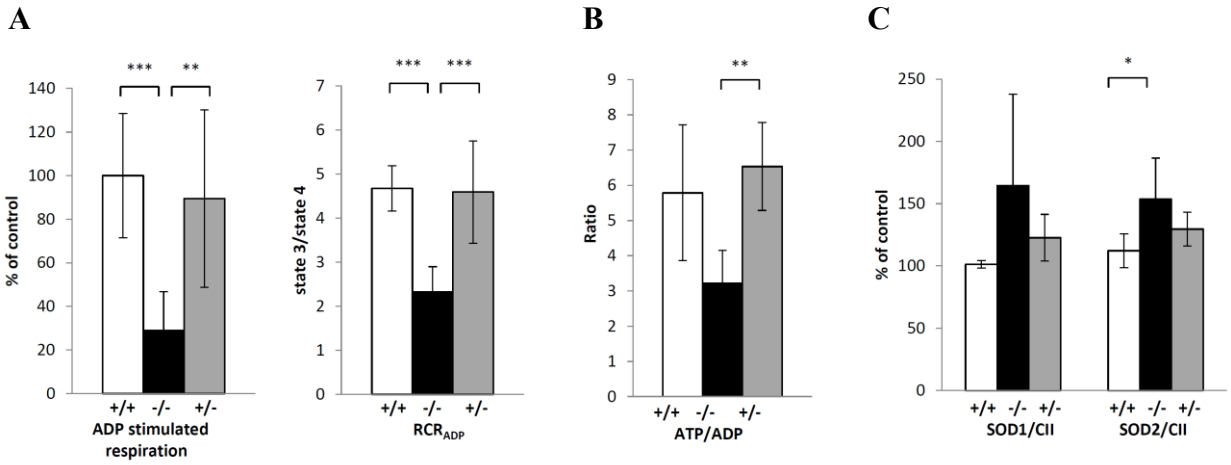

Figure 13. Altered mitochondrial energetic function in Tmem70$^{-/-}$ embryos. (A) *Seahorse oxygraphy of the whole embryo homogenates with respiratory substrates pyruvate + malate + succinate. ADP-stimulated, oligomycin-sensitive respiratory rates (normalized to CII content) and respiratory control ratio RCR$_{ADP}$.* ***(B)*** *ATP/ADP nucleotide content ratio in whole embryo extracts.* ***(C)*** *The level of superoxide dismutases in whole embryo extracts. SOD1 and SOD2 content was detected by SDS-PAGE and Western blot and normalised to CII content. Data are mean±SD, n ≥ 6 in **A**, 5 in **B**, 6 in **C**, Tmem70$^{+/+}$ (+/+), cTmem70$^{-/-}$ (-/-) and cTmem70$^{+/-}$ (+/-) E9.5 embryos were used. * p≤0.05, ** p≤0.01, *** p≤0.001.*

4.1.1.6 Affected postnatal heart phenotype of *Tmem70* heterozygous mice

Although c*Tmem70*$^{-/-}$ embryos were lethal, c*Tmem70*$^{+/-}$ mice were viable. We analysed them at the age of 5 and 14 weeks but no distinguishable differences were found in their growth parameters (body, heart weights) in comparison with *Tmem70*$^{+/+}$ littermates. BN-PAGE showed normal content of assembled ATP synthase without accumulation of F_1 intermediates, as well as normal content of respiratory chain complexes. Detailed characterisation of mitochondrial energetic function showed unchanged parameters of substrate oxidation (State 3-ADP, State 3-FCCP, ATP production, sensitivity to oligomycin). Similarly, measurements

of mitochondrial $\Delta\Psi_m$ did not reveal any changes at state 3 or state 4. For more information see the supplements of (Vrbacky et al., 2016).

Despite the lack of a biochemical phenotype, we observed mild systolic dysfunction of the cardiac left ventricle in c*Tmem70*$^{+/-}$ mice. Decrease of fractional shortening was detected in c*Tmem70*$^{+/-}$ mice compared to *Tmem70*$^{+/+}$ mice in both age groups (Table 5). In addition, the systolic wall thickness, which is related to a decreased fractional shortening, was significantly decreased at 14 weeks.

Table 5. Impaired heart function and growth parameters in c*Tmem70* $^{+/-}$ adult mice.

	5 weeks		**15 weeks**	
A	*Tmem70* $^{+/+}$	*cTmem70* $^{+/-}$	*Tmem70* $^{+/+}$	*cTmem70* $^{+/-}$
AWTd (mm)	0.62 ± 0.03	0.63 ± 0.04	0.70 ± 0.07	0.63 ± 0.05 *
LVDd (mm)	3.71 ±0.23	3.60 ± 0.17	4.30 ± 0.42	4.10 ± 0.36
PWTd (mm)	0.62 ± 0.06	0.64 ± 0.05	0.69 ± 0.08	0.62 ± 0.04 *
AWTs (mm)	1.02 ±0.08	0.98 ± 0.08	1.12 ± 0.09	0.94 ± 0.09 ***
LVDs (mm)	2.24 ± 0.18	2.33 ± 0.13	2.78 ± 0.33	2.89 ± 0.4
PWTs (mm)	1.06 ± 0.08	1.04 ± 0.11	1.13 ± 0.1	0.98 ± 0.1 **
FS (%)	39.41 ± 2.28	35.4 ± 2.56 **	35.5 ± 2.68	29.9 ± 4.26 **
HR	504 ± 49.2	521 ± 57	472 ± 38	501 ± 146
BW (g)	18.72 ± 1.61	18.85±0.87	28.56±2.17	28.42±1.75
HW (mg)	91±6.75	91±4.81	130±18.1	124±9.6
HW/BW (mg/g)	4.9±0.35	4.8±0.2	4.5±0.4	4.4±0.3

AWTd - diastolic anterior wall thickness, LVDd – left ventricle diastolic dimension, PWTd - diastolic posterior wall thickness, AWTs – systolic anterior wall thickness, LVDs – left ventricle systolic dimension, PWTs - systolic posterior wall thickness, FS – fractional shortening, HR - heart rate, BW - body weight and HW - heart weight parameters. Data are mean±SD values from 5-weeks-old mice (n=9) and 14-weeks-old mice (n=10-11); * $p<0.05$, ** $p<0.01$, *** $p<0.001$.

4.1.2 Inducible *Tmem70* knockout mouse (unpublished data)

4.1.2.1 Viability of i*Tmem70*$^{-/-}$ mice

As the constitutive knockout model of *Tmem70* was embryonic lethal, we further generated inducible constitutive knockout mice B6.Tmem70$^{tm1d(KOMP)Wtsi}$ (ROSA-Cre ERT2 x ACTFLPe/TMEM70; i*Tmem70*$^{-/-}$) to be able to study the presentation of TMEM70 deficiency on adult animal model. Induction of *Tmem70* knockout led to decrease of body weight (to 68 %) and food intake (to 84 %) and was lethal about 8 weeks after knockout induction (Figure 14 A). Heart weight (HW) and liver weight (LW) related to body weight did not differ between i*Tmem70*$^{-/-}$ and *Tmem70*$^{+/+}$ mice (Figure 14 B).

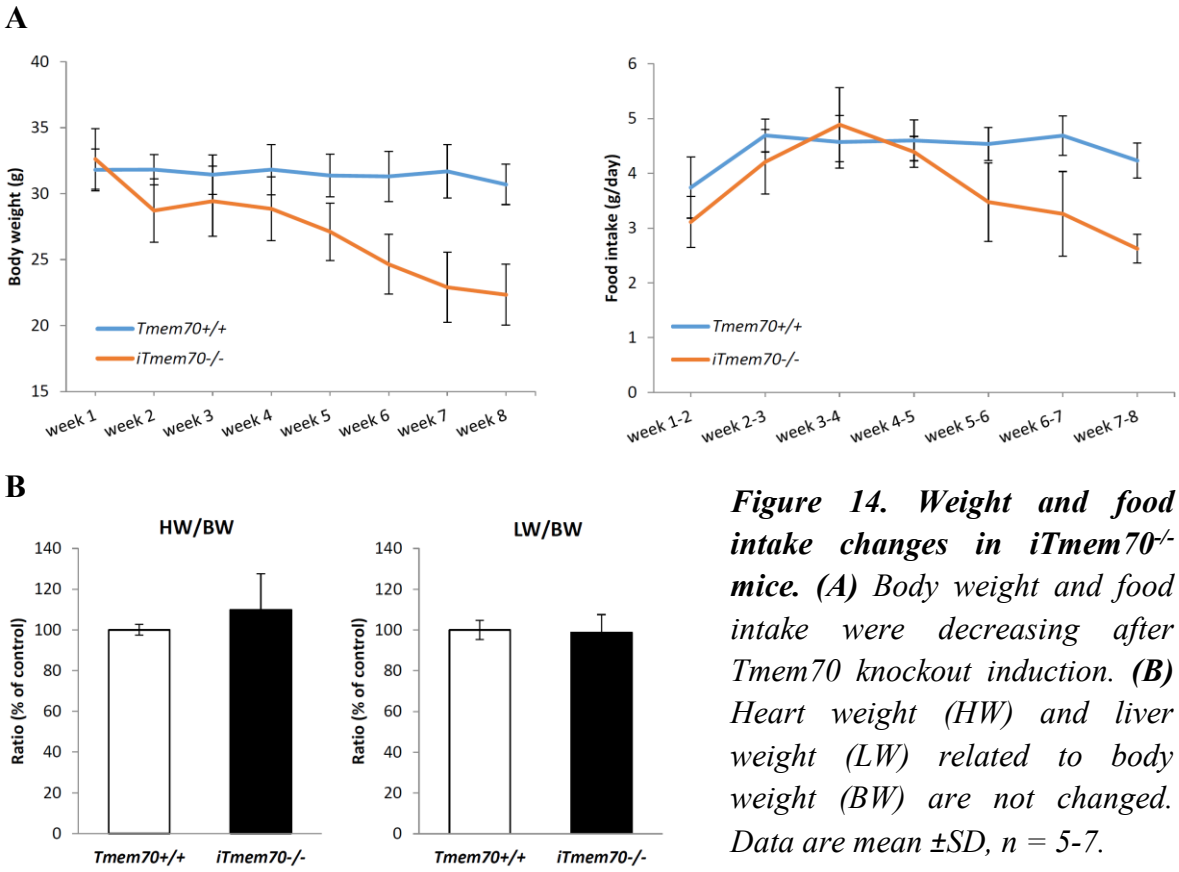

Figure 14. Weight and food intake changes in iTmem70$^{-/-}$ mice. ***(A)*** *Body weight and food intake were decreasing after Tmem70 knockout induction.* ***(B)*** *Heart weight (HW) and liver weight (LW) related to body weight (BW) are not changed. Data are mean ±SD, n = 5-7.*

4.1.2.2 Effectivity of *Tmem70* excision

We performed genotyping to analyse how effective was the excision of *Tmem70* in mouse tissues. We showed excision to be almost 100 % effective in most tissues but there was still some *Tmem70*$^{+/+}$ present in heart and brain (Figure 15 A). The expression of *Tmem70* quantified by RT-PCR was decreased both in liver and in heart of induced knockout mice. However, there was still more remaining *Tmem70* gene in heart (25±22 % relative to control animals) when compared to liver. Moreover, result demonstrates lower expression of *Tmem70* in liver tissue in comparison to heart (Figure 15 B), the tissue with higher energetic demands.

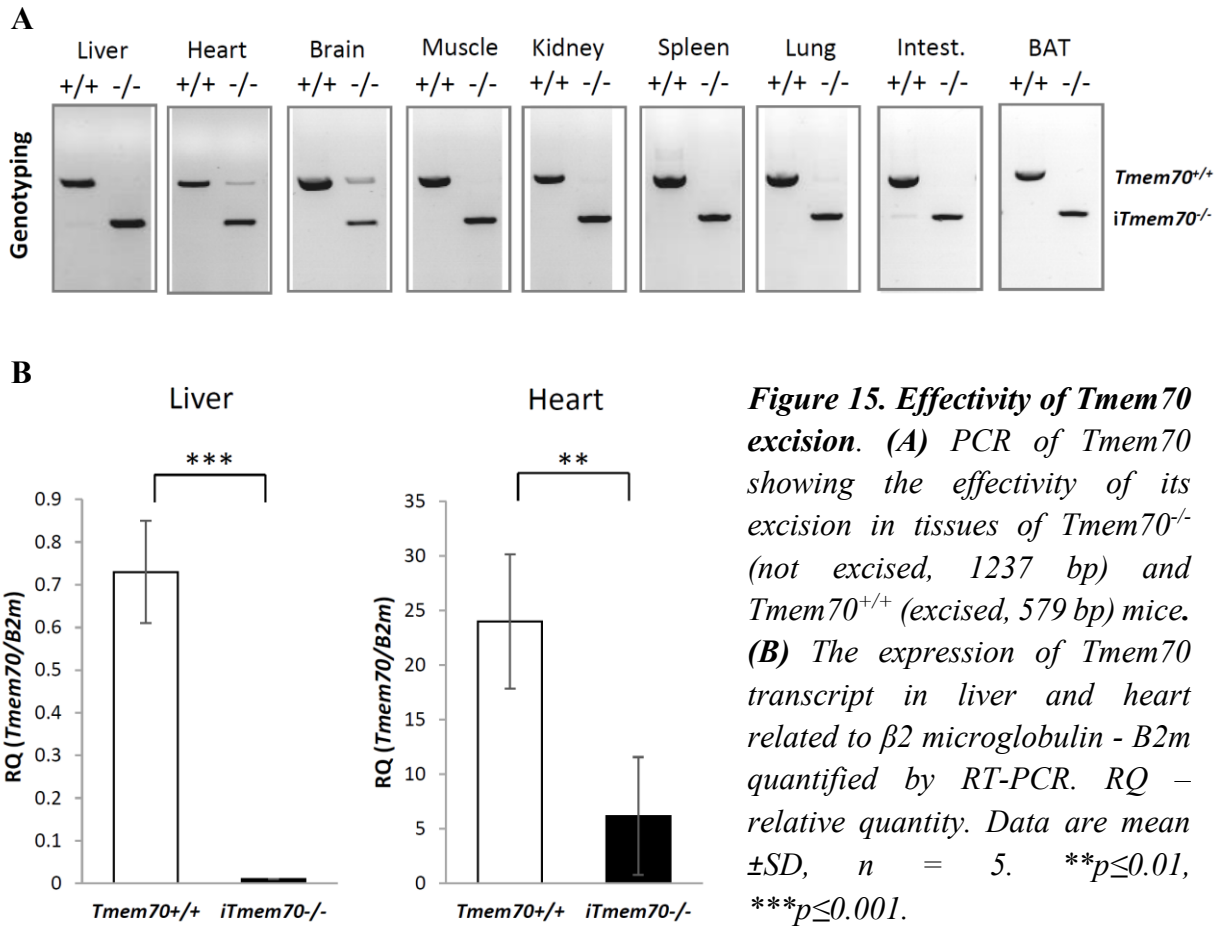

Figure 15. Effectivity of Tmem70 excision. ***(A)*** *PCR of Tmem70 showing the effectivity of its excision in tissues of Tmem70*$^{-/-}$ *(not excised, 1237 bp) and Tmem70*$^{+/+}$ *(excised, 579 bp) mice.* ***(B)*** *The expression of Tmem70 transcript in liver and heart related to β2 microglobulin - B2m quantified by RT-PCR. RQ – relative quantity. Data are mean ±SD, n = 5. **p≤0.01, ***p≤0.001.*

4.1.2.3 ATP synthase isolated deficiency i*Tmem70*$^{-/-}$ mice

To see the effectivity of *Tmem70* excision on ATP synthase biogenesis in different tissues (liver, heart, brain, muscle, kidney, spleen, lung, intestine, brown adipose tissue) and compare it with result on c*Tmem70*$^{-/-}$ embryos we performed native electrophoreses. Tissue homogenates of *Tmem70*$^{+/+}$ and i*Tmem70*$^{-/-}$ mice solubilised by n-dodecyl-β-D-maltoside (2g/g of protein) were separated by BN-PAGE. Subsequent Western blotting and immunodetection of F_1-α subunit showed that ATP synthase assembly is impaired with F_1 subcomplex accumulation in all tissues except heart. Interestingly, in brain we observed accumulation of F_1 subcomplex in i*Tmem70*$^{-/-}$ although, similarly to heart, there was still considerable quantity of non-excised *Tmem70* gene. ATPase in-gel hydrolytic activity assay performed on liver and heart homogenates, representing two extreme states, showed the same pattern (Figure 16 A).

Further analyses of mitochondria and ATP synthase assembly were done on heart and liver as two key organs with different amounts of ATP synthase. Heart represents organ with high energy demands but less impaired ATP synthase in i*Tmem70*$^{-/-}$ mice. On the other hand, liver represent the centre of metabolism with less ATP synthase which is highly affected in i*Tmem70*$^{-/-}$ mice. Thus, these tissues are suitable for deeper analysis of ATP synthase biogenesis.

To analyse ATP synthase biogenesis in detail we performed electrophoresis of liver homogenate under milder conditions. Surprisingly, hrCN-PAGE showed on samples solubilised by digitonin (2 g/g of protein) two more subcomplexes of ATP synthase, which were not observed in any of our previous models (Cizkova et al., 2008, Vrbacky et al., 2016). All observed subcomplexes contain F_1-α subunit but not F_o-c subunit (Figure 16 B). All three subcomplexes were also observed when using in-gel ATP synthase hydrolytic activity (Figure 16 B). Moreover, ATPase hydrolytic activity measured spectrophotometrically was decreased in the liver of i*Tmem70*$^{-/-}$ mice to 10 % of controls (Figure 16 C).

Because of the inter-individual variability of *Tmem70* excision efficiency in hearts of tested animals, we further decided to look at them individually and not at the cohort level. The content of accumulated F_1 subcomplex in heart homogenates of i*Tmem70*$^{-/-}$ mice differed among individual mice (Figure 17 A). The F_1 accumulation correlated with the level of *Tmem70* deficiency and with protein levels of F_1-γ and F_o-b subunits of ATP synthase (Figure 17 B; Table 6).

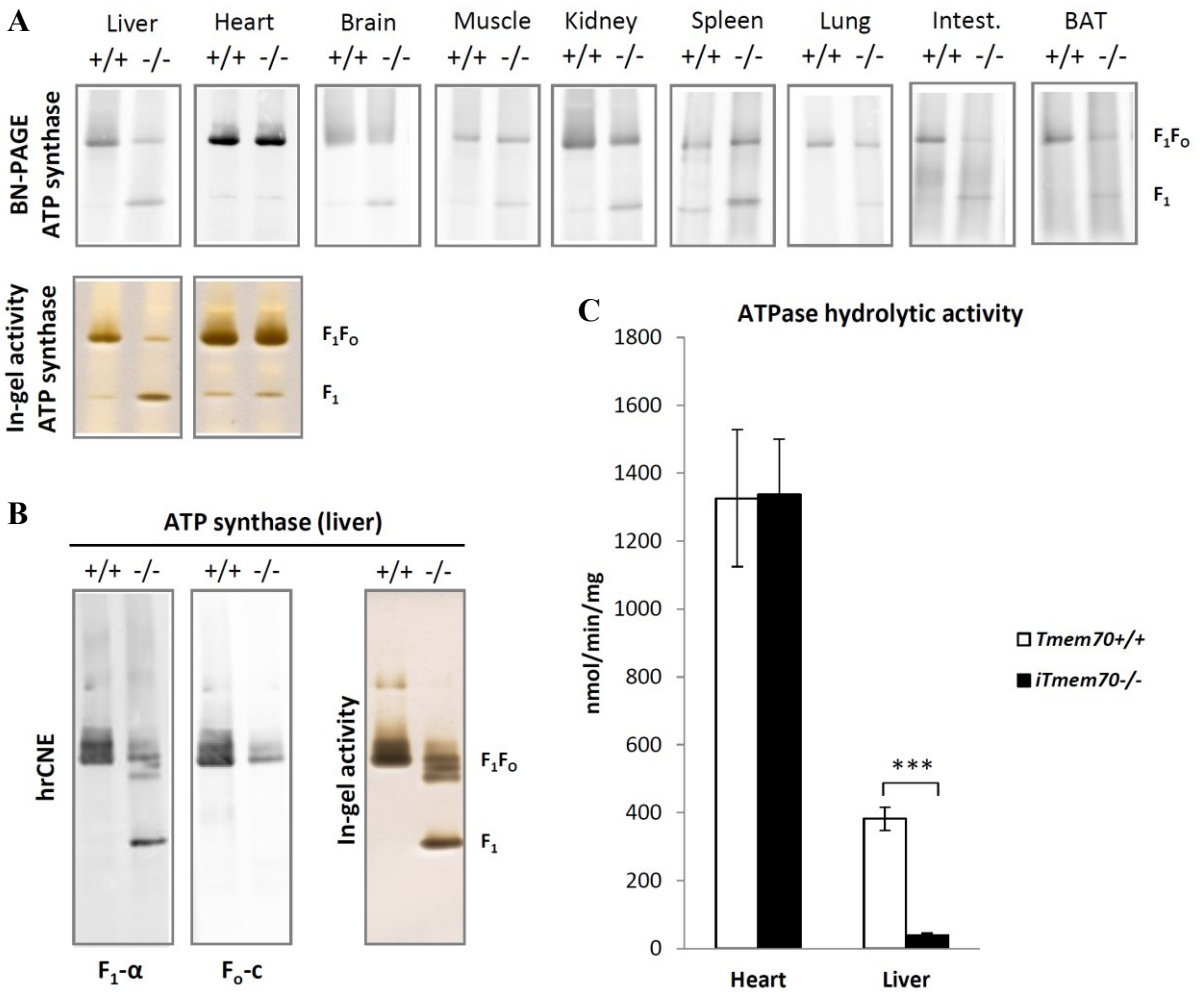

Figure 16. ATP synthase deficiency in iTmem70$^{-/-}$ mice. (A) *Impaired ATP synthase assembly in Tmem70$^{-/-}$ (-/-) mouse tissues analysed by BN-PAGE (samples solubilised by n-dodecyl-β-D-maltoside) and* ***(B)*** *in liver by hrCN-PAGE (samples solubilised by digitonin). ATP synthase was detected on western blots using antibody against F_1-α and F_o-c subunits or in gels by ATPase in-gel activity.* ***(C)*** *ATPase hydrolytic activity measured by spectrophotometer in iTmem70$^{-/-}$ (-/-) and Tmem70$^{+/+}$ (+/+) mice. Data are mean ±SD, n = 4-5. ***p≤0.001.*

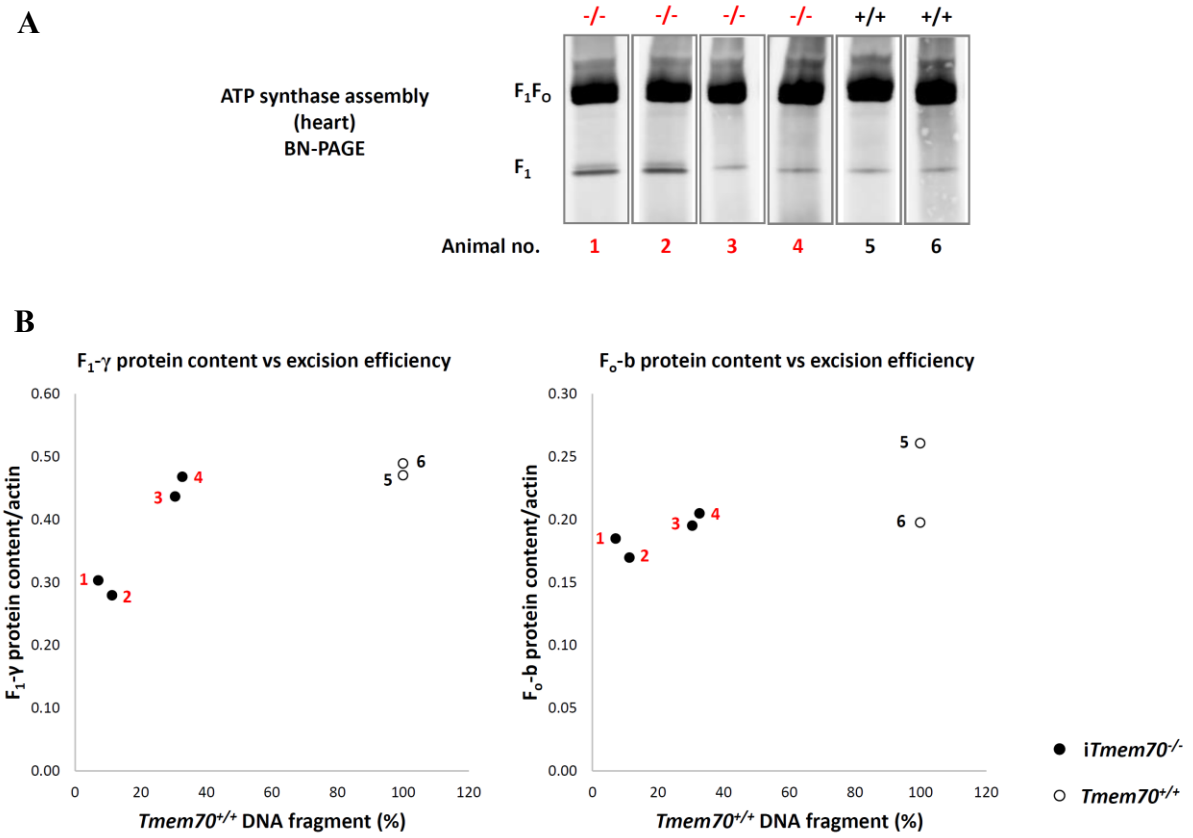

Figure 17. ATP synthase assembly and Tmem70 excision efficiency in heart. ***(A)*** *BN-PAGE analysis of ATP synthase assembly and F_1 accumulation in 4 iTmem70$^{-/-}$(1, 2, 3, 4 – black dots) and 2 Tmem70$^{+/+}$(5, 6 – black circles) mice.* ***(B)*** *Correlation of the content of PCR Tmem70 gene product (DNA fragment) in individual mice and their protein levels of ATP synthase subunits F_1-γ and F_o-b (related to actin) quantified by SDS-PAGE in heart mitochondria.*

Regarding the levels of other OXPHOS complexes, we analysed protein levels of representative subunits in liver mitochondria in control and *iTmem70*$^{-/-}$ mice. We found that subunits of CI (NDUFA9), CII (SDHA) and CIV (COX1 and COX4) were increased, while the content of CIII (Core 2) did not change. Subunits of CV (F_1-α, F_1-γ, F_o-b, F_o-c) were markedly decreased. When related to actin level, result is similar except subunit COX1 of complex IV, whose increase in this case did not reach statistical significance (Table 6). Analogous analysis on heart samples did not show any differences in OXPHOS complexes content (not shown).

Table 6. Protein content of subunits of protein OXPHOX complexes in liver.

	Protein content	**Per actin**
	% control ± SD	**% control ± SD**
CI (NDUFA9)	209±26***	204±34***
CII (SDHA)	159±27**	154±23**
CIII (Core 2)	108±8	105±9
CIV (COX1)	134±16**	131±28
CIV (COX4)	180±39**	175±33**
CV (F_1-α)	45±10***	44±10***
CV (F_1-γ)	24±11***	23±11***
CV (F_o-b)	24±6***	23±5***
CV (F_o-c)	17±4***	19±6***

*SDS-PAGE. Data are mean ±SD from 5 i$Tmem70^{-/-}$ and 4 $Tmem70^{+/+}$ mice. **p≤0.01, ***p≤0.001.*

4.1.2.4 Altered mitochondrial energetic function in i*Tmem70*$^{-/-}$ mice

To test the effect of ATP synthase defect on the mitochondrial function we analysed the respiration by Oxygraph O2k (Oroboros, Austria). Addition of cytochrome c led to systematically higher increase of oxygen consumption by liver mitochondria in homogenate of i$Tmem70^{-/-}$ mice to 178 % of increase in $Tmem70^{+/+}$ mice (Figure 18 A) indicating broken OMM. Maximal respiration with cytochrome *c*, pyruvate, malate, succinate and ADP did not differ between i$Tmem70^{-/-}$ *and* $Tmem70^{+/+}$ mice and inhibition of ATP synthase i$Tmem70^{-/-}$ by oligomycin was very low (not shown), which may point to damaged, uncoupled mitochondria. Respiratory control ratio (RCR) (State 3/State 4) in $Tmem70^{-/-}$ embryos decreased to 35 % of controls (Figure 18 B). Respiration of heart mitochondria was not affected (not shown).

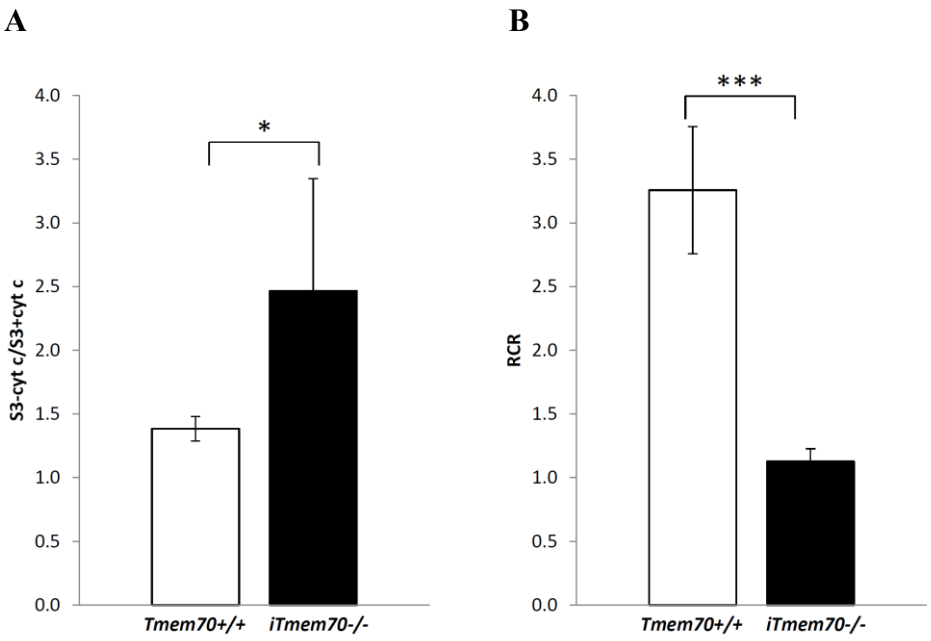

***Figure 18. Altered mitochondrial energetic function in induced Tmem70 knockout mice**. **(A)** Higher activation of oxygen consumption by cytochrome c in mitochondria of liver homogenate of iTmem70$^{-/-}$ mice **(B)** and decreased respiratory control ratio (RCR) in iTmem70$^{-/-}$ mice in comparison to Tmem70$^{+/+}$measured by oxygraphy. Data are mean ±SD from 5 animals in each group. *p≤0.05, ***p≤0.001.*

4.1.2.4 Oxidative stress in i*Tmem70*$^{-/-}$ mice

It was previously suggested that ATP synthase dysfunction is connected with increase of ROS production (Mracek et al., 2006) and indeed, c*Tmem70*$^{-/-}$ embryos had increased level of the matrix antioxidant superoxide dismutase 2 (SOD2) (see Figure 13). This was also confirmed in i*Tmem70*$^{-/-}$ liver. Defect in oxidative phosphorylation in liver led to the increase of SOD2 (161±25 % of controls), which indicates production of ROS. Superoxide dismutase 1 (SOD1) level were not changed (Figure 19 A). In addition, reduced antioxidant glutathione (GSH) supports the hypothesis of increased ROS production in liver of i*Tmem70*$^{-/-}$, because its levels were decreased to 64±10 % of *Tmem70*$^{+/+}$ due to its oxidation (Figure 19 B).

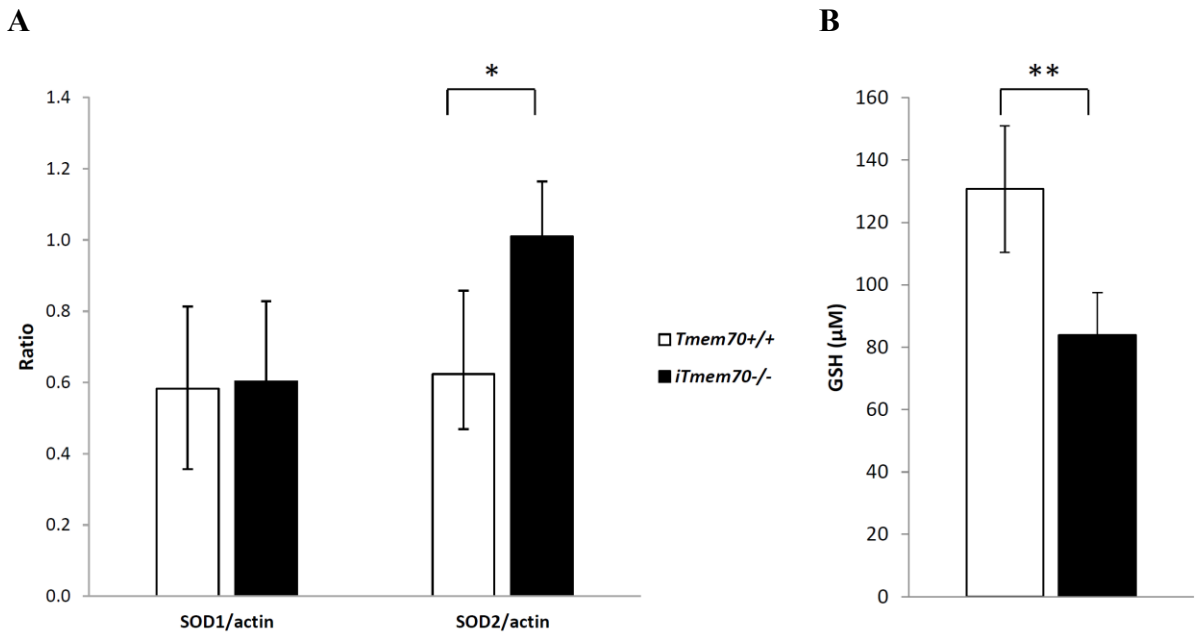

Figure 19. Oxidative stress in induced iTmem70$^{-/-}$ mice. (A) *Changes in antioxidants superoxide dismutases (SOD1 and SOD2) related to actin analysed by SDS-PAGE in mouse liver homogenates after knockout induction.* ***(B)*** *Change in reduced antioxidant glutathione (GSH) in iTmem70$^{-/-}$ liver homogenates. Measured by fluorescence assay. Data are mean ±SD from 5 animals in each group. *p≤0.05, **p≤0.01.*

4.1.2.5 Physiological parameters in liver of i*Tmem70*$^{-/-}$ mice

Liver mitochondria damage led to mild defect, which was indicated by liver fragility but also by increased plasma levels of alanine aminotransferase (ALT) and aspartate aminotransferase (AST) (Table 7). Increase of these markers indicate damaged cytoplasmic membrane of hepatocytes. Increase of NH_4^+ (hyperammonenmia) also indicates damage of liver due to urea cycle impairment. Moreover, haematological analysis revealed decrease in red and white blood cells. On the other hand, number of platelets was markedly increased (Table 7).

That the liver damage is linked to increased apoptosis was shown by significantly higher activities of pro-apoptotic enzymes caspase-3 and caspase-8. Caspase-3 increased in i*Tmem70*$^{-/-}$ liver to 225±104 % of controls and caspase-8 to 114±4.6 % (Figure 20). Caspase-9 was not changed (data not shown).

Table 7. Blood and plasma analysis.

Haematology		
	***Tmem70*$^{+/+}$**	***iTmem70*$^{-/-}$**
Red blood cells (10^{12}/l)	9.35±0.15	6.89±0.66 ***
White blood cells (10^{9}/l)	5.87±0.77	0.96±0.39 ***
Platelets (10^{9}/l)	965.25±108.97	1449.67±148.06 **
Haematocrit	0.45±0.01	0.34±0.03 ***
Plasma biochemistry		
	***Tmem70*$^{+/+}$**	***iTmem70*$^{-/-}$**
NH_4^+ (µmol/l)	36.43±13.06	106.83±43.28 **
ALT (U/l)	21.18±4.12	44.82±11.32 **
AST (U/l)	34.47±6.38	70±14.65 **

ALT - alanine aminotransferase, AST - aspartate aminotransferase
Data are mean ±SD from 5 animals in each group. **p≤0.01, ***p≤0.001.

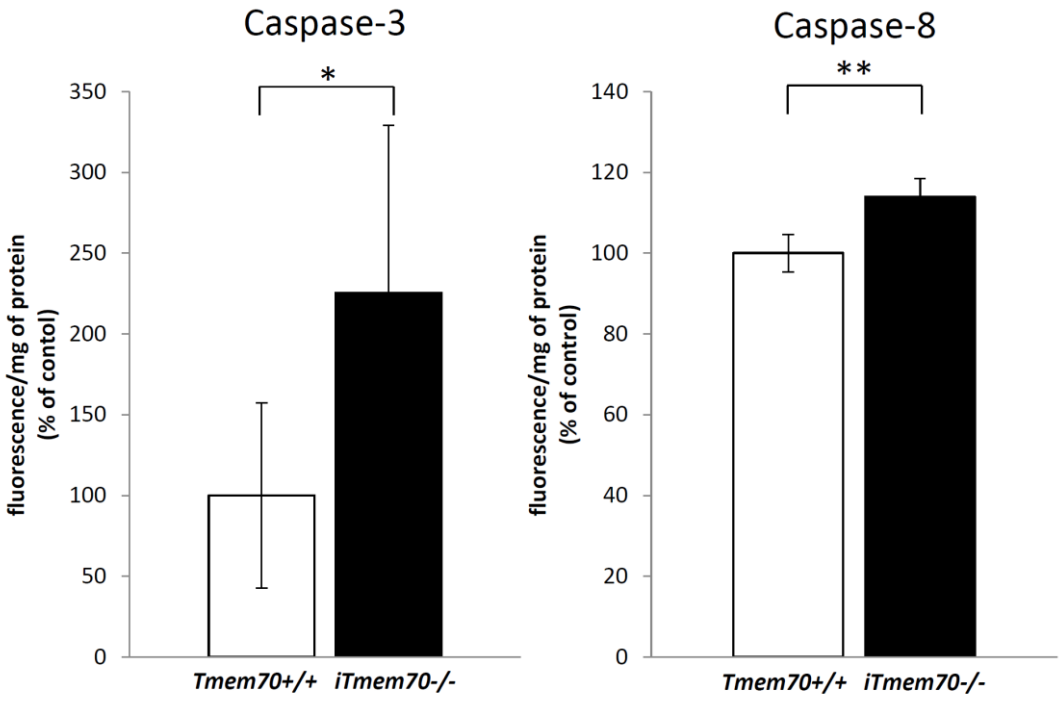

Figure 20. Increased apoptosis in induced iTmem70$^{-/-}$ mice. *Activities of caspase-3 and caspase-8 in Tmem70$^{+/+}$ and iTmem70$^{-/-}$ mouse liver homogenate. Measured by fluorescence assay. Data are mean ±SD from 5 animals in each group. *p≤0.05, **p≤0.01.*

4.2 Effect of DAPIT deficiency in rats (aim 2, unpublished data)

4.2.1 Lower body weight and heart hypertrophy of DAPIT deficient rats

Protein DAPIT, which is a new subunit of ATP synthase coded by nDNA gene *Usmg5*, was the second mitochondrial protein I focused on in this thesis. Our goal was to evaluate its role and position in ATP synthase complex. To achieve this, we generated *Usmg5*$^{-/-}$ deficient rats by zinc finger nucleases technology. *Usmg5*$^{-/-}$ rats were fully viable, albeit of smaller body size (Figure 21 A). Their body weight was 20-30 % lower in comparison to controls (*Usmg5*$^{+/+}$) (Figure 21 B). Moreover, *Usmg5*$^{-/-}$ rats had selective hypertrophy of right heart ventricle (RV) (127±21 % of controls) when related to body weight (Figure 21 C). On the other hand, they had decreased weight of epidydimal white adipose tissue (80±6 % of controls) and decrease of triglycerides in liver (86±6 %) (Figure 21 C).

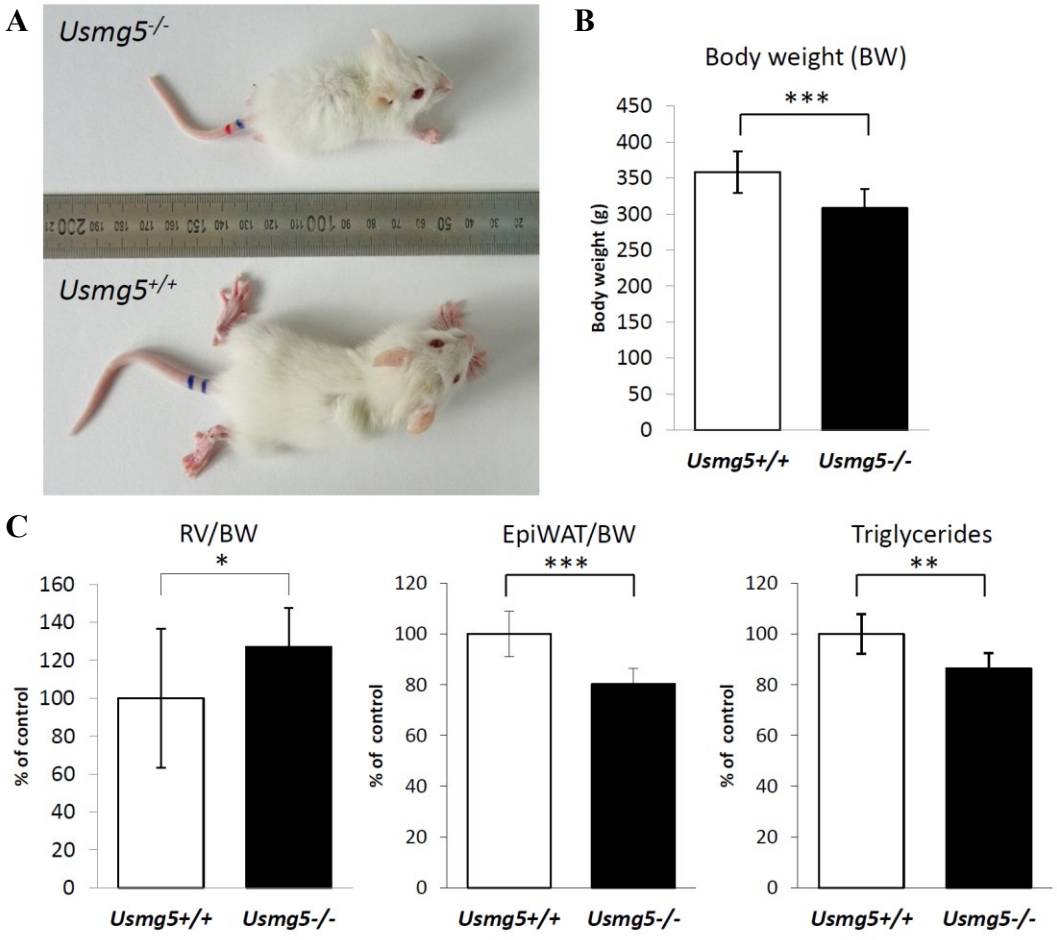

Figure 21. Body parameters of Usmg5$^{-/-}$ rats. (A) *Body size of Usmg5*$^{-/-}$ *rats and their controls (5-week-old).* ***(B)*** *The body weight (BW),* ***(C)*** *heart right ventricle (RV) weight, epididymal white adipose tissue weight (epiWAT) related to BW and level of triglycerides in liver of 6 months old rats. Data are mean ±SD from 16-18 animals in each group. *p≤0.05, **p≤0.01, ***p≤0.001.*

4.2.2 Affected heart function in DAPIT deficient rats

With regard to heart RV hypertrophy we tested rat heart function by echocardiography. It showed generalised heart dysfunction in *Usmg5*$^{-/-}$ rats presented by lower fractional shortening of left heart ventricle which was 84±10 % of controls (Figure 22 A). We also observed a pronounced change in pulmonary blood flow (pulmonary artery maximal velocity) which was in *Usmg5*$^{-/-}$ rats 166±80 % of their controls and was suggestive of pulmonary arterial hypertension (PAH) (Figure 22 B).

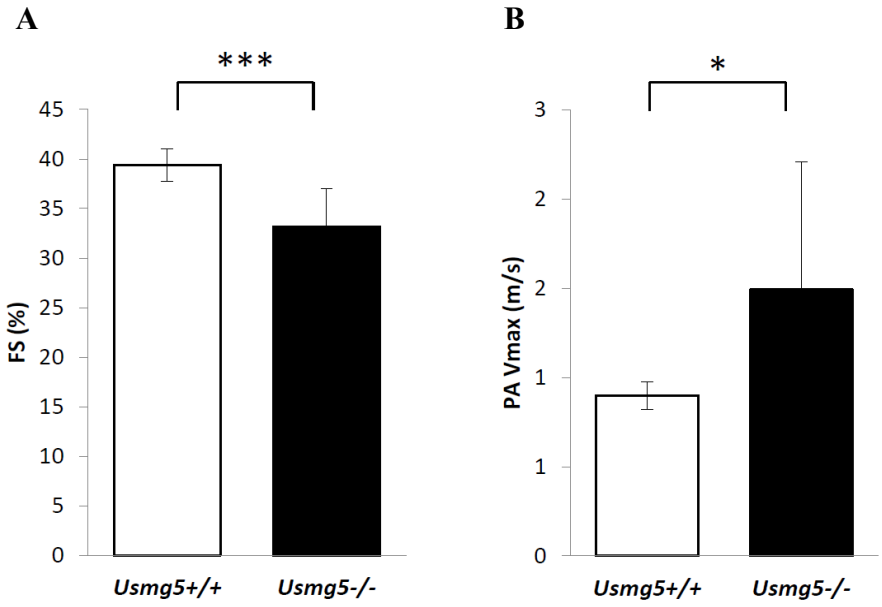

Figure 22. Affected heart function in DAPIT knockout rats. *Fractional shortening (FS) of heart left ventricle* ***(A)*** *and pulmonary artery maximal velocity (PA Vmax)* ***(B)*** *of Usmg5*$^{-/-}$ *and Usmg5*$^{+/+}$ *rats measured by echocardiography. Data are mean ±SD from 8 animals in each group. *p≤0.05, ***p≤0.001.*

4.2.3 ATP synthase defect in DAPIT deficient rats

BN-PAGE showed normal levels of ATP synthase in heart of *Usmg5*$^{-/-}$ rats. ATP synthase holoenzyme in *Usmg5*$^{-/-}$ animals was slightly smaller and apparently more labile, as judged by minor accumulation of F_1 subcomplex. Most interestingly, in *Usmg5*$^{-/-}$ animals we observed less dimers of ATP synthase (Figure 23 A). Subunit composition of ATP synthase monomers and dimers did not differ between *Usmg5*$^{-/-}$ and *Usmg5*$^{+/+}$ rats except of missing DAPIT subunit in *Usmg5*$^{-/-}$ rats (Figure 23 B). Spectrophotometrically measured ATPase (hydrolysing) activity was reduced but significantly only in liver to 81±8 % of controls (Figure 23 C).

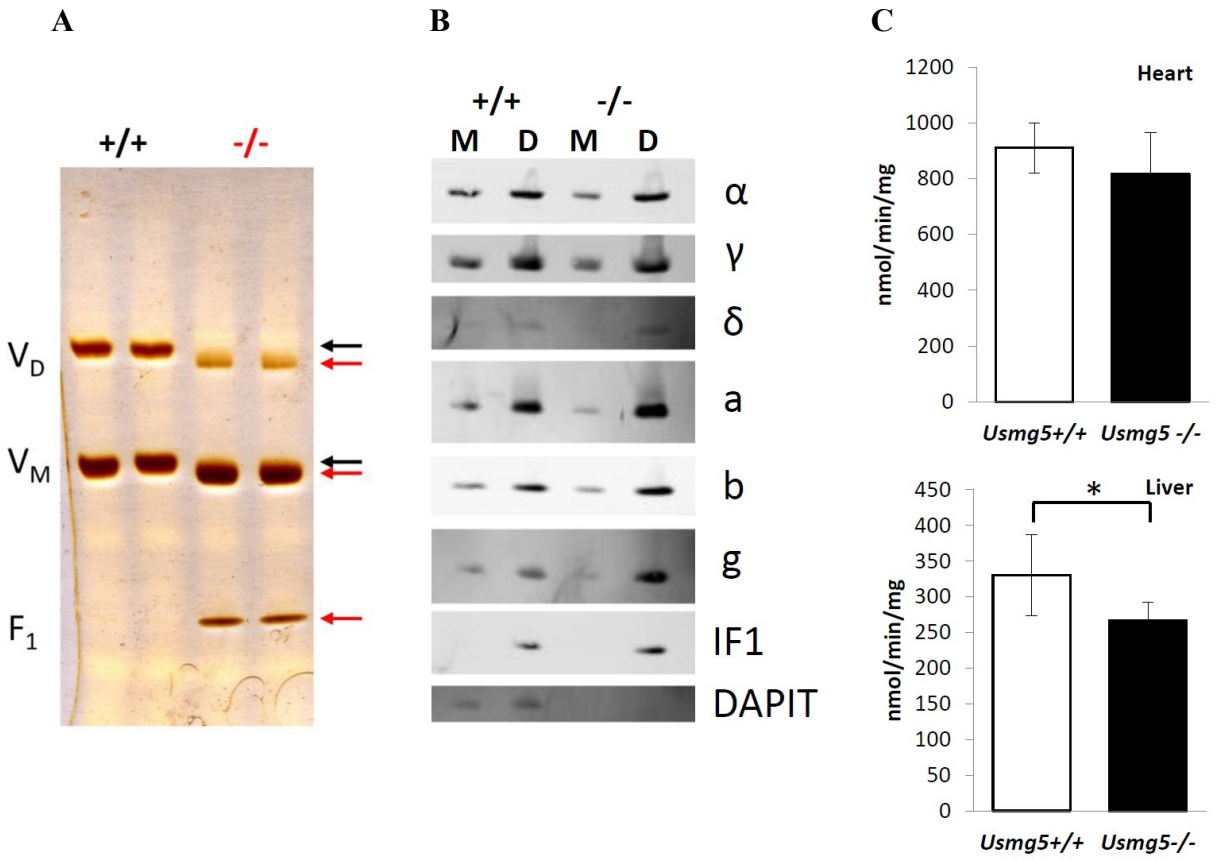

Figure 23. ATP synthase defect in Usmg5*$^{-/-}$ *rats. (A) *Heart ATPase of Usmg5*$^{-/-}$ *and Usmg5*$^{+/+}$ *detected by in-gel ATPase hydrolytic activity on gels after BN-PAGE (samples solubilised by digitonin). V_D - dimer of ATP synthase, V_M - monomer of ATP synthase, F_1 - subcomplex of ATP synthase.* ***(B)*** *Subunit composition of heart ATP synthase of Usmg5*$^{-/-}$ *and Usmg5*$^{+/+}$ *detected by SDS-PAGE. ATP synthase monomer (M) and dimer (D).* ***(C)*** *Spectrophotometrically measured ATPase hydrolytic activity in heart and liver homogenates. Data are mean ±SD from 8 animals in each group. *p≤0.05.*

ADP phosphorylating activity (state 3 respiration) measured by Oxygraph O2k was reduced in heart to 89±7 % and in liver to 91±2 % of controls (Figure 24). This ADP phosphorylating activity was titrated with ATP synthase F_o part inhibitor oligomycin or F_1 part inhibitor aurovertin. Interestingly, sensitivity to oligomycin was significantly higher in *Usmg5*$^{-/-}$ heart and liver in comparison to controls while aurovertin did not have any such effect and inhibited *Usmg5*$^{-/-}$ similarly to controls in both tissues (Figure 25).

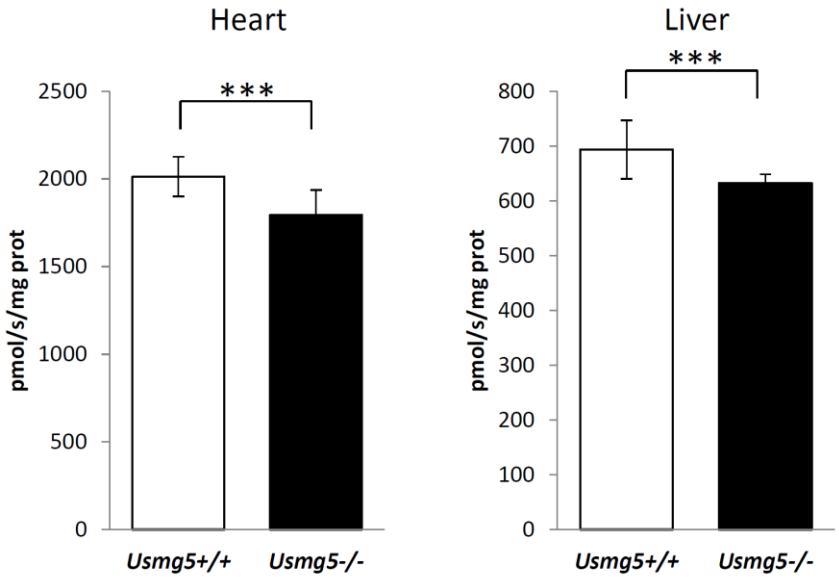

Figure 24. Altered energetic function in Usmg5$^{-/-}$ rats. *Maximal respiration of mitochondria in heart and liver homogenates in state 3 with substrates pyruvate, malate, and succinate and with cytochrome c and ADP measured by oxygraphy. Data are mean ±SD from 8 animals in each group. ***p≤0.001.*

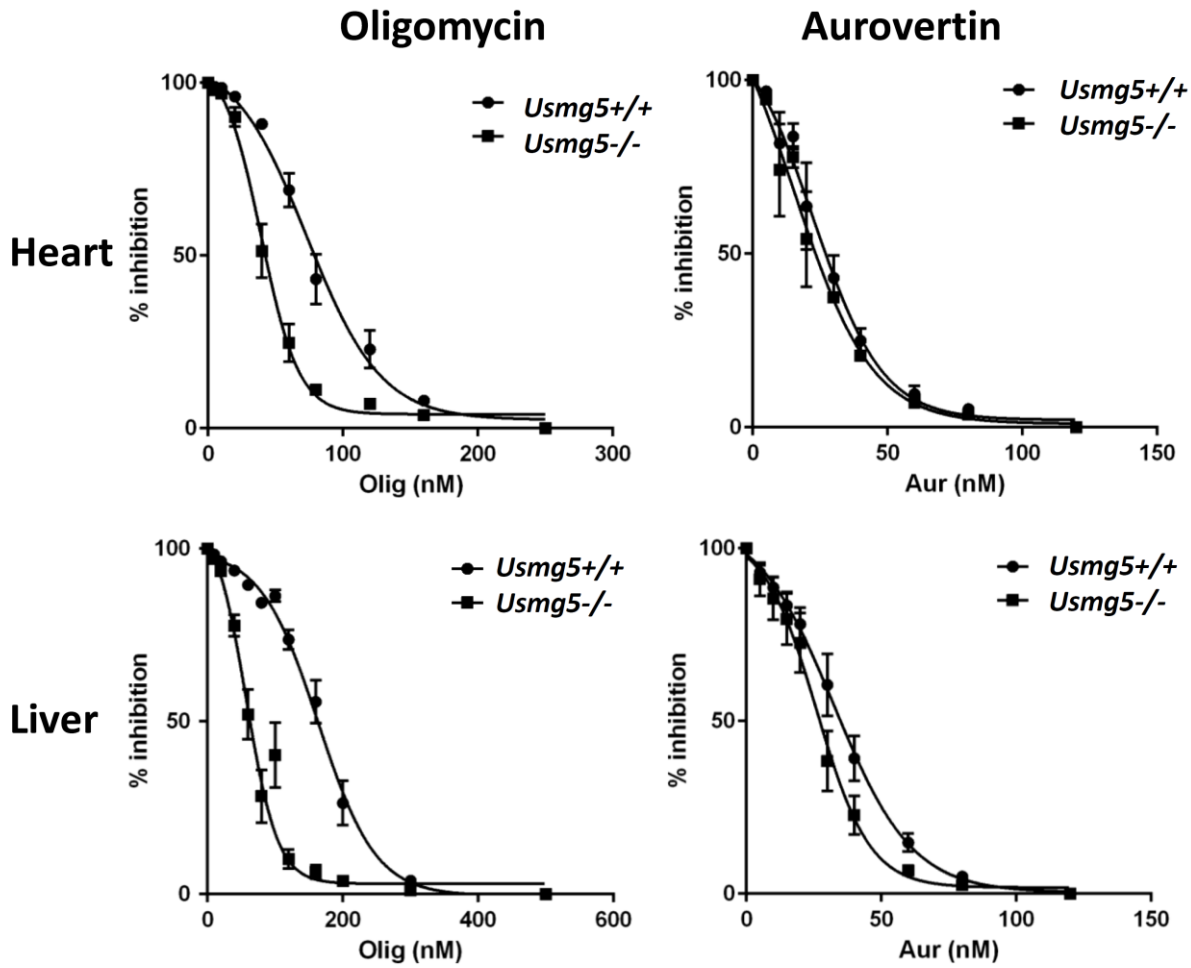

Figure 25. ATP synthase inhibition in Usmg5$^{-/-}$ rats. *Titration of maximal respiration of mitochondria in heart and liver homogenates in state 3 with substrates pyruvate, malate, and succinate and with cytochrome c and ADP with ATP synthase inhibitors oligomycin (F_o part inhibitor) or aurovertin (F_1 part inhibitor). Measured by oxygraphy. Data are mean ±SD from 6 animals in each group.*

4.3 Components of mitochondrial ATP synthasome in fibroblasts of patients with ATP synthase deficiency (aim 3, publication B)

It was proposed that ATP synthase forms higher structures. We decided to systematically explore the existence of putative ATP synthasome, which should be composed of ATP synthase, ANT and PiC. To achieve this, we decided to study tissues with varying amount of ATP synthase and cells from patients with ATP synthase deficiencies. In rat tissues we showed that the expression of mitochondrial carriers ANT and PiC is transcriptionally controlled in accordance with the ATP synthase amount. We demonstrated interaction of both ANT and PiC with ATP synthase but such association was minuscule one. Only 3 % of ANT and 16 % of PiC were incorporated into ATP synthasome and the majority exists as separate entities (Nuskova et al., 2015). To find out whether altered ATP synthase content change the proportion of PiC and ANT in fibroblasts of patients, we compared patients with decreased content of fully assembled ATP synthase (mutations in *TMEM70* and *ATP5E* - F_1-ε subunit) and patients with normal amount of assembled ATP synthase without ability to synthesise ATP (mutation in *MT-ATP6* - F_o-a subunit). The protein content of ANT and PiC was increased, respectively, to 150-240 % and 117-250 % of controls regardless of the different genetic origin or clinical and biochemical manifestation of ATP synthase defect (Figure 26 A). The relation of ANT and PiC to ATP synthase subunit F_1-β showed that ATP synthase dysfunctions are associated with an up to 7-fold increase between the carriers and ATP synthase (Figure 26 B). Moreover, we confirmed these results in liver homogenates of i*Tmem70*$^{-/-}$ mouse model. The level of ANT was increased when related to SDHA or content of ATP synthase (F_1-β) (Figure 26 C, D; Table 8).

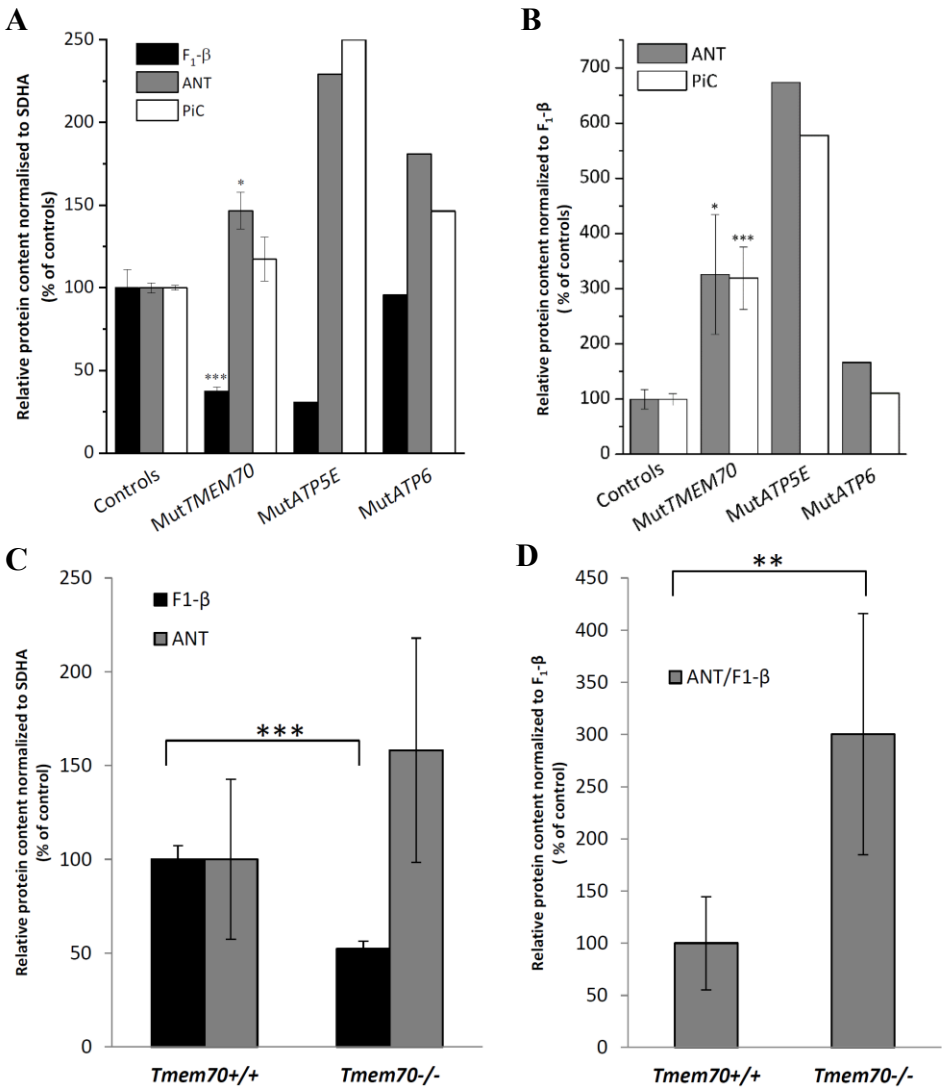

Figure 26. Components of mitochondrial ATP synthasome in fibroblasts of patients and mice with ATP synthase deficiency. ***(A)*** *SDS-PAGE of the protein content of ATP synthase subunit F_1-β, ANT and PiC in mitochondria from human fibroblasts of healthy controls, patients with mutated TMEM70 (mutTMEM70), ATPE (mutATP5E), and MT-ATP6 (mutATP6) analysed by western blots normalised to SDHA (complex II, CII) and* ***(B)*** *ANT and PiC normalised to F_1-β. Data are mean ±SD from 3 controls and 7 patients of mutTMEM70, mutATPE and mutATP6 represent multiple cultures of one patient each.* ***(C)*** *Protein content of ANT and F_1-β in $Tmem70^{+/+}$ and $iTmem70^{-/-}$ mouse liver homogenates normalised to SDHA and* ***(D)*** *protein content of ANT normalised to the ATP synthase content represented by F_1- β. Data are mean ±SD from 5 animals in each group. *p≤0.05, ***p≤0.001.*

Table 8. Protein content of ADP/ATP translocase (ANT) in i*Tmem70*$^{-/-}$ *mice.*

	Per SDHA	**Per actin**	**Per F_1-β**
ANT(% control ± SD)	158±60	226±91*	300±116**

*Data are mean ±SD from 5 $iTmem70^{-/-}$ and 5 $Tmem70^{+/+}$ mice. *p≤0.05, **p≤0.01.*

4.4 ATP synthase 'threshold' in ATP synthase deficiencies (aim 4, manuscript prepared for submission)

In general, in many cases of nuclear ATP synthase defects (including *Tmem70* mutations), the observed residual amount of the enzyme is approximately 30 % or less of controls (Houstek et al., 1999, Mayr et al., 2004, Sperl et al., 2006, Mayr et al., 2010). Constitutive mouse knockout of *Tmem70* and inducible *Tmem70* knockout led also to similar ATP synthase content decrease (chapter 3.1). To elucidate if there are any thresholds of ATP synthase deficiency in dependence on mitochondrial function and oxidative stress we produced range of clones of ATP synthase stalk subunits γ, δ, ε to cover the whole range of residual ATP synthase content and analysed functional parameters.

4.4.1 Knockdown of ATP synthase central stalk subunits - clone characterisation

From selected clones were chosen 9 clones (C1-C9) with different knockdown efficiency to cover the range of ~20 to 100 % of residual ATP synthase. These clones had differently lowered protein content of fully assembled ATP synthase (Figure 27). Knockdown clones contained 15-90 % of assembled ATP synthase compared to control clones. ATP synthase content correlated with the in-gel ATPase hydrolytic activity ATPase hydrolytic activity (Figure 27). Taken together, among 9 screened clones, the lowest ATP synthase content was approximately 15 %.

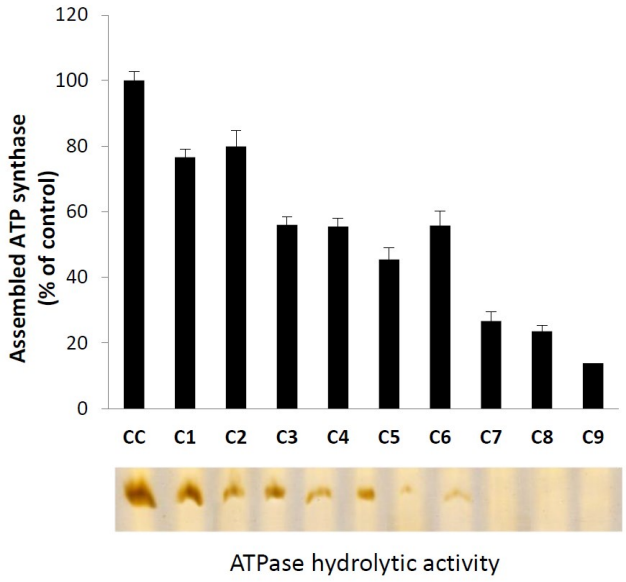

Figure 27. ATP synthase decrease in knockdown clones. *ATP synthase content (BN-PAGE, n-dodecyl-β-D-maltoside 2 g/g of protein) related to protein content (data are mean ±SEM from 5 repeated experiments) and in-gel ATPase hydrolytic activity after BN-PAGE in 9 clones of F_1-γ, F_1-δ and F_1-ε of HEK293 cells. CC- control HEK293 cells.*

4.4.2 Cellular energetics and ROS production in relation to residual ATP synthase activity

Cellular energetics was examined by Seahorse XF^{e}24 Analyzer. A decrease in the oligomycin-sensitive portion of basal respiration of intact cells (47 vs. 61 % in controls) was accompanied by an increase in the glycolytic flux (up to 20 %). The subsequent correlation of the basal respiratory rate, glycolytic flux and residual ATPase hydrolytic activity (measured spectrophotometrically) showed that clones with less than 30 % of residual ATPase activity switched their metabolism to enhanced glycolysis (Figure 28 A). On the other hand, clones with more than 30 % of residual activity showed no change in the respiration or in their basal glycolytic rate.

Due to ATP synthase deficiency, the knockdown clones exhibited reduced dissipation of $\Delta\Psi_m$ under ADP stimulation by up to 20 mV compared to controls (not shown). As a result of membrane hyperpolarisation, knockdown clones produced ROS. Their production was elevated by 23 % of controls in the most affected clones in comparison to controls (Figure 28 B). Basal ROS production also negatively correlated with residual ATPase hydrolytic activity. There was a threshold of 30 % residual ATP synthase for stimulation of ROS production (Figure 28 B).

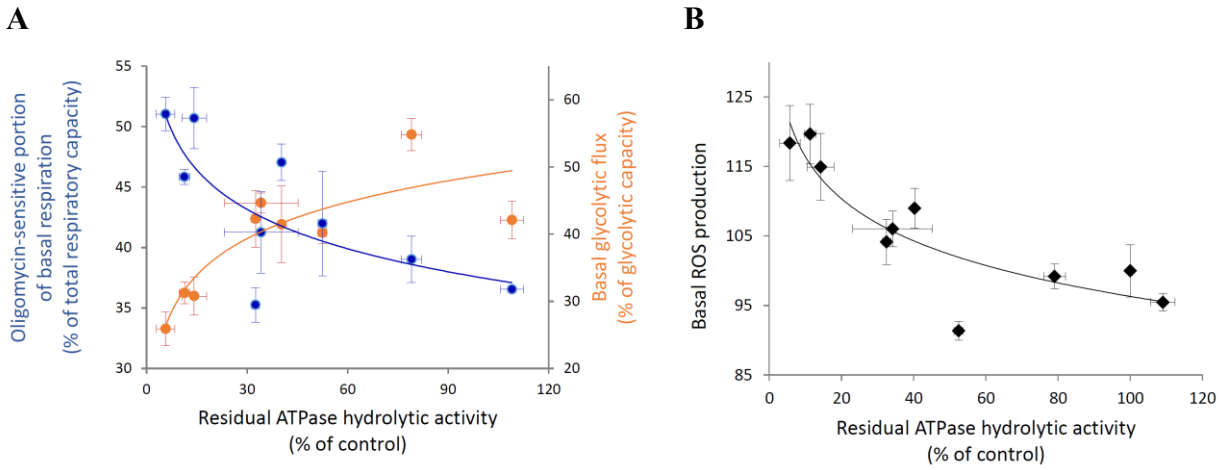

Figure 28. Cellular energetics and ROS production in relation to residual ATP synthase activity. (A) *Correlation of basal respiratory rate and basal glycolytic flux of C1-C9 clone cells and correlation of these parameters together with residual ATPase hydrolytic activity measured by Seahorse oxygraphy.* ***(B)*** *Correlation of basal ROS production and residual ATPase hydrolytic activity in control cells and C1-C9 clones. Measured by fluorescence assay. Data are mean ±SEM from 3 experiments (the basal respiratory rate and residual hydrolytic activity), 4 experiments (basal glycolytic flux, ROS production).*

MY CONTRIBUTION TO THE RESULTS

The presented data are result of team effort and also collaborations with other departments. Here I would like to highlight my personal experimental involvement:

1. Mice treatment with tamoxifen and subsequent monitoring of their body weight and food intake.

2. Animal tissue and blood collection, plasma isolation, embryos and tissue homogenisation and sample preparations.

3. Functional analyses of mitochondria - respiratory measurement by Seahorse XF^e24 Analyzer and Oxygraph O2k including ATP synthase inhibition.

4. Measurement of enzyme activities.

5. SDS electrophoreses to detect protein levels of OXPHOS, ANT, PiC, and superoxide dismutases in combination with Western blot and immunodetection.

6. Native electrophoreses to evaluate assembly of ATP synthase in combination with immunodetection on Western blots or ATPase in-gel activity.

7. Triglycerides level determination.

8. Genotyping - DNA isolation, PCR and agarose electrophoresis.

9. RNA isolation, reverse transcription and RT-PCR.

10. Cells cultivation.

5 DISCUSSION

All known human and mouse/rat mitochondrial proteins (mitoproteome) are nowadays listed in web databases, which contain over 1400 mitochondrial proteins (Pagliarini et al., 2008, Smith and Robinson, 2009, Smith et al., 2012, Uhlen et al., 2015, Calvo et al., 2016). Only 13 of these proteins are encoded in mtDNA and the rest of them encodes nDNA. Many of them have not yet been characterised. To elucidate their function and integration into mitochondrial processes is a goal of many scientists all over the world, because mitochondria have crucial function in energy production. Thus, mutations in genes coding mitochondrial proteins can cause serious diseases (Gorman et al., 2016) and possible therapy is still very limited. Cellular and animal models of these mutated genes have proven as a valuable tool for characterisation of their function (Iommarini et al., 2015, Torraco et al., 2015). For example, many animal models already improved our knowledge of OXPHOS enzymes and their assembly factors (Torraco et al., 2015).

The first protein I focused on in this thesis is **TMEM70**. It was shown in 2008 that *Tmem70* mutations cause isolated ATP synthase deficiency in patients, which leads to severe neonatal encephalocardiomyopathy (Cizkova et al., 2008). Many other following studies confirmed the importance of TMEM70 in ATP synthase biogenesis (Houstek et al., 2009, Hejzlarova et al., 2014). Using human cells, the protein characterisation clarified its molecular structure (Hejzlarova et al., 2011) and membrane topology (Jonckheere et al., 2011, Kratochvilova et al., 2014) but up to now, its detailed function is unknown. Since TMEM70 is specific only for higher eukaryotes, yeasts, which are also commonly used to model mitochondrial dysfunctions, are of no use here (Cizkova et al., 2008, Houstek et al., 2009). Thus, the animal model of *TMEM70* deficiency was chosen to elucidate its function as has been previously done for many other components of mitochondrial respiratory chain and their assembly factors (Iommarini et al., 2015, Torraco et al., 2015). Two different types of *Tmem70*$^{-/-}$ mouse knockout models were generated and analysed in our study.

The first generated model was **whole body constitutive knockout (c*Tmem70*$^{-/-}$)**, which exhibited developmental delay (Figure 10 C, 11 A) and embryonic lethality about E9.5, thus, demonstrated the importance of TMEM70 and assembled ATP synthase in early embryogenesis in mice. Similar embryonic lethality was observed in other knockout models of several structural components of respiratory chain enzymes (e.g. NDUFA5 subunit of complex I (Peralta et al., 2014), SDHD subunit of complex II (Piruat et al., 2004), RISP - Rieske iron

sulphur protein of complex III (Hughes and Hekimi, 2011)) or specific ancillary factors (e.g. Ndufs4 assembly factor of complex I (Ingraham et al., 2009), Cox15 factor of haem a biosynthesis (Viscomi et al., 2011) or Cox17 and Sco2 copper chaperones of complex IV (Takahashi et al., 2002, Yang et al., 2010). Moreover, many of genes included in the mtDNA replication, transcription and translation causing OXPHOS deficiencies were shown to be essential for mouse embryonal development (Iommarini et al., 2015). While these knockout models showed the requirement of functional respiratory chain complexes for embryogenesis, the phenotype of *Surf1* knockout, the gene for another assembly factor of complex IV, was very mild (Dell'agnello et al., 2007) compared to mostly fatal dysfunction of SURF1 in humans (Shoubridge, 2001). It reflected possible tissue specificity and species specificity of the role of Surf1 in biogenesis of this complex. Interestingly, in humans TMEM70 mimic SURF1 to some extent, as small amount of formed ATP synthase is present even in the absence of TMEM70. However, ATP synthase deficiency was found to be similarly pronounced (60-70 %) in different tissues or cells of patients lacking TMEM70 (Houstek et al., 1999, Sperl et al., 2006, Havlickova Karbanova et al., 2012) pointing to the same importance of TMEM70 function in various tissues and cells. Mouse *Tmem70* knockout further indicated that the resulting ATP synthase deficiency may have higher severity in rodents. This was further supported by analogous embryonic lethality of *Tmem70* knockout generated by ZFN nuclease in rats (Pravenec et al. unpublished).

On the other hand, ***Tmem70*$^{+/-}$ heterozygous mice** develop normally, indicating that one *Tmem70* allele is sufficient for viability. These mice had fully functional mitochondrial OXPHOS as well as the structure and function of ATP synthase did not show any difference from control *Tmem70*$^{+/+}$ mice. Rather unexpectedly then, the heart function measured by echocardiography was decreased. It reflects high energy demands and vulnerability of heart that is also primarily affected organ in patients lacking TMEM70 as well as in many other types of mitochondrial disorders of OXPHOS system (Brunel-Guitton et al., 2015). This may have broader implications in the human TMEM70 pathology but detailed anamnesis for parents of affected children is usually missing and it is difficult to establish, whether heterozygous *TMEM70* carriers may be more susceptible to heart dysfunction. For the patients, though, it is well established, that they suffer with early postnatal hypertrophic cardiomyopathy (HCMP) that was found in 76 % of patients (Honzik et al., 2010, Magner et al., 2015). Prenatally, mild thickening of the cardiac chambers, and also right sided clubfoot became first evident at sonography at weeks 28-30 of gestation (Spiegel et al., 2011). The mouse knockout model of *Tmem70* is embryonic lethal at the stage, when heart becomes functional and essential for

further development. However, despite of the developmental delay, no apparent morphological changes were observed in hearts of c*Tmem70*$^{-/-}$ embryos (Figure 11 A).

The second generated model was **whole body conditional Cre-inducible *Tmem70* knockout (i*Tmem70*$^{-/-}$)** which was lethal at about 8 weeks post *Tmem70* excision (Figure 14 A). Similarly, the conditional heart and skeletal muscle specific knockout mice of genes for proteins regulating mtDNA expression (TWINKLE, TFAM, POLRMT, LRPPRC, MTERF4) were lethal from <6 weeks (*Polrmt* knockout) to 21 weeks (*Mterf4* knockout). These deficiencies resulted in severe OXPHOS dysfunction and surprisingly, the disruption of mtDNA in hearts had severe effect on the mitochondrial CoQ synthesis (Kuhl et al., 2017).

Analysis of c*Tmem70*$^{-/-}$ embryos by BN-PAGE showed that TMEM70 deficiency prevents effective **biosynthesis of functional ATP synthase** resulting in lower amount of completely assembled ATP synthase complex and accumulation of F_1 subcomplex without any F_o subunits (Figure 12). Similar pattern was observed also in the most of i*Tmem70*$^{-/-}$ mouse tissues except heart (Figure 16 A). Heart was likely protected by relatively high expression levels of *Tmem70*, which were partially sustained even from the low remaining amount of wildtype *Tmem70* gene. Still, there was some accumulation of F_1 subcomplex, which correlated with excision efficiency. High amount of assembled ATP synthase in heart could be also explained by the different turnover of TMEM70 protein or ATP synthase itself among tissues (Kim et al., 2012). Mitochondrial proteins were shown to have very long half-lives, which can be extended by nutritional interventions such as caloric restriction (Dai et al., 2014). Such half-life extension may act as protective mechanism in heart of i*Tmem70*$^{-/-}$ animals.

We also showed much higher expression of mouse *Tmem70* in heart than in liver, which is in contrary to the results in humans who have higher *Tmem70* expression in liver than in heart (www.biogps.org (BioGPS - your Gene Portal System)). It suggests higher insufficiency of *Tmem70* in liver of i*Tmem70*$^{-/-}$ animals and might explain why patients suffer predominately with cardiologic defect.

Histologically, we observed focal necrosis in liver (not shown). Moreover, liver was fragile with higher levels of pro-apoptotic caspases (Figure 20). i*Tmem70*$^{-/-}$ mice also exhibited hyperammonemia, the marker of liver failure in blood similarly to patients (summarized in Table 2) There were also higher levels of ALT and AST in blood, which confirmed **liver damage** (Table 7). Moreover, blood analysis revealed pronounced leukocytopenia. Thus, mice might be more vulnerable to infection. Because red blood cells are also decreased, i*Tmem70*$^{-/-}$ mice have probably insufficient haematopoiesis. On the other hand, higher number of platelets

increases the risk of blood clotting [Table 7; (Hořejší et al., 2017); www.jax.org/strain/000664 (The Jackson Laboratory)].

Furthermore, more detailed hrCN-PAGE analysis of liver mitochondria from i*Tmem70*$^{-/-}$ animals surprisingly revealed **formation of large and labile vestigial ATP synthase subcomplexes**, which lacks subunit c (Figure 16 B) and falls apart due to Coomassie blue in BN-PAGE analysis. Thus, we demonstrated the presence of different profile of ATP synthase subcomplexes than in other models of ATP synthase deficiency (Cizkova et al., 2008, Vrbacky et al., 2016). The absence of subunit c is in contrast with phenotypes of central stalk subunits ε (Havlickova et al., 2010, Mayr et al., 2010), γ, or δ (Pecina et al., submitted). In all these cases the insufficient formation of F_1 was accompanied by accumulation of strongly hydrophobic subunits c. On the other hand, observed vestigial forms of ATP synthase correspond well with those described in knockout of all three isoforms of subunit c (He et al., 2017) and can indicate role for TMEM70 protein in the import, processing or assembly of ATP synthase subunit c. This is in line with our original hypothesis that TMEM70 is involved in early stage of ATP synthase biogenesis (Hejzlarova et al., 2014) and that it incorporates or stabilises subunit c in ATP synthase complex. However, immunoprecipitation and crosslinking did not show any direct interaction of F_1 or c subunits with TMEM70 (Kratochvilova et al., 2014). In this process additional protein might be included that would facilitate the regulatory role of TMEM70, thus, further studies are needed to find other possibilities of the interactions with TMEM70.

Moreover, ATP synthase has been shown to be essential in **cristae formation** (Strauss et al., 2008, Davies et al., 2012, Hahn et al., 2016). Ultrastructural mitochondrial degeneration was as well observed in patients with TMEM70 deficiency (Jonckheere et al., 2011, Braczynski et al., 2015). This was confirmed in c*Tmem70*$^{-/-}$ embryos, in which the defect of ATP synthase caused cristae disruption (Figure 13).

Analysis of the of other **OXPHOS complexes** in liver of i*Tmem70*$^{-/-}$ mice by SDS-PAGE revealed that their levels are also changed. Levels of protein subunits of complex I, complex II and complex IV were increased and level of complex V was decreased as expected (Table 6). This result points to compensation of low ATP production in case of dysfunctional ATP synthase by RC. In contrary, in patient's fibroblasts were significantly increased only levels of subunits of complex III and complex IV but similar increasing trend was observed in complex I (Havlickova Karbanova et al., 2012). These discrepancies could be explained by different cell type or tissue specificity. It is in contrast with results of Jonckheere et al. who demonstrated combined deficiency of complex V and I in patient cells with no effect on levels of complexes II, III, IV (Jonckheere et al., 2011). Moreover, TMEM70 was found

in assembly intermediates of complex I, suggesting that it may function also as complex I assembly factor (Guerrero-Castillo et al., 2017). On the other hand, we did not observe any changes in OXPHOS complexes I-IV in c*Tmem70*$^{-/-}$ embryos (Figure 11), in which the compensatory effect was probably not yet manifested.

As a consequence of ATP synthase deficiency, the **energetic function of mitochondria** of the c*Tmem70*$^{-/-}$ embryos and i*Tmem70*$^{-/-}$ mice was altered. H^+ electrochemical gradient generated on membrane by respiratory chain was not fully utilised by ATP synthase. It was shown in *cTmem70*$^{-/-}$ embryos that RCR and coupled ADP-stimulated respiration were strongly decreased (Figure 13 A). Also, induced i*Tmem70*$^{-/-}$ mice had lower RCR but it was caused by inefficient inhibition of ATP synthase by its inhibitors oligomycin and aurovertin. Moreover, the oxygen consumption was strongly increased after addition of cytochrome c, which indicated damaged OMM (Figure 18). The maximal uncoupled respiration of i*Tmem70*$^{-/-}$ mouse mitochondria was comparable to controls supposedly due to already uncoupled mitochondria. Similarly, substantial decrease in maximal respiration was not observed in lymphocytes of patients with TMEM70 deficiency (Pecina et al., 2014).

The stalled mitochondrial energy provision due to dysfunctional ATP synthase was followed by the decrease in ATP/ADP ratio in c*Tmem70*$^{-/-}$ embryos showing that the overall energetic state is compromised (Figure 13 B). It is additionally caused by accumulated catalytically active F_1 subcomplexes in that are not gated by F_o subunits and hydrolyse ATP. Free F_1 subcomplexes could be inhibited by endogenous ATP synthase inhibitor IF_1, however, its role *in vivo* is more complex at high values of $\Delta\Psi_m$ (Lippe et al., 1988) and may also inhibit the synthetic activity of ATP synthase (Formentini et al., 2014), that would make worse the impact of ATP synthase deficiency.

Early **embryonic development** is associated with marked changes in energy source depending on oxygen supply during different developmental stages. The concentration of oxygen in oviduct is lower than 40 % of atmospheric concentration (Leese, 1995) and it is much lower in *uterus* (3-5 %). It means that embryo is in hypoxic, nearly anoxic conditions during the preimplantation state and early implantation (Fischer and Bavister, 1993). During postimplantation period, the oxygen and nutrients are supplied to embryo by yolk sack. Then the trophectoderm invades endometrium of the uterus during early implantation and subsequently allantoic placenta supports embryonic development instead of yolk sac. Placenta begins to supply the high oxygen concentration to the embryo (New and Coppola, 1970). The energy metabolism changes during these periods from oxidative phosphorylation in early preimplantation stage to increasing role of glycolysis during compaction

and blastulation (E3-4), and in the end returns back to oxidative metabolism when chorionallantoic circulation is established and heart begins to function. Use of oxygen as energy substrate is accompanied by formation of ROS and activation of antioxidant defence system to balance the harmful and the natural regulatory effects of the imposed oxidative stress (Ufer and Wang, 2011). Analysis of c*Tmem70*$^{-/-}$ embryos at E9.5 showed upregulation of antioxidative enzymes SOD1 and SOD2, which indicates the higher level of ROS (Figure 12). This observation shows that the deficiency of ATP synthase in mouse embryos leads into both - the energy deprivation and enhanced **oxidative stress**. It is reminiscent of postnatal biochemical manifestation of ATP synthase deficiency in human patient with *TMEM70* mutation (Mracek et al., 2006). These results were confirmed by the increased level of mitochondrial SOD2 and reduced antioxidant glutathione in the liver of i*Tmem70*$^{-/-}$ mice caused by ROS increase (Figure 19).

In **patients** from families affected by mutations in *TMEM70* gene, frequent, but much less severe impairment of prenatal development was reported (Houstek 1999, Honzik 2010, Magner 2015, Sperl 2006). Out of 25 cases with identical homozygous c.317-2A>G *TMEM70* mutation preventing synthesis of TMEM70 protein, 68 % of patients were delivered prematurely and in 58 % patients was present intrauterine growth retardation (IUGR) (birth weight 2040±471 g, gestation age 36±2.6 weeks). Similarly, four of the six patients with other *TMEM70* mutations were born prematurely (Spiegel et al., 2011). This is different to the rodent models (mouse and rat) of TMEM70 deficiency, which are both lethal during early embryonic development. A few miscarriages were reported in some of the affected families (Houstek et al., 1999, Torraco et al., 2012, Braczynski et al., 2015) but it is mostly impossible to establish the reasons for miscarriages in common healthy population.

The second mitochondrial protein I focused on in this thesis was **DAPIT**, which was proven to be a new component of ATP synthase (Chen et al., 2007, Meyer et al., 2007, Lee et al., 2015). However, its detail function remains unclear. Therefore, we generated rat knockout model of DAPIT gene *Usmg5*$^{-/-}$ via ZFN technology to clarify DAPIT function. Knockout rats manifested lower body weight, decreased adiposity and triglyceride level in liver (Figure 21). Decreased adiposity can either stem from insufficient fatty acid storage or their preferential oxidation, which can be dissected in further experiments either by indirect calorimetry or by high fat diet regimen It was already published that DAPIT plays role in glucose metabolism (Paivarinne and Kainulainen, 2001, Kontro et al., 2015).

We also observed that *Usmg5*$^{-/-}$ rats had pronounced change in pulmonary blood flow (Figure 22 B) and defective heart function (Figure 22 A), manifested as hypertrophy of heart RV (Figure 21 C). It suggests pulmonary arterial hypertension (PAH; Figure 22 B). It was already shown, that PAH involves changes in pulmonary arteries leading to secondary RV failure (Paulin and Michelakis, 2014). Moreover, changes in mitochondrial dynamics (Chen et al., 2018) or mitochondrial calcium handling (Hong et al., 2017) can lead to pulmonary arteries smooth muscle proliferation and PAH.

DAPIT and also MLQ were identified in dimeric and in the monomeric bovine ATP synthase (Meyer et al., 2007). Using native electrophoresis, we also showed that DAPIT protein occurs in dimers and monomers but less dimers were formed and F_1 subcomplexes accumulated in heart of *Usmg5*$^{-/-}$ rats. The dimeric and monomeric forms of ATP synthase were smaller supposedly due to missing DAPIT protein (Figure 23 A). These results point at the role of DAPIT in dimer formation as was already predicted by Wittig and Schagger (Wittig and Schagger, 2008). The levels of other detected ATP synthase subunits were not changed (Figure 23 B) but the function of this complex was decreased (Figure 23 C, 24) similarly to the study of Ohsakaya et al. who showed unchanged expression of α and β subunits but decreased ATP synthase activity in HeLa cells with supressed *USMG5*$^{-/-}$ expression (Ohsakaya et al., 2011). Moreover, the inhibition of ATP synthase respiratory state 3 by its inhibitors oligomycin and aurovertin differed in effectivity between *Usmg5*$^{-/-}$ and *Usmg5*$^{+/+}$ rats. Interestingly, oligomycin was considerably more effective than aurovertin in both heart and liver of *Usmg5*$^{-/-}$ rats in comparison to controls (Figure 25). It might be explained by different binding specificity of these inhibitors on the ATP synthase. Oligomycin was shown to bind on F_o subcomplex and aurovertin on F_1 subcomplex (Hong and Pedersen, 2008). Thus, the enhanced sensitivity of *Usmg5*$^{-/-}$ mitochondria for oligomycin may indicate that DAPIT shields oligomycin binding side which is more accessible in *Usmg5*$^{-/-}$ rats. This is compatible with crosslinking studies demonstrating close apposition of DAPIT and a subunit (Lee et al., 2015).

We were also interested in the effect of ATP synthase defects on its previously suggested supramolecular structures. One of them is **ATP synthasome**, which is composed of ATP synthase and components necessary for ATP production - ADP/ATP translocase (ANT) and inorganic phosphate carrier (PiC) (Ko et al., 2003, Chen et al., 2004). While we confirmed the existence of such supercomplex, we also clearly showed that the majority of PiC and ANT do not interact with ATP synthase and exist in their free form. This may not be surprising, given the different kinetic properties of ATP synthase and the translocators, especially the ANT,

which demonstrates quite slow kinetics (Klingenberg, 2008). Our transcript and protein analyses of rat tissues revealed transcriptionally regulated PiC and ANT expression in concordance with ATP synthase biogenesis (Nuskova et al., 2015). Interestingly, their levels were increased in patient's fibroblasts with defective ATP synthase (Figure 26), which was confirmed in the liver of i*Tmem70*$^{-/-}$ mice (Figure 26, C, D; Table 8). This rather suggests compensatory type of response, similar to that seen for OXPHOS complexes (Table 6) and also (Havlickova Karbanova et al., 2012), driven by the low available ATP levels. It is also confirmation, that translocators and ATP synthase do not mutually depend on each other, and majority of their entities exist independently from ATP synthasome.

Looking back at reported cases of nuclear encoded ATP synthase pathologies, we usually see ATP synthase levels decreased to 30 % or less of controls (Houstek et al., 1999, Mayr et al., 2004, Sperl et al., 2006, Mayr et al., 2010). Decrease to < 10 % of ATP synthase compared to healthy individuals, is barely compatible with survival (Houstek et al., 2006). Similarly analyzed c*Tmem70*$^{-/-}$ embryos had only 20 % of remaining fully assembled ATP synthase activity (Figure 11). On the other hand, rats with DAPIT deficiency did not have such decrease of monomeric ATP synthase and they also had normal viability (Figure 24 A). To identify the **ATP synthase deficiency threshold** necessary for pathological presentation and to compare it with previously mentioned deficiencies, we generated 9 clones of F_1-γ, F_1-δ or F_1-ε of HEK293 cells with different level of ATP synthase deficiency and in-gel hydrolytic activity (Figure 27). Previously, decreased levels of assembled ATP synthase and absence of any assembly intermediates, such as F_1 subcomplex, were observed in knockdown cells of F_1-ε subunit (Havlickova et al., 2010) and recently also in knockdown cells of subunits F_1-γ and F_1-δ (Pecina et al., submitted). This makes central stalk knockdowns especially suitable model to study ATP synthase threshold levels, as the pathologic presentation is not mired by factors such as F_1 driven ATP hydrolysis. We showed that prepared clones with less than 30 % of residual ATPase activity switched their metabolism to enhanced glycolysis (Figure 28 A) and boosted the ROS production (Figure 28 B). This corresponds with other models of ATP synthase pathologies, where increased levels of oxidative stress could be seen. We have observed increased ROS in human patient with *TMEM70* mutation (Mracek et al., 2006) and in animal models of TMEM70 deficiency (Figure 13 C, 19). Similarly, the deficient ATP production and enhanced ROS generation were caused by mtDNA mutations of ATP6 subunit in cells (Mattiazzi et al., 2004). All those observations are in line with observed increase in ROS production under high levels of $\Delta\Psi_m$ (Korshunov et al., 1997). While direct increase in steady

state levels of $\Delta\Psi_m$ was observed only in some patients (Mattiazzi et al., 2004), the decreased ability to utilise $\Delta\Psi_m$ for ATP synthesis is clearly more general phenomenon (Mracek et al., 2006, Cizkova et al., 2008, Havlickova et al., 2010) and may explain the observed boost in ROS production. Importantly, we have observed similar threshold at circa 30 % of residual ATP synthase for all pathological presentations, indicating that below this level, cells cannot maintain their normal physiological function and pathology manifests.

Collectively, we have generated two unique novel animal models of *Tmem70* gene ablation and one rat model of *Usmg5* gene ablation. These deficiencies caused changes in ATP synthase biogenesis and function. Constitutive knockout of *Tmem70* led to embryonic lethality and inducible knockout mice also died not long after *Tmem70* deletion. We observed dramatic decrease of fully assembled ATP synthase and accumulation of its subcomplexes in both models of TMEM70 deficiency. We have also demonstrated, that ATP synthase deficiencies display clear threshold behaviour and decrease of the ATP synthase functional capacity below 30 % is necessary for pathologic presentation. Moreover, accumulated subcomplexes of ATP synthase did not contain subunit c indicating stalled ATP synthase biogenesis at the level of F_1 formation. Overall, mitochondrial energy production was critically impaired analogously to Tmem70 dysfunction in human patients. We convincingly demonstrated in rodent models that TMEM70 ancillary factor is essential for maintenance of ATP synthase biosynthesis and thus the supplying energy for the developing mammalian organism and that TMEM70 deficiency is not compatible with life of adult mice. Generated DAPIT deficient (*Usmg5*$^{-/-}$) rats had also slightly defective ATP synthase. We confirmed the importance of DAPIT protein in the formation of ATP synthase dimers. Furthermore, DAPIT supposedly shields the oligomycin binding pocket at ATP synthase pointing its position in this multiprotein complex. Finally, we showed, that ATP synthasome, ATP synthase supramolecular structure, components ANT and PiC were increased in patients and mice despite of the ATP synthase defects. It is likely due to a post-transcriptional adaptive mechanism.

6 CONCLUSIONS

From our studies on rodent knockout models, patient fibroblasts and knockdown cells, we can conclude that:

1. TMEM70 is essential for mouse embryonic development. ATP synthase of constitutive E9.5 *Tmem70*$^{-/-}$ embryos is not fully assembled and F_1 subcomplex is accumulated. This leads to insufficient energy provision, increased oxidative stress and disrupted cristae morphology. *Tmem70*$^{+/-}$ mice are viable but present with mild cardiological dysfunction. This can not be observed in embryos, which die before the heart morphology could be affected.

2. Inducible *Tmem70* mouse knockout model is lethal approximately 8 weeks post induction. Primarily impaired organ is liver, and symptoms thus resemble conditions during metabolic crises in patients.

3. Thanks to the *iTmem70*$^{-/-}$ model system, we can observe formation of large and labile ATP synthase complexes, which lack subunit c. We have demonstrated, that TMEM70 is important for incorporation of c-oligomer into ATP synthase.

4. DAPIT plays a role in formation of ATP synthase dimers. Levels of assembled monomeric ATP synthase are normal but its function is reduced by ~10 % in both liver and heart tissue. It seems that DAPIT shields oligomycin binding site at F_o moiety pointing at its position in ATP synthase multiprotein complex. *Usmg5*$^{-/-}$ rats have lower body weight and pronounced decrease of fat tissue, indicating an important role of DAPIT in regulation of metabolism.

5. Content of ANT and PiC in human and mouse ATP synthase deficiencies is increased, likely due to a post-transcriptional adaptive mechanism, probably as a compensation of isufficient ATP production.

6. The threshold limit for the presentation of ATP synthase related pathologies was shown to be ~30 %.

7 SUMMARY

Characterisation of new mitochondrial proteins TMEM70 and DAPIT function using unique knockout rodent models showed that TMEM70 is important for incorporation of c-oligomer into ATP synthase. Thus, TMEM70 protein might play the role in the import, processing or assembly of ATP synthase subunit c. Resulting ATP synthase deficiency reaches the threshold for its pathologic presentation, which was quantified at 30 %. Analogous to TMEM70 dysfunction in humans, it leads to critical impairment of mitochondrial energy provision essential for mouse embryonic development and life of adult mice. Induced *Tmem70* knockout mice have impaired primarily liver function, which resembles symptoms present during metabolic crises in patients. ANT and PiC components of ATP synthasome do not mutually depend on ATP synthase and reveal compensatory increase in ATP synthase pathologies.

DAPIT plays a role in the formation of ATP synthase dimers and likely shields oligomycin binding site at F_o moiety of ATP synthase. Furthermore, DAPIT seems to play an important role in metabolism regulation.

In general, we illustrate the importance of animal knockout models as a useful tool for mitochondrial proteins characterisation.

SOUHRN

Funkce nových mitochondriálních proteinů TMEM70 a DAPIT byla charakterizována pomocí unikátních hlodavčích modelů. Ukázalo se, že TMEM70 je důležitý pro přidání c-oligomeru do komplexu ATP syntázy. TMEM70 by tedy mohl hrát roli v importu, úpravě nebo asemblaci podjednotky c ATP syntázy. Výsledný nedostatek ATP syntázy dosahuje prahu projevu patologie, který jsme určili na 30 %. Podobně jako u pacientů dochází ke kritickému porušení tvorby energie, která je nezbytná pro embryonální vývoj myší a životaschopnost myší dospělých. U indukovaných *Tmem70* knockout myší docházelo primárně k jaternímu poškození, což se podobá symptomům v průběhu metabolické krize u pacientů. Dále komponenty ATP syntasomu ANT a PiC vzájemně nezávisí na ATP syntáze a jsou naopak u patologií ATP syntázy kompenzačně zvýšeny.

DAPIT je důležitý pro tvorbu dimerů ATP syntázy a pravděpodobně blokuje na F_o části ATP syntázy vazebné místo pro oligomycin. Také se zdá, že DAPIT hraje důležitou roli v regulaci metabolismu.

Potvrdili jsme, že zvířecí knockout modely jsou vhodné pro charakterizaci mitochondriálních proteinů.

8 REFERENCES

Abrahams, J. P., Leslie, A. G., Lutter, R. and Walker, J. E. (1994). "Structure at 2.8 A resolution of F1-ATPase from bovine heart mitochondria."Nature **370**(6491): 621-628.

Ackerman, S. H. and Tzagoloff, A. (2005). "Function, structure, and biogenesis of mitochondrial ATP synthase."Prog Nucleic Acid Res Mol Biol **80**: 95-133.

Allegretti, M., Klusch, N., Mills, D. J., Vonck, J., Kuhlbrandt, W. and Davies, K. M. (2015). "Horizontal membrane-intrinsic alpha-helices in the stator a-subunit of an F-type ATP synthase."Nature **521**(7551): 237-240.

Anderson, S., Bankier, A. T., Barrell, B. G., de Bruijn, M. H., Coulson, A. R., Drouin, J., Eperon, I. C., Nierlich, D. P., Roe, B. A., Sanger, F., Schreier, P. H., Smith, A. J., Staden, R. and Young, I. G. (1981). "Sequence and organization of the human mitochondrial genome."Nature **290**(5806): 457-465.

Andersson, S. G., Zomorodipour, A., Andersson, J. O., Sicheritz-Ponten, T., Alsmark, U. C., Podowski, R. M., Naslund, A. K., Eriksson, A. S., Winkler, H. H. and Kurland, C. G. (1998). "The genome sequence of Rickettsia prowazekii and the origin of mitochondria."Nature **396**(6707): 133-140.

Andrews, R. M., Kubacka, I., Chinnery, P. F., Lightowlers, R. N., Turnbull, D. M. and Howell, N. (1999). "Reanalysis and revision of the Cambridge reference sequence for human mitochondrial DNA."Nat Genet **23**(2): 147.

Antonicka, H. and Shoubridge, E. A. (2015). "Mitochondrial RNA Granules Are Centers for Posttranscriptional RNA Processing and Ribosome Biogenesis."Cell Rep.

Ardehali, H., Chen, Z., Ko, Y., Mejia-Alvarez, R. and Marban, E. (2004). "Multiprotein complex containing succinate dehydrogenase confers mitochondrial ATP-sensitive K+ channel activity."Proc Natl Acad Sci U S A **101**(32): 11880-11885.

Atay, Z., Bereket, A., Turan, S., Haliloglu, B., Memisoglu, A., Khayat, M., Shalev, S. A. and Spiegel, R. (2013). "A novel homozygous TMEM70 mutation results in congenital cataract and neonatal mitochondrial encephalo-cardiomyopathy."Gene **515**(1): 197-199.

Baracca, A., Amler, E., Solaini, G., Parenti Castelli, G., Lenaz, G. and Houstek, J. (1989). "Temperature-induced states of isolated F1-ATPase affect catalysis, enzyme conformation and high-affinity nucleotide binding sites."Biochim Biophys Acta **976**(1): 77-84.

Baracca, A., Sgarbi, G., Mattiazzi, M., Casalena, G., Pagnotta, E., Valentino, M. L., Moggio, M., Lenaz, G., Carelli, V. and Solaini, G. (2007). "Biochemical phenotypes associated with the mitochondrial ATP6 gene mutations at nt8993."Biochim Biophys Acta **1767**(7): 913-919.

Barrett, T., Wilhite, S. E., Ledoux, P., Evangelista, C., Kim, I. F., Tomashevsky, M., Marshall, K. A., Phillippy, K. H., Sherman, P. M., Holko, M., Yefanov, A., Lee, H., Zhang, N., Robertson, C. L., Serova, N., Davis, S. and Soboleva, A. (2013). "NCBI GEO: archive for functional genomics data sets--update."Nucleic Acids Res **41**(Database issue): D991-995.

Barupala, D. P., Dzul, S. P., Riggs-Gelasco, P. J. and Stemmler, T. L. (2016). "Synthesis, delivery and regulation of eukaryotic heme and Fe-S cluster cofactors."Arch Biochem Biophys **592**: 60-75.

Belogrudov, G. I. (2002). "Factor B is essential for ATP synthesis by mitochondria."Arch Biochem Biophys **406**(2): 271-274.

Belogrudov, G. I. (2010). "Coupling factor B affects the morphology of mitochondria."J Bioenerg Biomembr **42**(1): 29-35.

Bereiter-Hahn, J. (1990). "Behavior of mitochondria in the living cell."Int Rev Cytol **122**: 1-63.

Bezawork-Geleta, A., Rohlena, J., Dong, L., Pacak, K. and Neuzil, J. (2017). "Mitochondrial Complex II: At the Crossroads."Trends Biochem Sci **42**(4): 312-325.

BioGPS - your Gene Portal System, www.biogps.org, 6.3.2018

Birling, M. C., Dierich, A., Jacquot, S., Herault, Y. and Pavlovic, G. (2012). "Highly-efficient, fluorescent, locus directed cre and FlpO deleter mice on a pure C57BL/6N genetic background."Genesis **50**(6): 482-489.

Bogenhagen, D. F., Martin, D. W. and Koller, A. (2014). "Initial steps in RNA processing and ribosome assembly occur at mitochondrial DNA nucleoids."Cell Metab **19**(4): 618-629.

Bourgeron, T., Rustin, P., Chretien, D., Birch-Machin, M., Bourgeois, M., Viegas-Pequignot, E., Munnich, A. and Rotig, A. (1995). "Mutation of a nuclear succinate dehydrogenase gene results in mitochondrial respiratory chain deficiency."Nat Genet **11**(2): 144-149.

Boyer, P. D. (1975). "A model for conformational coupling of membrane potential and proton translocation to ATP synthesis and to active transport."FEBS Lett **58**(1): 1-6.

Braczynski, A. K., Vlaho, S., Muller, K., Wittig, I., Blank, A. E., Tews, D. S., Drott, U., Kleinle, S., Abicht, A., Horvath, R., Plate, K. H., Stenzel, W., Goebel, H. H., Schulze, A., Harter, P. N., Kieslich, M. and Mittelbronn, M. (2015). "ATP synthase deficiency due to TMEM70 mutation leads to ultrastructural mitochondrial degeneration and is amenable to treatment."Biomed Res Int **2015**: 462592.

Bradford, M. M. (1976). "A rapid and sensitive method for the quantitation of microgram quantities of protein utilizing the principle of protein-dye binding."Anal Biochem **72**: 248-254.

Brunel-Guitton, C., Levtova, A. and Sasarman, F. (2015). "Mitochondrial Diseases and Cardiomyopathies."Can J Cardiol **31**(11): 1360-1376.

Brzezniak, L. K., Bijata, M., Szczesny, R. J. and Stepien, P. P. (2011). "Involvement of human ELAC2 gene product in 3' end processing of mitochondrial tRNAs."RNA Biol **8**(4): 616-626.

Calvo, S., Jain, M., Xie, X., Sheth, S. A., Chang, B., Goldberger, O. A., Spinazzola, A., Zeviani, M., Carr, S. A. and Mootha, V. K. (2006). "Systematic identification of human mitochondrial disease genes through integrative genomics."Nat Genet **38**(5): 576-582.

Calvo, S. E. and Mootha, V. K. (2010). "The mitochondrial proteome and human disease."Annu Rev Genomics Hum Genet **11**: 25-44.

Calvo, S. E., Clauser, K. R. and Mootha, V. K. (2016). "MitoCarta2.0: an updated inventory of mammalian mitochondrial proteins."Nucleic Acids Res **44**(D1): D1251-1257.

Cameron, J. M., Levandovskiy, V., Mackay, N., Ackerley, C., Chitayat, D., Raiman, J., Halliday, W. H., Schulze, A. and Robinson, B. H. (2011). "Complex V TMEM70 deficiency results in mitochondrial nucleoid disorganization."Mitochondrion **11**(1): 191-199.

Carroll, J., Fearnley, I. M. and Walker, J. E. (2006). "Definition of the mitochondrial proteome by measurement of molecular masses of membrane proteins."Proc Natl Acad Sci U S A **103**(44): 16170-16175.

Catteruccia, M., Verrigni, D., Martinelli, D., Torraco, A., Agovino, T., Bonafe, L., D'Amico, A., Donati, M. A., Adorisio, R., Santorelli, F. M., Carrozzo, R., Bertini, E. and Dionisi-Vici, C. (2014). "Persistent pulmonary arterial hypertension in the newborn (PPHN): a frequent manifestation of TMEM70 defective patients."Mol Genet Metab **111**(3): 353-359.

Chen, C., Ko, Y., Delannoy, M., Ludtke, S. J., Chiu, W. and Pedersen, P. L. (2004). "Mitochondrial ATP synthasome: three-dimensional structure by electron microscopy of the ATP synthase in complex formation with carriers for Pi and ADP/ATP."J Biol Chem **279**(30): 31761-31768.

Chen, K. H., Dasgupta, A., Lin, J., Potus, F., Bonnet, S., Iremonger, J., Fu, J., Mewburn, J., Wu, D., Dunham-Snary, K., Theilmann, A. L., Jing, Z. C., Hindmarch, C., Ormiston, M. L., Lawrie, A. and Archer, S. L. (2018). "Epigenetic Dysregulation of the Drp1 Binding Partners MiD49 and MiD51 Increases Mitotic Mitochondrial Fission and Promotes Pulmonary Arterial Hypertension: Mechanistic and Therapeutic Implications."Circulation.

Chen, R., Runswick, M. J., Carroll, J., Fearnley, I. M. and Walker, J. E. (2007). "Association of two proteolipids of unknown function with ATP synthase from bovine heart mitochondria."FEBS Lett **581**(17): 3145-3148.

Cizkova, A., Stranecky, V., Mayr, J. A., Tesarova, M., Havlickova, V., Paul, J., Ivanek, R., Kuss, A. W., Hansikova, H., Kaplanova, V., Vrbacky, M., Hartmannova, H., Noskova, L., Honzik, T., Drahota, Z., Magner, M., Hejzlarova, K., Sperl, W., Zeman, J., Houstek, J. and Kmoch, S. (2008). "TMEM70 mutations cause isolated ATP synthase deficiency and neonatal mitochondrial encephalocardiomyopathy."Nat Genet **40**(11): 1288-1290.

Craven, L., Tang, M. X., Gorman, G. S., De Sutter, P. and Heindryckx, B. (2017). "Novel reproductive technologies to prevent mitochondrial disease."Hum Reprod Update **23**(5): 501-519.

Dahout-Gonzalez, C., Nury, H., Trezeguet, V., Lauquin, G. J., Pebay-Peyroula, E. and Brandolin, G. (2006). "Molecular, functional, and pathological aspects of the mitochondrial ADP/ATP carrier."Physiology (Bethesda) **21**: 242-249.

Dai, D. F., Karunadharma, P. P., Chiao, Y. A., Basisty, N., Crispin, D., Hsieh, E. J., Chen, T., Gu, H., Djukovic, D., Raftery, D., Beyer, R. P., MacCoss, M. J. and Rabinovitch, P. S. (2014). "Altered proteome turnover and remodeling by short-term caloric restriction or rapamycin rejuvenate the aging heart."Aging Cell **13**(3): 529-539.

Davies, K. M., Anselmi, C., Wittig, I., Faraldo-Gomez, J. D. and Kuhlbrandt, W. (2012). "Structure of the yeast F1Fo-ATP synthase dimer and its role in shaping the mitochondrial cristae."Proc Natl Acad Sci U S A **109**(34): 13602-13607.

De Meirleir, L., Seneca, S., Lissens, W., De Clercq, I., Eyskens, F., Gerlo, E., Smet, J. and Van Coster, R. (2004). "Respiratory chain complex V deficiency due to a mutation in the assembly gene ATP12."J Med Genet **41**(2): 120-124.

Dell'agnello, C., Leo, S., Agostino, A., Szabadkai, G., Tiveron, C., Zulian, A., Prelle, A., Roubertoux, P., Rizzuto, R. and Zeviani, M. (2007). "Increased longevity and refractoriness to Ca(2+)-dependent neurodegeneration in Surf1 knockout mice."Hum Mol Genet **16**(4): 431-444.

Dimauro, S. and Davidzon, G. (2005). "Mitochondrial DNA and disease."Ann Med **37**(3): 222-232.

Diodato, D., Invernizzi, F., Lamantea, E., Fagiolari, G., Parini, R., Menni, F., Parenti, G., Bollani, L., Pasquini, E., Donati, M. A., Cassandrini, D., Santorelli, F. M., Haack, T. B., Prokisch, H., Ghezzi, D., Lamperti, C. and Zeviani, M. (2015). "Common and Novel TMEM70 Mutations in a Cohort of Italian Patients with Mitochondrial Encephalocardiomyopathy."JIMD Rep **15**: 71-78.

Dolce, V., Iacobazzi, V., Palmieri, F. and Walker, J. E. (1994). "The sequences of human and bovine genes of the phosphate carrier from mitochondria contain evidence of alternatively spliced forms."J Biol Chem **269**(14): 10451-10460.

Dolce, V., Scarcia, P., Iacopetta, D. and Palmieri, F. (2005). "A fourth ADP/ATP carrier isoform in man: identification, bacterial expression, functional characterization and tissue distribution."FEBS Lett **579**(3): 633-637.

Dubot, A., Godinot, C., Dumur, V., Sablonniere, B., Stojkovic, T., Cuisset, J. M., Vojtiskova, A., Pecina, P., Jesina, P. and Houstek, J. (2004). "GUG is an efficient initiation codon to translate the human mitochondrial ATP6 gene."Biochem Biophys Res Commun **313**(3): 687-693.

Falkenberg, M., Larsson, N. G. and Gustafsson, C. M. (2007). "DNA replication and transcription in mammalian mitochondria."Annu Rev Biochem **76**: 679-699.

Falkenberg, M., Gaspari, M., Rantanen, A., Trifunovic, A., Larsson, N. G. and Gustafsson, C. M. (2002). "Mitochondrial transcription factors B1 and B2 activate transcription of human mtDNA."Nat Genet **31**(3): 289-294.

Fearnley, I. M. and Walker, J. E. (1986). "Two overlapping genes in bovine mitochondrial DNA encode membrane components of ATP synthase."EMBO J **5**(8): 2003-2008.

Fernandez-Vizarra, E. and Zeviani, M. (2015). "Nuclear gene mutations as the cause of mitochondrial complex III deficiency."Front Genet **6**: 134.

Fiermonte, G., Dolce, V. and Palmieri, F. (1998). "Expression in Escherichia coli, functional characterization, and tissue distribution of isoforms A and B of the phosphate carrier from bovine mitochondria."J Biol Chem **273**(35): 22782-22787.

Fischer, B. and Bavister, B. D. (1993). "Oxygen tension in the oviduct and uterus of rhesus monkeys, hamsters and rabbits."J Reprod Fertil **99**(2): 673-679.

Flachs, P., Novotny, J., Baumruk, F., Bardova, K., Bourova, L., Miksik, I., Sponarova, J., Svoboda, P. and Kopecky, J. (2002). "Impaired noradrenaline-induced lipolysis in white fat of aP2-Ucp1 transgenic mice is associated with changes in G-protein levels."Biochem J **364**(Pt 2): 369-376.

Floyd, B. J., Wilkerson, E. M., Veling, M. T., Minogue, C. E., Xia, C., Beebe, E. T., Wrobel, R. L., Cho, H., Kremer, L. S., Alston, C. L., Gromek, K. A., Dolan, B. K., Ulbrich, A., Stefely, J. A., Bohl, S. L., Werner, K. M., Jochem, A., Westphall, M. S., Rensvold, J. W., Taylor, R. W., Prokisch, H., Kim, J. P., Coon, J. J. and Pagliarini, D. J. (2016). "Mitochondrial Protein Interaction Mapping Identifies Regulators of Respiratory Chain Function."Mol Cell **63**(4): 621-632.

Formentini, L., Pereira, M. P., Sanchez-Cenizo, L., Santacatterina, F., Lucas, J. J., Navarro, C., Martinez-Serrano, A. and Cuezva, J. M. (2014). "In vivo inhibition of the mitochondrial H+-ATP synthase in neurons promotes metabolic preconditioning."EMBO J **33**(7): 762-778.

Frazier, A. E., Thorburn, D. R. and Compton, A. G. (2017). "Mitochondrial energy generation disorders: genes, mechanisms and clues to pathology."J Biol Chem.

Gaspari, M., Falkenberg, M., Larsson, N. G. and Gustafsson, C. M. (2004). "The mitochondrial RNA polymerase contributes critically to promoter specificity in mammalian cells."EMBO J **23**(23): 4606-4614.

Gene Ontology, C. (2008). "The Gene Ontology project in 2008."Nucleic Acids Res **36**(Database issue): D440-444.

Gorman, G. S., Chinnery, P. F., DiMauro, S., Hirano, M., Koga, Y., McFarland, R., Suomalainen, A., Thorburn, D. R., Zeviani, M. and Turnbull, D. M. (2016). "Mitochondrial diseases."Nat Rev Dis Primers **2**: 16080.

Gorman, G. S., Schaefer, A. M., Ng, Y., Gomez, N., Blakely, E. L., Alston, C. L., Feeney, C., Horvath, R., Yu-Wai-Man, P., Chinnery, P. F., Taylor, R. W., Turnbull, D. M. and McFarland, R. (2015). "Prevalence of nuclear and mitochondrial DNA mutations related to adult mitochondrial disease."Ann Neurol **77**(5): 753-759.

Guerrero-Castillo, S., Baertling, F., Kownatzki, D., Wessels, H. J., Arnold, S., Brandt, U. and Nijtmans, L. (2017). "The Assembly Pathway of Mitochondrial Respiratory Chain Complex I."Cell Metab **25**(1): 128-139.

Guidotti, G. (1972). "Membrane proteins."Annu Rev Biochem **41**: 731-752.

Guo, H., Bueler, S. A. and Rubinstein, J. L. (2017). "Atomic model for the dimeric FO region of mitochondrial ATP synthase."Science **358**(6365): 936-940.

Hahn, A., Parey, K., Bublitz, M., Mills, D. J., Zickermann, V., Vonck, J., Kuhlbrandt, W. and Meier, T. (2016). "Structure of a Complete ATP Synthase Dimer Reveals the Molecular Basis of Inner Mitochondrial Membrane Morphology."Mol Cell **63**(3): 445-456.

Han, S., Udeshi, N. D., Deerinck, T. J., Svinkina, T., Ellisman, M. H., Carr, S. A. and Ting, A. Y. (2017). "Proximity Biotinylation as a Method for Mapping Proteins Associated with mtDNA in Living Cells."Cell Chem Biol **24**(3): 404-414.

Havlickova Karbanova, V., Cizkova Vrbacka, A., Hejzlarova, K., Nuskova, H., Stranecky, V., Potocka, A., Kmoch, S. and Houstek, J. (2012). "Compensatory upregulation of respiratory chain complexes III and IV in isolated deficiency of ATP synthase due to TMEM70 mutation."Biochim Biophys Acta **1817**(7): 1037-1043.

Havlickova, V., Kaplanova, V., Nuskova, H., Drahota, Z. and Houstek, J. (2010). "Knockdown of F1 epsilon subunit decreases mitochondrial content of ATP synthase and leads to accumulation of subunit c."Biochim Biophys Acta **1797**(6-7): 1124-1129.

He, J., Ford, H. C., Carroll, J., Ding, S., Fearnley, I. M. and Walker, J. E. (2017). "Persistence of the mitochondrial permeability transition in the absence of subunit c of human ATP synthase."Proc Natl Acad Sci U S A **114**(13): 3409-3414.

Hejzlarova, K., Mracek, T., Vrbacky, M., Kaplanova, V., Karbanova, V., Nuskova, H., Pecina, P. and Houstek, J. (2014). "Nuclear genetic defects of mitochondrial ATP synthase."Physiol Res **63 Suppl 1**: S57-71.

Hejzlarova, K., Kaplanova, V., Nuskova, H., Kovarova, N., Jesina, P., Drahota, Z., Mracek, T., Seneca, S. and Houstek, J. (2015). "Alteration of structure and function of ATP synthase and cytochrome c oxidase by lack of Fo-a and Cox3 subunits caused by mitochondrial DNA 9205delTA mutation."Biochem J **466**(3): 601-611.

Hejzlarova, K., Tesarova, M., Vrbacka-Cizkova, A., Vrbacky, M., Hartmannova, H., Kaplanova, V., Noskova, L., Kratochvilova, H., Buzkova, J., Havlickova, V., Zeman, J., Kmoch, S. and Houstek, J. (2011). "Expression and processing of the TMEM70 protein."Biochim Biophys Acta **1807**(1): 144-149.

Hensen, F., Cansiz, S., Gerhold, J. M. and Spelbrink, J. N. (2014). "To be or not to be a nucleoid protein: a comparison of mass-spectrometry based approaches in the identification of potential mtDNA-nucleoid associated proteins."Biochimie **100**: 219-226.

Herrmann, J. M. and Riemer, J. (2010). "The intermembrane space of mitochondria."Antioxid Redox Signal **13**(9): 1341-1358.

Holme, E., Greter, J., Jacobson, C. E., Larsson, N. G., Lindstedt, S., Nilsson, K. O., Oldfors, A. and Tulinius, M. (1992). "Mitochondrial ATP-synthase deficiency in a child with 3-methylglutaconic aciduria."Pediatr Res **32**(6): 731-735.

Holt, I. J., Harding, A. E., Petty, R. K. and Morgan-Hughes, J. A. (1990). "A new mitochondrial disease associated with mitochondrial DNA heteroplasmy."Am J Hum Genet **46**(3): 428-433.

Holzmann, J., Frank, P., Loffler, E., Bennett, K. L., Gerner, C. and Rossmanith, W. (2008). "RNase P without RNA: identification and functional reconstitution of the human mitochondrial tRNA processing enzyme."Cell **135**(3): 462-474.

Hong, S. and Pedersen, P. L. (2008). "ATP synthase and the actions of inhibitors utilized to study its roles in human health, disease, and other scientific areas."Microbiol Mol Biol Rev **72**(4): 590-641, Table of Contents.

Hong, Z., Chen, K. H., DasGupta, A., Potus, F., Dunham-Snary, K., Bonnet, S., Tian, L., Fu, J., Breuils-Bonnet, S., Provencher, S., Wu, D., Mewburn, J., Ormiston, M. L. and Archer, S. L. (2017). "MicroRNA-138 and MicroRNA-25 Down-regulate Mitochondrial Calcium Uniporter, Causing the Pulmonary Arterial Hypertension Cancer Phenotype."Am J Respir Crit Care Med **195**(4): 515-529.

Honzik, T., Tesarova, M., Mayr, J. A., Hansikova, H., Jesina, P., Bodamer, O., Koch, J., Magner, M., Freisinger, P., Huemer, M., Kostkova, O., van Coster, R., Kmoch, S., Houstek, J., Sperl, W. and Zeman, J. (2010). "Mitochondrial encephalocardio-myopathy with early neonatal onset due to TMEM70 mutation."Arch Dis Child **95**(4): 296-301.

Hořejší, V., Bartůňková, J., Brdička, T. and Spíšek, R. (2017). Základy imunologie.6, Triton.

Horvath, S. E. and Daum, G. (2013). "Lipids of mitochondria."Prog Lipid Res **52**(4): 590-614.

Houstek, J., Kmoch, S. and Zeman, J. (2009). "TMEM70 protein - a novel ancillary factor of mammalian ATP synthase."Biochim Biophys Acta **1787**(5): 529-532.

Houstek, J., Mracek, T., Vojtiskova, A. and Zeman, J. (2004). "Mitochondrial diseases and ATPase defects of nuclear origin."Biochim Biophys Acta **1658**(1-2): 115-121.

Houstek, J., Pickova, A., Vojtiskova, A., Mracek, T., Pecina, P. and Jesina, P. (2006). "Mitochondrial diseases and genetic defects of ATP synthase."Biochim Biophys Acta **1757**(9-10): 1400-1405.

Houstek, J., Klement, P., Floryk, D., Antonicka, H., Hermanska, J., Kalous, M., Hansikova, H., Hout'kova, H., Chowdhury, S. K., Rosipal, T., Kmoch, S., Stratilova, L. and Zeman, J. (1999). "A novel deficiency of mitochondrial ATPase of nuclear origin."Hum Mol Genet **8**(11): 1967-1974.

Hughes, B. G. and Hekimi, S. (2011). "A mild impairment of mitochondrial electron transport has sex-specific effects on lifespan and aging in mice."PLoS One **6**(10): e26116.

Ingraham, C. A., Burwell, L. S., Skalska, J., Brookes, P. S., Howell, R. L., Sheu, S. S. and Pinkert, C. A. (2009). "NDUFS4: creation of a mouse model mimicking a Complex I disorder."Mitochondrion **9**(3): 204-210.

Iommarini, L., Peralta, S., Torraco, A. and Diaz, F. (2015). "Mitochondrial Diseases Part II: Mouse models of OXPHOS deficiencies caused by defects in regulatory factors and other components required for mitochondrial function."Mitochondrion **22**: 96-118.

Isidoro, A., Martinez, M., Fernandez, P. L., Ortega, A. D., Santamaria, G., Chamorro, M., Reed, J. C. and Cuezva, J. M. (2004). "Alteration of the bioenergetic phenotype of mitochondria is a hallmark of breast, gastric, lung and oesophageal cancer."Biochem J **378**(Pt 1): 17-20.

Iwata, S., Lee, J. W., Okada, K., Lee, J. K., Iwata, M., Rasmussen, B., Link, T. A., Ramaswamy, S. and Jap, B. K. (1998). "Complete structure of the 11-subunit bovine mitochondrial cytochrome bc1 complex."Science **281**(5373): 64-71.

The Jackson Laboratory, www.jax.org/strain/000664, 6.3.2018

Jesina, P., Tesarova, M., Fornuskova, D., Vojtiskova, A., Pecina, P., Kaplanova, V., Hansikova, H., Zeman, J. and Houstek, J. (2004). "Diminished synthesis of subunit a (ATP6) and altered function of ATP synthase and cytochrome c oxidase due to the mtDNA 2 bp microdeletion of TA at positions 9205 and 9206."Biochem J **383**(Pt. 3): 561-571.

Jonckheere, A. I., Renkema, G. H., Bras, M., van den Heuvel, L. P., Hoischen, A., Gilissen, C., Nabuurs, S. B., Huynen, M. A., de Vries, M. C., Smeitink, J. A. and Rodenburg, R. J. (2013). "A complex V ATP5A1 defect causes fatal neonatal mitochondrial encephalopathy."Brain **136**(Pt 5): 1544-1554.

Jonckheere, A. I., Huigsloot, M., Lammens, M., Jansen, J., van den Heuvel, L. P., Spiekerkoetter, U., von Kleist-Retzow, J. C., Forkink, M., Koopman, W. J., Szklarczyk, R., Huynen, M. A., Fransen, J. A., Smeitink, J. A. and Rodenburg, R. J. (2011). "Restoration of complex V deficiency caused by a novel deletion in the human TMEM70 gene normalizes mitochondrial morphology."Mitochondrion **11**(6): 954-963.

Jonckheere, A. I., Hogeveen, M., Nijtmans, L. G., van den Brand, M. A., Janssen, A. J., Diepstra, J. H., van den Brandt, F. C., van den Heuvel, L. P., Hol, F. A., Hofste, T. G., Kapusta, L., Dillmann, U., Shamdeen, M. G., Smeitink, J. A. and Rodenburg, R. J. (2008). "A novel mitochondrial ATP8 gene mutation in a patient with apical hypertrophic cardiomyopathy and neuropathy."J Med Genet **45**(3): 129-133.

Junge, W., Lill, H. and Engelbrecht, S. (1997). "ATP synthase: an electrochemical transducer with rotatory mechanics."Trends Biochem Sci **22**(11): 420-423.

Kadenbach, B. and Huttemann, M. (2015). "The subunit composition and function of mammalian cytochrome c oxidase."Mitochondrion **24**: 64-76.

Kim, T. Y., Wang, D., Kim, A. K., Lau, E., Lin, A. J., Liem, D. A., Zhang, J., Zong, N. C., Lam, M. P. and Ping, P. (2012). "Metabolic labeling reveals proteome dynamics of mouse mitochondria."Mol Cell Proteomics **11**(12): 1586-1594.

Klingenberg, M. (2008). "The ADP and ATP transport in mitochondria and its carrier."Biochim Biophys Acta **1778**(10): 1978-2021.

Klusch, N., Murphy, B. J., Mills, D. J., Yildiz, O. and Kuhlbrandt, W. (2017). "Structural basis of proton translocation and force generation in mitochondrial ATP synthase."Elife **6**.

The Knockout Mouse Project, www.komp.org, 14.2.2018

Ko, Y. H., Delannoy, M., Hullihen, J., Chiu, W. and Pedersen, P. L. (2003). "Mitochondrial ATP synthasome. Cristae-enriched membranes and a multiwell detergent screening assay yield dispersed single complexes containing the ATP synthase and carriers for Pi and ADP/ATP."J Biol Chem **278**(14): 12305-12309.

Kolarov, J., Kuzela, S., Krempasky, V., Lakota, J. and Ujhazy, V. (1978). "ADP, ATP translocator protein of rat heart, liver and hepatoma mitochondria exhibits immunological cross-reactivity."FEBS Lett **96**(2): 373-376.

Kontro, H., Hulmi, J. J., Rahkila, P. and Kainulainen, H. (2012). "Cellular and tissue expression of DAPIT, a phylogenetically conserved peptide."Eur J Histochem **56**(2): e18.

Kontro, H., Cannino, G., Rustin, P., Dufour, E. and Kainulainen, H. (2015). "DAPIT Over-Expression Modulates Glucose Metabolism and Cell Behaviour in HEK293T Cells."PLoS One **10**(7): e0131990.

Korshunov, S. S., Skulachev, V. P. and Starkov, A. A. (1997). "High protonic potential actuates a mechanism of production of reactive oxygen species in mitochondria."FEBS Lett **416**(1): 15-18.

Kratochvilova, H., Hejzlarova, K., Vrbacky, M., Mracek, T., Karbanova, V., Tesarova, M., Gombitova, A., Cmarko, D., Wittig, I., Zeman, J. and Houstek, J. (2014). "Mitochondrial membrane assembly of TMEM70 protein."Mitochondrion **15**: 1-9.

Kuhl, I., Miranda, M., Atanassov, I., Kuznetsova, I., Hinze, Y., Mourier, A., Filipovska, A. and Larsson, N. G. (2017). "Transcriptomic and proteomic landscape of mitochondrial dysfunction reveals secondary coenzyme Q deficiency in mammals."Elife **6**.

Kukat, C. and Larsson, N. G. (2013). "mtDNA makes a U-turn for the mitochondrial nucleoid."Trends Cell Biol **23**(9): 457-463.

Kukat, C., Davies, K. M., Wurm, C. A., Spahr, H., Bonekamp, N. A., Kuhl, I., Joos, F., Polosa, P. L., Park, C. B., Posse, V., Falkenberg, M., Jakobs, S., Kuhlbrandt, W. and Larsson, N. G. (2015). "Cross-strand binding of TFAM to a single mtDNA molecule forms the mitochondrial nucleoid."Proc Natl Acad Sci U S A **112**(36): 11288-11293.

Lee, J., Ding, S., Walpole, T. B., Holding, A. N., Montgomery, M. G., Fearnley, I. M. and Walker, J. E. (2015). "Organization of Subunits in the Membrane Domain of the Bovine F-ATPase Revealed by Covalent Cross-linking."J Biol Chem **290**(21): 13308-13320.

Leese, H. J. (1995). "Metabolic control during preimplantation mammalian development."Hum Reprod Update **1**(1): 63-72.

Lippe, G., Sorgato, M. C. and Harris, D. A. (1988). "Kinetics of the release of the mitochondrial inhibitor protein. Correlation with synthesis and hydrolysis of ATP."Biochim Biophys Acta **933**(1): 1-11.

Lodish, H., Berk, A., Kaiser, C. A., Krieger, M., Scott, M., Bretscher, A., Ploegh, H. and Matsudaira, P. (2007). Molecular Cell Biology.6, W. H. Freeman and Company, New York.

Magner, M., Dvorakova, V., Tesarova, M., Mazurova, S., Hansikova, H., Zahorec, M., Brennerova, K., Bzduch, V., Spiegel, R., Horovitz, Y., Mandel, H., Eminoglu, F. T., Mayr, J. A., Koch, J., Martinelli, D., Bertini, E., Konstantopoulou, V., Smet, J., Rahman, S., Broomfield, A., Stojanovic, V., Dionisi-Vici, C., van Coster, R., Morava, E., Sperl, W., Zeman, J. and Honzik, T. (2015). "TMEM70 deficiency: long-term outcome of 48 patients."J Inherit Metab Dis **38**(3): 417-426.

Mai, N., Chrzanowska-Lightowlers, Z. M. and Lightowlers, R. N. (2017). "The process of mammalian mitochondrial protein synthesis."Cell Tissue Res **367**(1): 5-20.

Mattiazzi, M., Vijayvergiya, C., Gajewski, C. D., DeVivo, D. C., Lenaz, G., Wiedmann, M. and Manfredi, G. (2004). "The mtDNA T8993G (NARP) mutation results in an impairment of oxidative phosphorylation that can be improved by antioxidants."Hum Mol Genet **13**(8): 869-879.

Mayr, J. A., Paul, J., Pecina, P., Kurnik, P., Forster, H., Fotschl, U., Sperl, W. and Houstek, J. (2004). "Reduced respiratory control with ADP and changed pattern of respiratory chain enzymes as a result of selective deficiency of the mitochondrial ATP synthase."Pediatr Res **55**(6): 988-994.

Mayr, J. A., Havlickova, V., Zimmermann, F., Magler, I., Kaplanova, V., Jesina, P., Pecinova, A., Nuskova, H., Koch, J., Sperl, W. and Houstek, J. (2010). "Mitochondrial ATP synthase deficiency due to a mutation in the ATP5E gene for the F1 epsilon subunit."Hum Mol Genet **19**(17): 3430-3439.

McFarland, M. A., Ellis, C. E., Markey, S. P. and Nussbaum, R. L. (2008). "Proteomics analysis identifies phosphorylation-dependent alpha-synuclein protein interactions."Mol Cell Proteomics **7**(11): 2123-2137.

Meyer, B., Wittig, I., Trifilieff, E., Karas, M. and Schagger, H. (2007). "Identification of two proteins associated with mammalian ATP synthase."Mol Cell Proteomics **6**(10): 1690-1699.

Milenkovic, D., Blaza, J. N., Larsson, N. G. and Hirst, J. (2017). "The Enigma of the Respiratory Chain Supercomplex."Cell Metab **25**(4): 765-776.

Milenkovic, D., Matic, S., Kuhl, I., Ruzzenente, B., Freyer, C., Jemt, E., Park, C. B., Falkenberg, M. and Larsson, N. G. (2013). "TWINKLE is an essential mitochondrial helicase required for synthesis of nascent D-loop strands and complete mtDNA replication."Hum Mol Genet **22**(10): 1983-1993.

Minczuk, M., He, J., Duch, A. M., Ettema, T. J., Chlebowski, A., Dzionek, K., Nijtmans, L. G., Huynen, M. A. and Holt, I. J. (2011). "TEFM (c17orf42) is necessary for transcription of human mtDNA."Nucleic Acids Res **39**(10): 4284-4299.

Mitchell, P. (1961). "Coupling of phosphorylation to electron and hydrogen transfer by a chemi-osmotic type of mechanism."Nature **191**: 144-148.

Mizukami, S., Yafune, A., Watanabe, Y., Nakajima, K., Jin, M., Yoshida, T. and Shibutani, M. (2017). "Identification of epigenetically downregulated Tmem70 and Ube2e2 in rat liver after 28-day treatment with hepatocarcinogenic thioacetamide showing gene product downregulation in hepatocellular preneoplastic and neoplastic lesions produced by tumor promotion."Toxicol Lett **266**: 13-22.

Mizukami, S., Watanabe, Y., Nakajima, K., Hasegawa-Baba, Y., Jin, M., Yoshida, T. and Shibutani, M. (2017). "Downregulation of TMEM70 in Rat Liver Cells After Hepatocarcinogen Treatment Related to the Warburg Effect in Hepatocarcinogenesis Producing GST-P-Expressing Proliferative Lesions."Toxicol Sci **159**(1): 211-223.

Mracek, T., Pecinova, A., Vrbacky, M., Drahota, Z. and Houstek, J. (2009). "High efficiency of ROS production by glycerophosphate dehydrogenase in mammalian mitochondria."Arch Biochem Biophys **481**(1): 30-36.

Mracek, T., Pecina, P., Vojtiskova, A., Kalous, M., Sebesta, O. and Houstek, J. (2006). "Two components in pathogenic mechanism of mitochondrial ATPase deficiency: energy deprivation and ROS production."Exp Gerontol **41**(7): 683-687.

Murray, J., Marusich, M. F., Capaldi, R. A. and Aggeler, R. (2004). "Focused proteomics: monoclonal antibody-based isolation of the oxidative phosphorylation machinery and detection of phosphoproteins using a fluorescent phosphoprotein gel stain."Electrophoresis **25**(15): 2520-2525.

Nelson, D. L. and Cox, M. (2017). Lehninger Principles of Biochemistry: International Edition.7 WH Freeman.

New, D. A. and Coppola, P. T. (1970). "Effects of different oxygen concentrations on the development of rat embryos in culture."J Reprod Fertil **21**(1): 109-118.

Nicholls, D. G. and Ferguson, S. J. (2013). Bioenergetics 4.4, Elsevier Science.

Nuskova, H., Mracek, T., Mikulova, T., Vrbacky, M., Kovarova, N., Kovalcikova, J., Pecina, P. and Houstek, J. (2015). "Mitochondrial ATP synthasome: Expression and structural interaction of its components."Biochem Biophys Res Commun **464**(3): 787-793.

Ohsakaya, S., Fujikawa, M., Hisabori, T. and Yoshida, M. (2011). "Knockdown of DAPIT (diabetes-associated protein in insulin-sensitive tissue) results in loss of ATP synthase in mitochondria."J Biol Chem **286**(23): 20292-20296.

Osman, C., Wilmes, C., Tatsuta, T. and Langer, T. (2007). "Prohibitins interact genetically with Atp23, a novel processing peptidase and chaperone for the F1Fo-ATP synthase."Mol Biol Cell **18**(2): 627-635.

Pagliarini, D. J., Calvo, S. E., Chang, B., Sheth, S. A., Vafai, S. B., Ong, S. E., Walford, G. A., Sugiana, C., Boneh, A., Chen, W. K., Hill, D. E., Vidal, M., Evans, J. G., Thorburn, D. R., Carr, S. A. and Mootha, V. K. (2008). "A mitochondrial protein compendium elucidates complex I disease biology."Cell **134**(1): 112-123.

Paivarinne, H. and Kainulainen, H. (2001). "DAPIT, a novel protein down-regulated in insulin-sensitive tissues in streptozotocin-induced diabetes."Acta Diabetol **38**(2): 83-86.

Palade, G. E. (1953). "An electron microscope study of the mitochondrial structure."J Histochem Cytochem **1**(4): 188-211.

Paulin, R. and Michelakis, E. D. (2014). "The metabolic theory of pulmonary arterial hypertension."Circ Res **115**(1): 148-164.

Pecina, P., Houstkova, H., Mracek, T., Pecinova, A., Nuskova, H., Tesarova, M., Hansikova, H., Janota, J., Zeman, J. and Houstek, J. (2014). "Noninvasive diagnostics of mitochondrial disorders in isolated lymphocytes with high resolution respirometry."BBA Clin **2**: 62-71.

Pecinova, A., Drahota, Z., Nuskova, H., Pecina, P. and Houstek, J. (2011). "Evaluation of basic mitochondrial functions using rat tissue homogenates."Mitochondrion **11**(5): 722-728.

Peralta, S., Torraco, A., Wenz, T., Garcia, S., Diaz, F. and Moraes, C. T. (2014). "Partial complex I deficiency due to the CNS conditional ablation of Ndufa5 results in a mild chronic encephalopathy but no increase in oxidative damage."Hum Mol Genet **23**(6): 1399-1412.

Piruat, J. I., Pintado, C. O., Ortega-Saenz, P., Roche, M. and Lopez-Barneo, J. (2004). "The mitochondrial SDHD gene is required for early embryogenesis, and its partial deficiency results

in persistent carotid body glomus cell activation with full responsiveness to hypoxia."Mol Cell Biol **24**(24): 10933-10940.

Pogoryelov, D., Krah, A., Langer, J. D., Yildiz, O., Faraldo-Gomez, J. D. and Meier, T. (2010). "Microscopic rotary mechanism of ion translocation in the F(o) complex of ATP synthases."Nat Chem Biol **6**(12): 891-899.

Rak, M., Gokova, S. and Tzagoloff, A. (2011). "Modular assembly of yeast mitochondrial ATP synthase."EMBO J **30**(5): 920-930.

Rak, M., Zeng, X., Briere, J. J. and Tzagoloff, A. (2009). "Assembly of F0 in Saccharomyces cerevisiae."Biochim Biophys Acta **1793**(1): 108-116.

Rossignol, R., Letellier, T., Malgat, M., Rocher, C. and Mazat, J. P. (2000). "Tissue variation in the control of oxidative phosphorylation: implication for mitochondrial diseases."Biochem J **347 Pt 1**: 45-53.

Rossignol, R., Faustin, B., Rocher, C., Malgat, M., Mazat, J. P. and Letellier, T. (2003). "Mitochondrial threshold effects."Biochem J **370**(Pt 3): 751-762.

Ruhle, T. and Leister, D. (2015). "Assembly of F1F0-ATP synthases."Biochim Biophys Acta **1847**(9): 849-860.

Ruiz-Pesini, E., Lott, M. T., Procaccio, V., Poole, J. C., Brandon, M. C., Mishmar, D., Yi, C., Kreuziger, J., Baldi, P. and Wallace, D. C. (2007). "An enhanced MITOMAP with a global mtDNA mutational phylogeny."Nucleic Acids Res **35**(Database issue): D823-828.

Sagan, L. (1967). "On the origin of mitosing cells."J Theor Biol **14**(3): 255-274.

Sanchez-Caballero, L., Guerrero-Castillo, S. and Nijtmans, L. (2016). "Unraveling the complexity of mitochondrial complex I assembly: A dynamic process."Biochim Biophys Acta **1857**(7): 980-990.

Sarajlija, A., Magner, M., Djordjevic, M., Kecman, B., Grujic, B., Tesarova, M. and Minic, P. (2017). "Late-presenting congenital diaphragmatic hernia in a child with TMEM70 deficiency."Congenit Anom (Kyoto) **57**(2): 64-65.

Scaglia, F., Scheuerle, A. E., Towbin, J. A., Armstrong, D. L., Sweetman, L. and Wong, L. J. (2002). "Neonatal presentation of ventricular tachycardia and a Reye-like syndrome episode associated with disturbed mitochondrial energy metabolism."BMC Pediatr **2**: 12.

Scarpulla, R. C. (2006). "Nuclear control of respiratory gene expression in mammalian cells."J Cell Biochem **97**(4): 673-683.

Schagger, H., Link, T. A., Engel, W. D. and von Jagow, G. (1986). "Isolation of the eleven protein subunits of the bc1 complex from beef heart."Methods Enzymol **126**: 224-237.

Seelert, H. and Dencher, N. A. (2011). "ATP synthase superassemblies in animals and plants: two or more are better."Biochim Biophys Acta **1807**(9): 1185-1197.

Shchelochkov, O. A., Li, F. Y., Wang, J., Zhan, H., Towbin, J. A., Jefferies, J. L., Wong, L. J. and Scaglia, F. (2010). "Milder clinical course of Type IV 3-methylglutaconic aciduria due to a novel mutation in TMEM70."Mol Genet Metab **101**(2-3): 282-285.

Shi, Y., Dierckx, A., Wanrooij, P. H., Wanrooij, S., Larsson, N. G., Wilhelmsson, L. M., Falkenberg, M. and Gustafsson, C. M. (2012). "Mammalian transcription factor A is a core component of the mitochondrial transcription machinery."Proc Natl Acad Sci U S A **109**(41): 16510-16515.

Shoubridge, E. A. (2001). "Nuclear genetic defects of oxidative phosphorylation."Hum Mol Genet **10**(20): 2277-2284.

Skarnes, W. C., Rosen, B., West, A. P., Koutsourakis, M., Bushell, W., Iyer, V., Mujica, A. O., Thomas, M., Harrow, J., Cox, T., Jackson, D., Severin, J., Biggs, P., Fu, J., Nefedov, M., de Jong, P. J., Stewart, A. F. and Bradley, A. (2011). "A conditional knockout resource for the genome-wide study of mouse gene function."Nature **474**(7351): 337-342.

Sladkova, J., Spacilova, J., Capek, M., Tesarova, M., Hansikova, H., Honzik, T., Martinek, J., Zamecnik, J., Kostkova, O. and Zeman, J. (2015). "Analysis of Mitochondrial Network Morphology in Cultured Myoblasts from Patients with Mitochondrial Disorders."Ultrastruct Pathol **39**(5): 340-350.

Smith, A. C. and Robinson, A. J. (2009). "MitoMiner, an integrated database for the storage and analysis of mitochondrial proteomics data."Mol Cell Proteomics **8**(6): 1324-1337.

Smith, A. C. and Robinson, A. J. (2016). "MitoMiner v3.1, an update on the mitochondrial proteomics database."Nucleic Acids Res **44**(D1): D1258-1261.

Smith, A. C., Blackshaw, J. A. and Robinson, A. J. (2012). "MitoMiner: a data warehouse for mitochondrial proteomics data."Nucleic Acids Res **40**(Database issue): D1160-1167.

Spelbrink, J. N., Li, F. Y., Tiranti, V., Nikali, K., Yuan, Q. P., Tariq, M., Wanrooij, S., Garrido, N., Comi, G., Morandi, L., Santoro, L., Toscano, A., Fabrizi, G. M., Somer, H., Croxen, R., Beeson, D., Poulton, J., Suomalainen, A., Jacobs, H. T., Zeviani, M. and Larsson, C. (2001). "Human mitochondrial DNA deletions associated with mutations in the gene encoding Twinkle, a phage T7 gene 4-like protein localized in mitochondria."Nat Genet **28**(3): 223-231.

Sperl, W., Jesina, P., Zeman, J., Mayr, J. A., Demeirleir, L., VanCoster, R., Pickova, A., Hansikova, H., Houst'kova, H., Krejcik, Z., Koch, J., Smet, J., Muss, W., Holme, E. and Houstek, J. (2006). "Deficiency of mitochondrial ATP synthase of nuclear genetic origin."Neuromuscul Disord **16**(12): 821-829.

Spiegel, R., Khayat, M., Shalev, S. A., Horovitz, Y., Mandel, H., Hershkovitz, E., Barghuti, F., Shaag, A., Saada, A., Korman, S. H., Elpeleg, O. and Yatsiv, I. (2011). "TMEM70 mutations are a common cause of nuclear encoded ATP synthase assembly defect: further delineation of a new syndrome."J Med Genet **48**(3): 177-182.

Stepien, G., Torroni, A., Chung, A. B., Hodge, J. A. and Wallace, D. C. (1992). "Differential expression of adenine nucleotide translocator isoforms in mammalian tissues and during muscle cell differentiation."J Biol Chem **267**(21): 14592-14597.

Stojanovic, V. and Doronjski, A. (2013). "Mild form of 3-methylglutaconic aciduria type IV and mutation in the TMEM70 genes."J Pediatr Endocrinol Metab **26**(1-2): 151-154.

Strauss, M., Hofhaus, G., Schroder, R. R. and Kuhlbrandt, W. (2008). "Dimer ribbons of ATP synthase shape the inner mitochondrial membrane."EMBO J **27**(7): 1154-1160.

Szabo, I. and Zoratti, M. (2014). "Mitochondrial channels: ion fluxes and more."Physiol Rev **94**(2): 519-608.

Takahashi, Y., Kako, K., Kashiwabara, S., Takehara, A., Inada, Y., Arai, H., Nakada, K., Kodama, H., Hayashi, J., Baba, T. and Munekata, E. (2002). "Mammalian copper chaperone Cox17p has an essential role in activation of cytochrome C oxidase and embryonic development."Mol Cell Biol **22**(21): 7614-7621.

Timohhina, N., Guzun, R., Tepp, K., Monge, C., Varikmaa, M., Vija, H., Sikk, P., Kaambre, T., Sackett, D. and Saks, V. (2009). "Direct measurement of energy fluxes from mitochondria into cytoplasm in permeabilized cardiac cells in situ: some evidence for Mitochondrial Interactosome."J Bioenerg Biomembr **41**(3): 259-275.

Tomecki, R., Dmochowska, A., Gewartowski, K., Dziembowski, A. and Stepien, P. P. (2004). "Identification of a novel human nuclear-encoded mitochondrial poly(A) polymerase."Nucleic Acids Res **32**(20): 6001-6014.

Torraco, A., Peralta, S., Iommarini, L. and Diaz, F. (2015). "Mitochondrial Diseases Part I: mouse models of OXPHOS deficiencies caused by defects in respiratory complex subunits or assembly factors."Mitochondrion **21**: 76-91.

Torraco, A., Verrigni, D., Rizza, T., Meschini, M. C., Vazquez-Memije, M. E., Martinelli, D., Bianchi, M., Piemonte, F., Dionisi-Vici, C., Santorelli, F. M., Bertini, E. and Carrozzo, R. (2012). "TMEM70: a mutational hot spot in nuclear ATP synthase deficiency with a pivotal role in complex V biogenesis."Neurogenetics **13**(4): 375-386.

Tort, F., Del Toro, M., Lissens, W., Montoya, J., Fernandez-Burriel, M., Font, A., Bujan, N., Navarro-Sastre, A., Lopez-Gallardo, E., Arranz, J. A., Riudor, E., Briones, P. and Ribes, A. (2011). "Screening for nuclear genetic defects in the ATP synthase-associated genes TMEM70, ATP12 and ATP5E in patients with 3-methylglutaconic aciduria."Clin Genet **80**(3): 297-300.

Tsukihara, T., Aoyama, H., Yamashita, E., Tomizaki, T., Yamaguchi, H., Shinzawa-Itoh, K., Nakashima, R., Yaono, R. and Yoshikawa, S. (1996). "The whole structure of the 13-subunit oxidized cytochrome c oxidase at 2.8 A."Science **272**(5265): 1136-1144.

Tyynismaa, H., Sembongi, H., Bokori-Brown, M., Granycome, C., Ashley, N., Poulton, J., Jalanko, A., Spelbrink, J. N., Holt, I. J. and Suomalainen, A. (2004). "Twinkle helicase is essential for mtDNA maintenance and regulates mtDNA copy number."Hum Mol Genet **13**(24): 3219-3227.

Ufer, C. and Wang, C. C. (2011). "The Roles of Glutathione Peroxidases during Embryo Development."Front Mol Neurosci **4**: 12.

Uhlen, M., Fagerberg, L., Hallstrom, B. M., Lindskog, C., Oksvold, P., Mardinoglu, A., Sivertsson, A., Kampf, C., Sjostedt, E., Asplund, A., Olsson, I., Edlund, K., Lundberg, E., Navani, S., Szigyarto, C. A., Odeberg, J., Djureinovic, D., Takanen, J. O., Hober, S., Alm, T.,

Edqvist, P. H., Berling, H., Tegel, H., Mulder, J., Rockberg, J., Nilsson, P., Schwenk, J. M., Hamsten, M., von Feilitzen, K., Forsberg, M., Persson, L., Johansson, F., Zwahlen, M., von Heijne, G., Nielsen, J. and Ponten, F. (2015). "Proteomics. Tissue-based map of the human proteome."Science **347**(6220): 1260419.

Vafai, S. B. and Mootha, V. K. (2012). "Mitochondrial disorders as windows into an ancient organelle."Nature **491**(7424): 374-383.

Vik, S. B. and Antonio, B. J. (1994). "A mechanism of proton translocation by F1F0 ATP synthases suggested by double mutants of the a subunit."J Biol Chem **269**(48): 30364-30369.

Viscomi, C. (2016). "Toward a therapy for mitochondrial disease."Biochem Soc Trans **44**(5): 1483-1490.

Viscomi, C., Bottani, E., Civiletto, G., Cerutti, R., Moggio, M., Fagiolari, G., Schon, E. A., Lamperti, C. and Zeviani, M. (2011). "In vivo correction of COX deficiency by activation of the AMPK/PGC-1alpha axis."Cell Metab **14**(1): 80-90.

Vrbacky, M., Kovalcikova, J., Chawengsaksophak, K., Beck, I. M., Mracek, T., Nuskova, H., Sedmera, D., Papousek, F., Kolar, F., Sobol, M., Hozak, P., Sedlacek, R. and Houstek, J. (2016). "Knockout of Tmem70 alters biogenesis of ATP synthase and leads to embryonal lethality in mice."Hum Mol Genet **25**(21): 4674-4685.

Walker, J. E. (2013). "The ATP synthase: the understood, the uncertain and the unknown."Biochem Soc Trans **41**(1): 1-16.

Wang, L., Zuo, L., Hu, J., Shao, H., Lei, C., Qi, W., Liu, Y., Miao, Y., Ma, X., Huang, C. L., Wang, B., Zhou, X., Zhang, Y. and Liu, L. (2016). "Dual LQT1 and HCM phenotypes associated with tetrad heterozygous mutations in KCNQ1, MYH7, MYLK2, and TMEM70 genes in a three-generation Chinese family."Europace **18**(4): 602-609.

Wang, Z. G., White, P. S. and Ackerman, S. H. (2001). "Atp11p and Atp12p are assembly factors for the F(1)-ATPase in human mitochondria."J Biol Chem **276**(33): 30773-30778.

Wasilewski, M., Chojnacka, K. and Chacinska, A. (2017). "Protein trafficking at the crossroads to mitochondria."Biochim Biophys Acta **1864**(1): 125-137.

Wirth, C., Brandt, U., Hunte, C. and Zickermann, V. (2016). "Structure and function of mitochondrial complex I."Biochim Biophys Acta **1857**(7): 902-914.

Wittig, I. and Schagger, H. (2008). "Structural organization of mitochondrial ATP synthase."Biochim Biophys Acta **1777**(7-8): 592-598.

Wittig, I. and Schagger, H. (2009). "Native electrophoretic techniques to identify protein-protein interactions."Proteomics **9**(23): 5214-5223.

Wittig, I., Braun, H. P. and Schagger, H. (2006). "Blue native PAGE."Nat Protoc **1**(1): 418-428.

Wittig, I., Karas, M. and Schagger, H. (2007). "High resolution clear native electrophoresis for in-gel functional assays and fluorescence studies of membrane protein complexes."Mol Cell Proteomics **6**(7): 1215-1225.

Wittig, I., Meyer, B., Heide, H., Steger, M., Bleier, L., Wumaier, Z., Karas, M. and Schagger, H. (2010). "Assembly and oligomerization of human ATP synthase lacking mitochondrial subunits a and A6L."Biochim Biophys Acta **1797**(6-7): 1004-1011.

Wortmann, S. B., Rodenburg, R. J., Jonckheere, A., de Vries, M. C., Huizing, M., Heldt, K., van den Heuvel, L. P., Wendel, U., Kluijtmans, L. A., Engelke, U. F., Wevers, R. A., Smeitink, J. A. and Morava, E. (2009). "Biochemical and genetic analysis of 3-methylglutaconic aciduria type IV: a diagnostic strategy."Brain **132**(Pt 1): 136-146.

Yang, H., Brosel, S., Acin-Perez, R., Slavkovich, V., Nishino, I., Khan, R., Goldberg, I. J., Graziano, J., Manfredi, G. and Schon, E. A. (2010). "Analysis of mouse models of cytochrome c oxidase deficiency owing to mutations in Sco2."Hum Mol Genet **19**(1): 170-180.

Young, M. J. and Copeland, W. C. (2016). "Human mitochondrial DNA replication machinery and disease."Curr Opin Genet Dev **38**: 52-62.

Zeng, X., Neupert, W. and Tzagoloff, A. (2007). "The metalloprotease encoded by ATP23 has a dual function in processing and assembly of subunit 6 of mitochondrial ATPase."Mol Biol Cell **18**(2): 617-626.

Zhang, L., Yu, C., Vasquez, F. E., Galeva, N., Onyango, I., Swerdlow, R. H. and Dobrowsky, R. T. (2010). "Hyperglycemia alters the schwann cell mitochondrial proteome and decreases coupled respiration in the absence of superoxide production."J Proteome Res **9**(1): 458-471.

Zhou, A., Rohou, A., Schep, D. G., Bason, J. V., Montgomery, M. G., Walker, J. E., Grigorieff, N. and Rubinstein, J. L. (2015). "Structure and conformational states of the bovine mitochondrial ATP synthase by cryo-EM."Elife **4**: e10180.

9 APPENDIX

Thesis is based on these publications with IF:

Publication A

Vrbacký M.*, Kovalčíková J.*, Chawengsaksophak K., Beck I.M., Mráček T., Nůsková H., Sedmera D., Papoušek F., Kolář F., Sobol M., Hozák P., Sedlacek R., Houštěk J. *"Knockout of Tmem70 alters biogenesis of ATP synthase and leads to embryonal lethality in mice."* Human Molecular Genetics, 2016, 25(21): 4674-4685. IF_{2016}=5.340

*Equal contribution

Publication B

Nůsková H., Mráček T., Mikulová T., Vrbacký M., Kovářová N., Kovalčíková J., Pecina P., Houštek J.*"Mitochondrial ATP synthasome: expression and structural interaction of its components."* Biochemical and Biophysical Research Communications, 2015, 464(3): 787-793. IF_{2016}=2.466